UNIVERSIDADE DE LISBOA
FACULDADE DE CIÊNCIAS
DEPARTAMENTO DE FÍSICA

Evolutionary Dynamics of Collective Action in Structured Populations

Marta Daniela de Almeida Santos

Tese orientada pelo Prof. Doutor Jorge Manuel dos Santos Pacheco e pela Prof.ª Doutora Ana Maria Ribeiro Ferreira Nunes, especialmente elaborada para a obtenção do grau de doutor em Física

2012

Para a minha mãe ☺

Abstract

The pervasiveness of cooperation in Nature is not easily explained. If evolution is characterized by competition and survival of the fittest, why should selfish individuals cooperate with each other? Evolutionary Game Theory (**EGT**) provides a suitable mathematical framework to study this problem, central to many areas of science. Conventionally, interactions between individuals are modeled in terms of one-shot, symmetric 2-Person Dilemmas of Cooperation, but many real-life situations involve decisions within groups with more than 2 individuals, which are best-dealt in the framework of N-Person games. In this Thesis, we investigate the evolutionary dynamics of two paradigmatic collective social dilemmas - the N-Person Prisoner's Dilemma (**NPD**) and the N-Person Snowdrift Game (**NSG**) on structured populations, modeled by networks with diverse topological properties.

Cooperative strategies are just one example of the many traits that can be transmitted on social networks. Several recent studies based on empirical evidence from a medical database have suggested the existence of a *3 degrees of influence rule*, according to which not only our "friends", but also our friends' friends, and our friends' friends' friends, have a non-trivial influence on our decisions. We investigate the degree of peer influence that emerges from the spread of cooperative strategies, opinions and diseases on populations with distinct underlying networks of contacts. Our results show that networks naturally entangle individuals into interactions of many-body nature and that for each network class considered different processes lead to identical degrees of influence.

Keywords: Evolutionary Game Theory, Complex Social Networks, Evolution of Cooperation, N-Person Social Dilemmas, Peer Influence.

Resumo

De uma perspectiva Darwinista, a evolução das espécies resulta da acção conjunta da selecção natural e da mutação (ao nível genético). A sobrevivência dos mais fortes - ou melhor, a sobrevivência dos melhor adaptados às exigências do ambiente circundante - pode ser entendida como um processo de competição em que indivíduos egoístas, que se preocupam em prolongar o seu tempo de sobrevivência de forma a maximizar a probabilidade de propagação dos seus genes para a próxima geração, acabam por ganhar. Não é pois de esperar que existam quaisquer manifestações de ajuda, de *cooperação*, entre indivíduos, em que se quantifica um acto cooperativo como aquele que envolve um custo c para quem coopera resultando num benefício b a quem o recebe $(b > c)$.

A Natureza no entanto revela-nos evidências do contrário em todas as escalas, desde a origem dos organismos multi-celulares, ao desenvolvimento da cultura humana, que só foram possíveis graças à existência de cooperação. Como explicar então a ocorrência de tantos exemplos de cooperação na Natureza, e como solucionar este (aparente) paradoxo? Esta é uma questão central em áreas científicas tão diversas como a Biologia, a Matemática, as Ciências Sociais ou a Física, e tem recebido uma atenção crescente nas últimas décadas. Nesta tese, começamos por estudar a dinâmica da cooperação associada a diferentes dilemas sociais colectivos em populações estruturadas, isto é, em que os indivíduos não interagem com quaisquer outros indivíduos mas apenas com um sub-conjunto fixo de indivíduos determinado por uma arquitectura complexa. Estas estruturas podem ser facilmente modeladas recorrendo a redes, em que os seus nodos representam indivíduos e as ligações determinam o padrão de interacções entre eles. Estas redes podem ser encontradas nos mais diversos contextos, desde redes eléctricas a redes de transportes (como tráfego aéreo e auto-estradas) e redes sociais reais e virtuais (isto é, baseadas na Internet). Neste último caso, a franca expansão da Internet, associada à sua crescente democratização e à utilização em massa de ferramentas como o Facebook ou o Twitter tem permitido, pela primeira vez, o estudo exaustivo de redes sociais com milhares ou milhões de indivíduos. A ciência de redes acompanhou este desenvolvimento, registando um enorme crescimento nos últimos anos, e permitiu

aprofundar as principais características destas estruturas e avaliar as suas propriedades. A avaliação do impacto de populações estruturadas na dinâmica evolutiva da cooperação é um tópico de investigação muito recente, para o qual esta tese procura contribuir.

A Teoria de Jogos Evolutiva permite estudar situações estratégicas em que o sucesso de cada indivíduo depende das escolhas de outro ou outros, e proporciona o formalismo matemático adequado ao estudo da emergência e evolução da cooperação. A abordagem mais convencional consiste em considerar indivíduos sem memória que interagem 2 a 2 podendo optar por duas estratégias unilaterais, Cooperar ou Não Cooperar. Adicionalmente, também se consideram que as populaçoes são infinitas e sem estrutura e que a dinâmica evolutiva é modelada através da equação do replicador. Estas hipóteses são aproximações mas, como demonstraremos, constitutem uma referência importante para a avaliação do impacto de populações estruturadas.

Muitos dilemas cooperativos envolvem decisões resultantes de grupos que englobam $N \geq 2$ individuos. Desde a participação em projectos comunitários, ao pagamento de impostos, passando por aquele que será um dos mais importantes problemas de acção colectiva da actualidade e que envolve todos os indivíduos do planeta - a questão das alterações climáticas e o que podemos fazer para as minorar - os exemplos são inúmeros. O Dilema do Prisioneiro para N Pessoas surge como o modelo adequado a descrever problemas em que o beneficio é proporcional ao número de cooperadores no grupo sendo, no contexto dos dilemas de bem público aquele que tem sido alvo de maior atenção na literatura. À semelhança do que sucede no dilema do prisioneiro envolvendo 2 pessoas, em populações sem estrutura aqueles que não cooperam estão sempre em vantagem, e portanto a cooperação está condenada à extinção.

Neste trabalho, estudamos não só qual o impacto de tornar as interacções localizadas através da introdução de estrutura na população, como também quais as consequências da mudança de paradigma contributivo. Tradicionalmente, assumia-se que todos os cooperadores contribuiam com um mesmo esforço em cada um dos dilemas em que participavam. No entanto, a introdução de estrutura na população fez com que tivéssemos de rever esse paradigma. Demonstramos que, assumindo que cada cooperador reparte o seu esforço igualmente pelos vários dilemas em que participa, os níveis de cooperação disparam. Em suma, no contexto deste modelo os nossos resultados demonstram uma mensagem que consideramos encorajadora - o acto de dar é mais relevante que o montante dado.

Também existem situações em que o benefício, quando obtido, é fixo, independente do número de Cooperadores, e está igualmente disponível a todos os elementos do grupo. Nestes casos, o modelo mais adequado é o Jogo da Avalanche de N Pessoas, que facilita a emergência da cooperação. Com efeito verifica-se que mesmo no cenário tradicional de população sem estrutura, este modelo prevê uma coexistência entre cooperadores e não-cooperadores.

No decurso deste trabalho, adoptamos uma nova abordagem para estudar o impacto de populações estruturadas na evolução da cooperação. Através do cálculo numérico de um análogo em populações estruturadas da equação do replicador - o *Gradiente de Selecção* - , torna-se possível acompanhar e analisar em detalhe a evolução do sistema para o seu estado estacionário. Esta informação, que se perdia na abordagem convencional, permite retirar conclusões surpreendentes. Demonstramos que o jogo global, por consequência das interacções localizadas impostas pela rede de contactos, é distinto das regras locais do Jogo da Avalanche de N Pessoas, e que diferentes redes de contacto dão origem a diferentes jogos globais.

Estratégias cooperativas são um dos muitos exemplos possíveis de comportamentos, ideias, em suma, informação, que se propagam nas redes sociais. Partindo da análise de uma base de dados médica, e do estudo de correlações entre indivíduos em relação a aspectos tão distintos como o consumo de álcool, hábitos tabágicos, obesidade, felicidade ou cooperação, foi recentemente proposta uma regra de *3 graus de influência* para a propagação de informação em redes sociais. Estas correlações reflectem o aumento relativo da probabilidade, quando comparada com uma distribuição aleatória, de dois indivíduos partilharem a mesma característica em função da distância social, medida como o número mínimo de ligações que separam esses indivíduos na rede. Observou-se a emergência de padrões de influência semelhantes e não triviais estendendo-se até uma distância social de aproximadamente 3. Por outras palavras, não apenas os nossos "amigos", mas também os seus amigos e os amigos deles exibem uma correlação positiva connosco em relação a determinada característica. Com o intuito de comprender a origem de tal padrão, modelamos interacções a 2 pessoas, não apenas no contexto da Teoria de Jogos Evolutiva, mas recorrendo também a modelos epidemiológicos e modelos simples de formação de opiniões. Mostramos que, para cada classe de rede social considerada, *diferentes* processos dinâmicos conduzem a *iguais* graus de influência, o que sugere que a influência de pares não depende do processo em causa, e que a topologia da rede associada determina o padrão de correlações emergente. Isto é, as redes sociais efectivamente alargam, de uma forma não-trivial, as interacções diádicas das

quais partimos: sempre que estamos sujeitos a influência dos nossos contactos sociais, não apenas aqueles com quem interagimos directamente afectam as nossas escolhas, mas o nível de influência a que estamos sujeitos é definido pelas propriedades da rede em que estamos inseridos.

Palavras-chave: Teoria de Jogos Evolutiva, Redes Sociais Complexas, Evolução da Cooperação, Dilemas Sociais de N Pessoas, Influência de Pares.

Agradecimentos

Realizar este doutoramento foi para mim uma jornada tanto científica como pessoal. Não apenas os sucessos, mas também (e sobretudo) os problemas e as falhas ensinaram-me a não desistir, a ser persistente, a tentar outras abordagens. Muitos foram aqueles que ao longo dos últimos 4 anos me deram o apoio e força necessários para chegar até aqui.

Em primeiro lugar, quero agradecer ao Prof. Jorge Pacheco, meu orientador, que me recebeu no grupo ATP (Applications of Theoretical Physics) e meu deu todo o apoio em todos os projectos em que trabalhei. Obrigada por todos os conhecimentos que me transmitiu ao longo destes 4 anos, e pela sua constante disponibilidade para me ajudar com as minhas dúvidas sempre que necessário. Agradeço tambem à Prof. Ana Nunes, minha co-supervisora, pelos seus conselhos e palavras de encorajamento constantes, que tornaram todo este percurso mais fácil.

O Prof. Francisco Santos esteve presente em todos os projectos que desenvolvi, e a ele devo a ajuda para encontrar a soluçao de diversos problemas científicos com os quais me fui deparando. A sua paciência para me ajudar e as suas palavras sempre positivas foram uma parte muito importante na concretização de todo o trabalho que aqui apresento.

O trabalho interdisciplinar que desenvolvi e apresento nesta tese não teria sido possível se não estivesse inserida num grupo tão heterogéneo como o ATP. Cada um dos meus colegas, com os seus conhecimentos e a sua experiência, me ensinou coisas que de uma ou outra forma estão aqui espelhadas. Muito obrigada pelo vosso companheirismo e pela vossa ajuda.

A fase final do doutoramento, de escrita da tese, pode ser particularmente esgotante – foi-o, pelo menos, no meu caso. Quero deixar o meu muito obrigada aos meus colegas e amigos Stefan Wieland, Ramona e Pedro Neves pelo seu especial apoio nesta fase final. Os pequenos momentos que partilhamos no dia a dia, as conversas aparentemente sem significado ao almoço e ao lanche, as vossas palavras de incentivo, foram fundamentais para me dar ânimo. Agradeço tambem ao Pedro a sua paciência e empenho na revisão desta tese: ela estaria muito diferente (para pior...) se não fosse o seu olho clínico e as suas observações sempre certeiras. Muito obrigada!

Agradeço a todos os meus amigos o terem tido (muita) paciência comigo durante estes anos por não ter estado tão presente quanto gostaria, e a sua compreensão por, por diversas vezes, não conseguir ter outro tema de conversa que não o trabalho. Está na hora de colocarmos a conversa em dia!

Não poderia terminar sem deixar o meu maior agradecimento, por tudo, à minha mãe: por acreditar sempre em mim (mais do que eu acredito em mim mesma, na maior parte das vezes...), pelo seu apoio, por me encorajar, por me ajudar, por me fazer ultrapassar os momentos mais difíceis. Sem ela, nada disto teria sido possível. Obrigada mãe ☺

Agradeço financiamento dos projectos

- *Cultural Evolution and Cooperation Genetics*, PDCT/HEC/60360/2004
- *Mathematical Models of Evolutionary Processes*, PTDC/MAT/66426/2006
- *Modeling of Complex Evolutionary Processes*, PTDC/FIS/70973/2006
- *Co-evolution and Self-organization of Cooperation*, PTDC/FIS/101248/2008

para participação em conferências nacionais e internacionais (projectos atribuídos pela Fundaçãao para a Ciência e Tecnologia, FCT, ao grupo ATP - Applications of Theoretical Physics).

Agradeço à FCT a bolsa de doutoramento com a referência SFRH / BD / 43282 / 2008, sem a qual este trabalho não teria sido possível.

Contents

List of Figures

1

Introduction

> *No man is an island.*
>
> – John Donne, in "Devotions upon emergent occasions" (1624)

Contrary to being solitary we participate, to a greater or lesser extent, in each other's lives: we act and live integrated in communities – and we cooperate with others. Human culture is a living and evolving proof of such cooperation: the interchange of tools, food and methods allowed the individuals involved in such exchange to gradually rely on the knowledge and achievements of others and become specialized. Cooperation paved the way to specialization and exchange of ideas, which have culminated in a rich and fast evolving culture.

Many philosophers have tried to understand why, we humans, cooperate. Wouldn't it be easier to be egotistical and pursue only our own interests? Along history, there have been many and contradictory views on this subject, with philosophers trying to understand the role of society on the nature of the individual: from Thomas Hobbes, who claimed that humans are born selfish and society teaches them better, to Jean-Jacques Rousseau, who defended that humans are born cooperative and society later corrupts them.

Cooperation seems to have played a fundamental role in some of the major transitions in evolution. According to John Maynard Smith and Eörs Szathmáry,

> "*Major transitions are major stages in the evolution of complexity that involve a change in the level of organization, and hence the level of selection.*"
>
> – John Maynard Smith and Eörs Szathmáry in "The major transitions in evolution" (1995)

Take for instance the emergence of multicellular organisms, that is, the transition from protists (organisms that are unicellular, or multicellular but without specialized tissues) to complex multicellular organisms such as animals, plants and fungi. This transition occurred presumably at approximately 6 x 10^8 years ago, and required the cooperation of cells. In this context, we do not refer to *cooperation* as a conscious decision, of course, but as an interaction between elements in which each of the simple constituent elements may be interpreted as paying a cost c and obtaining a benefit b (with $b > c$). Associated with the cost c in this transition from protists to multicellular organisms is for instance the fact that single cells are not able to replicate independently anymore when they are part of the larger and more complex entity (the multicellular organism). One of the advantages associated with the benefit b in this transition is the fact that in a multicellular organism each cell does not have to ensure the execution of several functions but can become specialized in a particular one.

Or take instead the most recent major transition in evolution, from primate societies to the human societies of nowadays. This transition required the emergence of a new way of transmitting information – it fostered the evolution of *language*. With language, individuals were able to exchange more and more detailed information, and specialized in particular tasks instead of having to ensure all tasks necessary for their survival. They then came to rely on the knowledge of other individuals and gradually construct a *culture*.

Human societies are embedded in complex social networks, determined by the pattern of interactions between individuals. Despite social networks' massive popularization, thanks to the democratization of the Internet and the massive access to social online networking tools such as Facebook, Twitter and MySpace, this concept has been widely used for over a century to describe complex sets of relationships between elements of social systems. Although their systematic study began before, in the first decades of the last century, they comprised only small-scale networks, with a few dozen of individual at most, as it was not yet possible at the time to obtain more significant data. Only recently it has been possible to start exploring the vast networks by which we are in fact interconnected – structures with thousands, millions of elements.

Network science comprises a whole set of mathematical tools to analyze its topological properties, but despite its recent bloom its roots date back to approximately three centuries ago. Inadvertently and as a consequence of his simple and elegant reasoning, Leonhard Euler founded graph theory with the publication of his 1736 paper with the solution of the problem known as "The Seven Bridges of Königsberg". Königsberg was

a city of Prussia (now Kalinningrad, in Russia) that consisted in two islands – these were inter-connected and connected to the mainland by a total of seven bridges. The challenge – which Euler proved to be impossible – was to devise a route that would transverse each bridge exactly once. He based his reasoning, for the first time in the history of Mathematics, in an abstract representation which eliminated all features except the bridges and the land masses. The interest in graphs, its properties and applications bloomed, and several renowned mathematicians contributed to the field in the centuries that followed.

In this thesis we aim to contribute for a better understanding of what is the impact of population structure on the evolutionary dynamics of **i)** collective social dilemmas, and **ii)** dyadic contact processes representative of propagation of behaviors and ideas in social networks. Therefore, we start by discussing some central concepts of Network Science in chapter 2, which will be recurrently used in the rest of the thesis. In chapter 3 we present the mathematical framework of Evolutionary Game Theory (**EGT**), which traditionally addresses the problem of evolution of cooperation in well-mixed populations (i.e. populations in which each and every individual has the same probability of interacting with every other in the population). Although real populations are far from being well-mixed and infinite, these theoretical foundations provide a solid background for the analysis of the impact of the introduction of structure in a population in the dynamical processes studied here. Chapters 2 and 3 correspond to the theoretical introduction necessary for the understanding and discussion of the original results presented in the chapters that follow.Finally, in chapters 4 to 6 we present and discuss the results obtained in three distinct projects. In each of these chapters, we start by presenting a brief discussion of the evolutionary dynamics of the model under study in well-mixed populations (results already known in the literature), and then proceed to discuss our original results in structured populations. In figure 1.1 we present a flowchart with a brief outline of the thesis. The projects we discuss in chapters 4 to 6 are the following:

- Chapter 4: The N-Person Prisoner's Dilemma (**NPD**) is the most suitable model to describe situations in which a benefit obtained from the completion of a task is proportional to the number of cooperators in the group. We investigate not only the impact of localized interactions in the average level of cooperation in a population, but also the impact of modifying the contributive paradigm. We show that in highly heterogeneous populations, when cooperators share their effort equally among all the dilemmas in which they participate cooperation blooms.

Our results demonstrate what we believe is an encouraging message – the act of giving is more important than the amount given.

- Chapter 5: Less studied than the **NPD**, the N-Person Snowdrift Game (**NSG**) is an interesting alternative to study the evolution of cooperation, appropriate for situations in which the benefit, when obtained, is fixed and equally available to all members of the group. We investigate the impact of structured populations in the evolutionary dynamics of **NSG** resorting to a numerical analogue of the replicator equation for structured populations – the *gradient of selection*. This new approach provides information concerning the evolution towards the steady state which in the end proves crucial, and how population structure affects the global dilemma played in the population.

- Chapter 6: Cooperative strategies are just one of many possible examples of a trait that may propagate in social networks. Recently, a *3 degrees of influence* rule was proposed for the propagation of traits in social networks, after analyzing empirical correlations among individuals for traits as diverse as alcohol consumption, smoking habits, obesity, cooperation or happiness in a social network extracted from a medical database. Throughout this thesis, we refer to *peer influence* as a synonym of this empirical observation that individuals influence the behavior of their nearest neighbors. Similar and non-trivial patterns of correlation were observed for each of these traits, extending to a social distance of approximately 3. We adopt simple dyadic interaction models, not only in the framework of **EGT** but also epidemiological models and opinion formation models, and show how, for each class of network modeling population structure, different dynamical processes lead to similar degrees of influence. This suggests that peer influence does not depend on the trait or dynamical process, and that network structure may ultimately determine the pattern of peer influence.

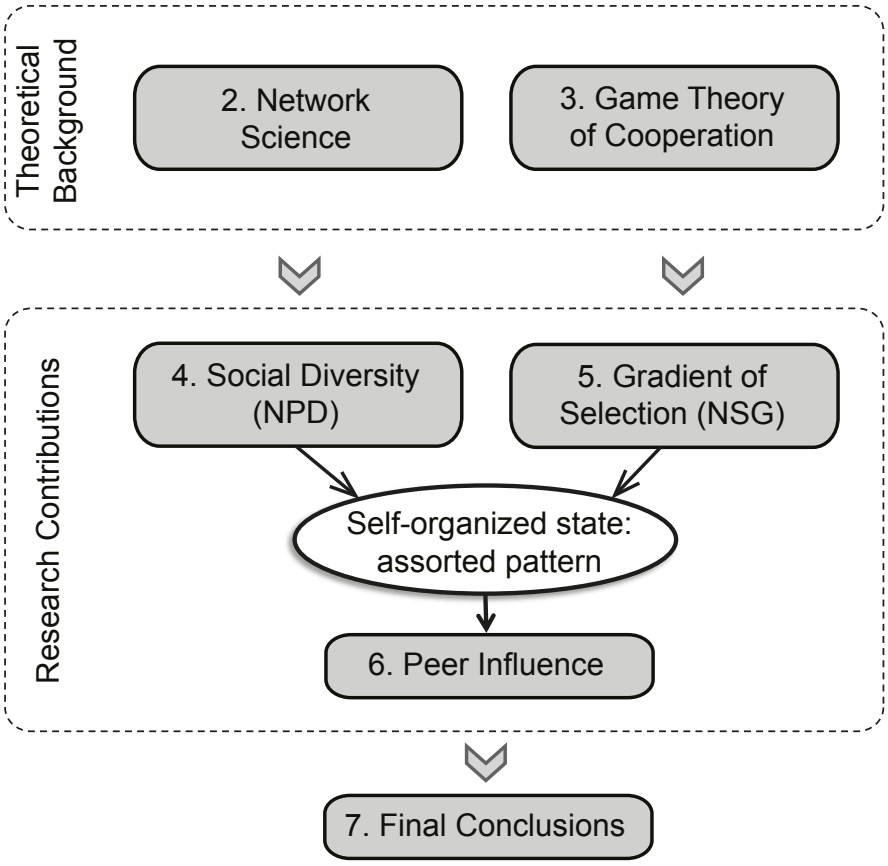

Figure 1.1: Outline of the thesis - Brief outline of the organization of the thesis, highlighting what are the research contributions and the necessary theoretical background.

2

Network Science

2.1 Introduction

Consider a system composed of several individual parts connected with each other in some way. The complete study of such a system can follow diverse routes, as one can investigate

- the properties of its individual elements,
- the nature of the interactions between them, and also
- the *pattern of interactions* between those elements.

Such pattern can be captured by a *network* (or a *graph*) – formally, a collection of *nodes* connected by *links* or *edges* according to a certain structure.

In figure 2.1 we show two examples of systems of very different nature and their respective networks: a railroad network of United States of America (panel A), and a snapshot of the structure of the Internet (panel B). In the former case, the nodes are cities, linked together by railroads; while in the latter nodes are computers and routers, linked together by physical links, like cables and other data connections. On both examples, when we study *just* the network a significant amount of information is lost: it is not possible to know when the rails and roads were built, and the traffic in each of them; or the operating systems of the computers and how many times they are accessed. But the same simplification occurs in countless physical models. The central point here is that networks may provide a convenient and useful formalism for studying the *interaction* between the elements of a system. Perhaps because of this very

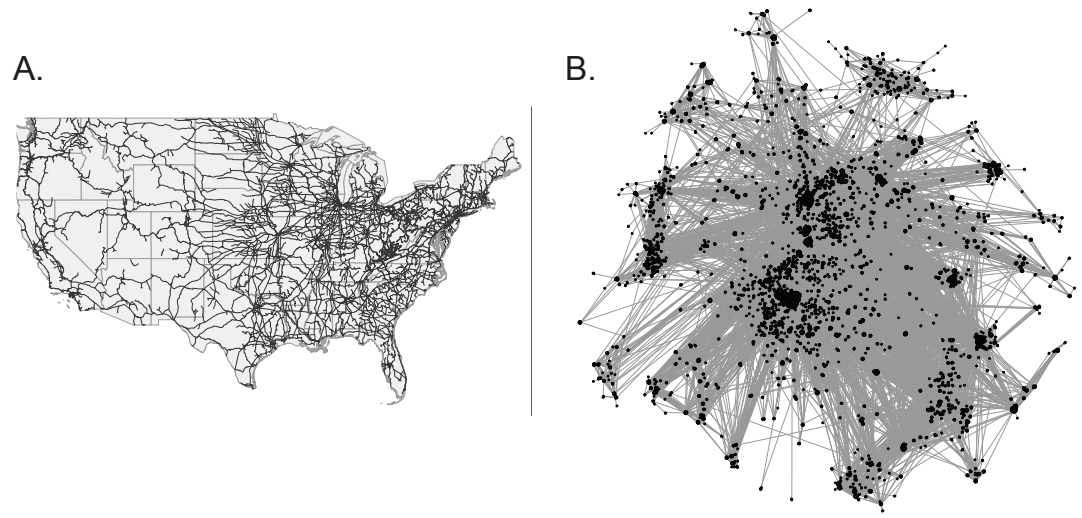

Figure 2.1: Examples of real world networks - **A.** The United States of America rail network, which connects the main road systems (source: Wolfram Mathematica (3)). **B.** A symmetrized snapshot of the structure of the Internet at the level of autonomous systems (4) ; layout obtained using the algorithm OpenOrd (5), optimized for the representation of large scale networks, of software Gephi (6)).

reason they have become fundamental in every area of Science and Technology – from Mathematics, to Physics, Social Sciences, Biology or Telecommunications, to cite a few.

Networks will be a central element to all the original results discussed in this thesis. Consequently, in this chapter we start with a brief introduction to the mathematical formalism of network theory, and then proceed to present some of the most emblematic network models and explore some of its topological properties. Theoretical elements presented in this chapter will be limited to the scope of this thesis; a more detailed exposition can be found, for instance, in (1, 2).

2.2 Quantifying Network Structure

In this thesis, we will consider only networks in which all links have the same weight or strength, in which there are no multi-links (more than one link connecting the same pair of nodes), no loops (links connecting a node to itself) and no directed links (if node i is connected to node j then j is also connected to i). The structure of a network can be mathematically represented in the framework of graph theory by its *adjacency*

matrix $\mathbf{A} = A_{ij}$, a square matrix whose elements are simply given by

$$A_{ij} = \begin{cases} 1 & \text{if there is a link between nodes } i \text{ and } j \\ 0 & \text{otherwise} \end{cases} \tag{2.1}$$

A simple example is represented in figure 2.2. With the above mentioned simplifying assumptions, the adjacency matrix is symmetric and all its diagonal elements are zero. Also note that computationally speaking, depending on the network size, storing network structure using its adjacency matrix can demand huge amounts of memory. Although in this thesis we restrict ourselves to networks with a few thousands of nodes at most, we use adjacency lists (a list of the neighbors of each node) to store information instead of adjacency matrices, so as to ensure fast processing and low memory consumption.

The number E of edges of a network with Z nodes is given by

$$E = \frac{1}{2}\sum_{i=1}^{Z} k_i, \tag{2.2}$$

where k_i represents the *degree* or *connectivity* of a node i – the number of nodes to which it is connected. In the equation above we count the links of each of the Z nodes of the network and therefore each link is counted twice, hence the factor $\frac{1}{2}$. Equivalently, we can have $E = \frac{Z\langle k\rangle}{2}$, where

$$\langle k\rangle = \frac{\sum_{i=1}^{Z} k_i}{Z} \tag{2.3}$$

is the *average degree* or *average connectivity* of a network, an important measure that will be used recurrently in the next chapters. The degree of a node is sometimes referred to as its *degree centrality*, to emphasize that it can be regarded as a measure of the importance of that node in the network. Of course, depending on the particular dynamical process being modeled in a network, the concept of importance can take different forms. Degree centrality is the simplest of such measures, counting the number of connections of each node, but despite its simplicity it can be elucidating: regarding the spread of a disease, rumor or idea on a (social) network, it is reasonable to think that individuals with more neighbors will simultaneously be more exposed to it and more able to infect or influence individuals.

One of the most important network properties is its *degree distribution* $D(k)$ – the frequency of nodes in the network exhibiting degree k or, equivalently, the probability

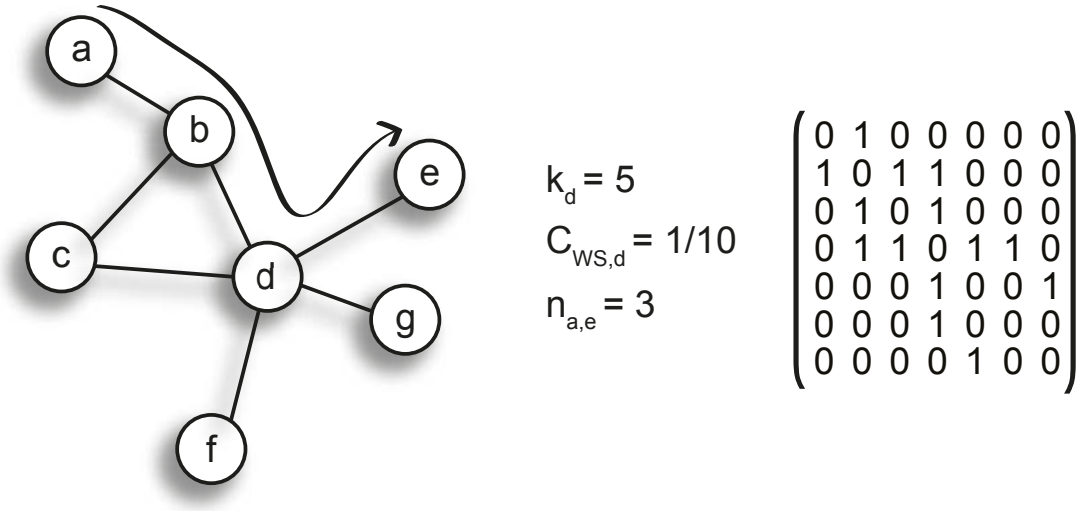

Figure 2.2: Quantifying network structure - We represent a simple network composed of 7 nodes, without multi-links, loops and directed links. The degree (k), clustering coefficient (C_{WS}) and shortest path length (n_{ij}) are given for specific nodes, and the corresponding adjacency matrix is given on the right.

that a node of an infinite network has degree k. The degree distribution $D(k)$ is given by

$$D(k) = \frac{n(k)}{Z} \tag{2.4}$$

where $n(k)$ is the number of nodes with degree k in a network of size Z. Alternatively, one can also define the *accumulated degree distribution*, $D_{acc}(k)$, which measures the frequency of nodes with degree higher or equal to k:

$$D_{acc}(k) = \frac{\sum_{i=k}^{k_{max}} D(k_i)}{Z} \tag{2.5}$$

where k_{max} represents the maximum degree observed in the network. An important distinction will be recurrent in the next chapters, between *homogeneous* and *heterogeneous* networks: in heterogeneous networks, different nodes may have different number of connections – some relevant examples, which will be discussed in more detail in the following sections, are represented on panels B and C of figure 2.3. As for homogeneous networks, all nodes have the same degree k, and therefore the degree distribution is simply a Kronecker delta in k, examples being lattices and ring networks, depicted in panel A of figure 2.3.

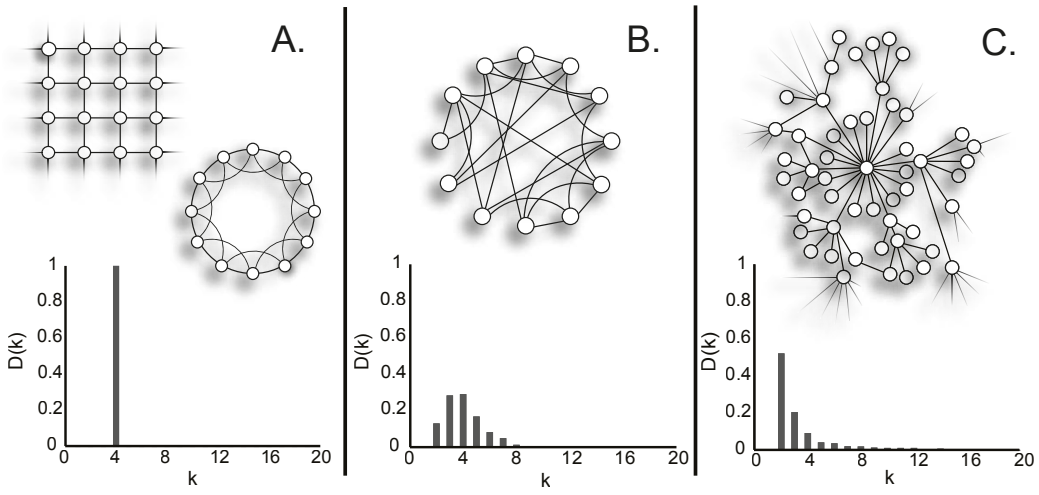

Figure 2.3: Network classes according to degree distribution - **A.** Lattices and ring regular networks are examples of homogeneous networks, in which all nodes have the same number of neighbors, and for which the degree distribution is simply $D(k) = \delta(i-k)$. **B.** The degree distribution of random networks follows a Poisson distribution. **C.** Scale-free networks are characterized by a marked degree of heterogeneity and small-world effects. Its degree distribution follows a power-law.

The average degree of the network, $\langle k \rangle$, is given by the first moment of the degree distribution $D(k)$, $\langle k \rangle = \sum_{k=1}^{k_{max}} kD(k)$,while the second moment allows us to compute the variance of k, σ_k^2:

$$\sigma_k^2 = \sum_{k=1}^{k_{max}} k^2 D\left(k\right) - \left[\sum_{k=1}^{k_{max}} kD\left(k\right)\right]^2 = \langle k^2 \rangle - \langle k \rangle \tag{2.6}$$

But $D(k)$ (or $D_{acc}(k)$) does not provide a complete description of a network – for a given network size Z, there can be several different networks for the same $D(k)$ and $D_{acc}(k)$. Other important topological quantities can be measured that further characterize a network and have been shown to have a significant impact on the dynamical processes modeled on networks. One of such properties is the propensity that two neighbors of a given node are themselves neighbors of each other. The *clustering coefficient*, as proposed in 1998 by Watts and Strogatz (7) in the context of the analysis of the *small-world effect* (see section 2.3), can be evaluated locally for each node. Suppose nodes j and m are both neighbors of node i. If j and m are also connected to each other themselves, we say that i, j and m form a *triangle*. The local clustering coefficient of

node i, $C_{WS}(i)$, measures in how many triangles i takes part, over all possible triangles that could be formed with i, that is,

$$C_{WS}(i) = \frac{\#\text{ pairs of neighbors of } i \text{ that are connected}}{\#\text{ pairs of neighbors of } i} \tag{2.7}$$

The global clustering coefficient of the network, C_{WS}, is simply an average over the clustering coefficient of all the nodes of the network:

$$C_{WS} = \frac{\sum_{i=1}^{Z} C_{WS}(i)}{Z} \tag{2.8}$$

Transitivity, Tr, on the other hand, was proposed in 2002 by Newman, Watts and Strogatz (8), and at the time was claimed to be equivalent to C_{WS}. Transitivity corresponds to counting how many triangles exist on the network over all the triangles that could be formed or, alternatively,

$$Tr = \frac{(\#\text{ triangles}) \text{ x } 6}{\#\text{ paths of length } 2} \tag{2.9}$$

where the factor 6 comes from the fact that each triangle is counted 6 times when counting the number of paths of length 2; if we assume that nodes i, j and m form a triangle, then we count the paths ijm, jmi, mij, mji, jim,imj. As first noted in (9, 10), these two quantities can in fact differ significantly when measured for the same network. In this thesis we chose to use C_{WS}. We are aware that in heterogeneous networks the values obtained for C_{WS} need to be taken into account with some cautions, as smaller degree nodes will contribute more to the global clustering coefficient, and for those nodes it is also easier to achieve higher local values of the clustering coefficient. However, this will not affect the conclusions extracted from our results.

Last but not least, there are other important topological concepts which are related with the distance between pairs of nodes in a network – measured as the number of edges that lie in a path between them. Of special interest is the determination of the *geodesic paths*, or *shortest paths*: denoting as n_{ij} the shortest distance between nodes i and j (that is, the geodesic path between i and j), the *average path length* L is simply an average over the shortest path lengths between all pairs of nodes in the network, that is,

$$L = \frac{1}{Z(Z-1)} \sum_{i,j \in Z, i \neq j} n_{ij} \tag{2.10}$$

The average path length L plays an important role in the dynamical processes modeled on networks – intuitively, the smaller this quantity the easier a trait will spread over

	Z	E	L	C_{WS}
Network of Jazz Bands (11)	198	2 742	2.235	0.617
Coauthorship in Network Science (12)	1 589	2 742	5.823	0.638
C. Elegans Neuronal Network (7, 13)	306	2 345	3.992	0.284
Power Grid (7, 14)	4 941	6 594	18.989	0.08
Marvel Social Network (15)	10 469	178 115	2.889	0.458
Internet	22 963	48 436	3.842	0.23

Table 2.1: Number of nodes (Z) and edges (E), average path length L and clustering coefficient C_{WS} for: **i)** a network of jazz musicians, **ii)** a network of co-authorships in Network Science (publications up to early 2006), **iii)** the C. Elegans neuronal network, **iv)** a power grid, **v)** the Marvel social network, and **vi)** the Internet, also graphically represented in panel B of Figure 2.1. Values for the topological properties obtained using the Gephi software (6).

a population located on the nodes of the network and inter-connected through the links. Conversely, we can also determine a network's *diameter*: the length of the longest geodesic path between any pair of nodes in the network for which a path actually exists. Note that without this last remark, the diameter of networks composed of disconnected components would be infinite. However, we will be only concerned with connected networks (in which there is at least one path between any pair of nodes). In figure 2.2 we illustrate the concepts of adjacency matrix, connectivity, local clustering coefficient and shortest path length for a simple and small network.

In table 2.1 we present the number of nodes (Z) and edges (E), the average path length (L) and the clustering coefficient (C_{WS}) of some real world networks from different nature, from power grids to neuronal networks and a network of jazz bands that performed between 1912 and 1940. Note that, to the exception of the power grid network, all exhibit a significant value of clustering coefficient and a small average path length. The Internet, the largest network analyzed in table 2.1, even exhibits an average path length smaller than the network of co-authorships in network science, despite the huge difference in the size of these two networks. These differences are related with how nodes and links are organized in each of the networks, that is, with the specific mechanisms that led to the growth of these networks. These mechanisms have of course an impact in the degree distribution of the networks – an aspect which

we will discuss in the following section.

2.3 The Regular, the Random, and the Small-World in between

Random networks were the first heterogeneous networks studied in detail. In general, we say that a network is *random* if, while certain characteristics are fixed (say, the number of nodes and/or links, the degree distribution, etc), the remaining ones are random. Therefore, the random network model is not defined by a single network but by an *ensemble* of all possible networks in which only the specified properties are fixed.

Although these networks were first studied by Solomonoff and Rapoport (16, 17), this model is often associated with the names of Paul Erdös and Alfréd Rényi, who published a series of papers in the late 1950s about a random network model in which the number of nodes Z is fixed and a link between any pair of nodes would be established with probability p. They have shown that, in the limit of large Z ($Z \to \infty$), the degree distribution of the network follows a Poisson distribution, that is,

$$D(k) \to \frac{(Zp)^k e^{-Zp}}{k!}, Zp = \text{const} \tag{2.11}$$

The rail network depicted in panel A of figure 2.1 is one example of a random network whose degree distribution, in the limit of large Z, would follow a Poisson distribution. The physical impossibility (and the inefficiency) of building hundreds of rails connecting the major roads causes the degree distribution of this network to be approximately Poisson; in this case, the majority of nodes (roads) have 5 to 6 connections (railways).

Almost half century before the **ER** model, on December 11, 1909, Gugliemo Marconi shared the Nobel Prize for Physics with Karl Ferdinand Braun "...in recognition of their contributions to the development of wireless telegraphy". The possibility of communicating across long distances was a revolutionary mark in human history, and the Nobel Prize reception speech of Marconi was visionary: he suggested that, on average, it required only 5.83 radio delay stations to communicate over the entire globe. To such a large and populated world, this sounded almost like science fiction. It is said that these declarations inspired the author Frigyes Karinthy to write the short story "Chains", 20 years later, in which he suggested that, as a consequence of technological advancements in communication and travel, human beings were becoming more and more inter-connected and the world was shrinking.

This *small-world effect* was first observed experimentally in a series of famous experiments undertaken in the 1960s by Stanley Milgram (18), an American social psychologist who was assistant professor in Harvard University at the time (he would be denied tenure shortly after, most probably because of his polemic experiments on obedience to authority (19)). Milgram sent several packages to randomly chosen individuals in the U.S. cities of Omaha and Wichita; the packages' final destination was a target individual located in Boston. The recipients of the package were only informed of his name and home city. Each recipient was asked to forward the package to this target individual or, if they did not know him (which was the most probable), to someone who they thought could know him. Of the 296 packages sent, only 64 reached their destination (one of the main criticisms to the conclusions taken from this experiment); of these, the average number of links separating sender from recipient was close to 6 – giving rise to the expression *6 degrees of separation*, although Milgram himself never used it.

Despite some relevant criticisms pointed to this experiment, more recently several other studies have reached similar qualitative conclusions, reinforcing the idea that we indeed live in a small world. In 2003 (20) Dodds, Muhamad and Watts replicated Milgram's experiment using electronic mail, and reached a similar average path length. Also, in 2008 a study of the Microsoft Messenger instant-messaging system revealed that the average chain of contacts between its users was of 6.6 people (21). The Erdös number (the same Erdös from the **ER** model), a humorous tribute to the prolific output of the Hungarian mathematician Paul Erdös which measures an individual's degree of separation from Erdös based on article co-authorship, is another example: the fact that approximately 90% of the mathematicians have an Erdös number smaller than 8 reveals the small world nature of the mathematical community.

In 1998, Watts and Strogatz (7) proposed an algorithm which consisted in rewiring each edge of a regular ring network with Z nodes and E edges, with a probability p_{rewire}, and monitored both the clustering coefficient C_{WS} and the average path length L of the resulting networks as a function of p_{rewire} (an example of the application of such algorithm is given in figure 2.4). The limiting cases $p_{rewire} \to 0$ ($p_{rewire} \to 1$) are characterized by large C_{WS} and L (low C_{WS} and L) respectively. The authors showed that there is a region of p_{rewire} values for which, while C_{WS} remains high, L is quite small due to the introduction of a few long range links that connect nodes that would otherwise be far apart.

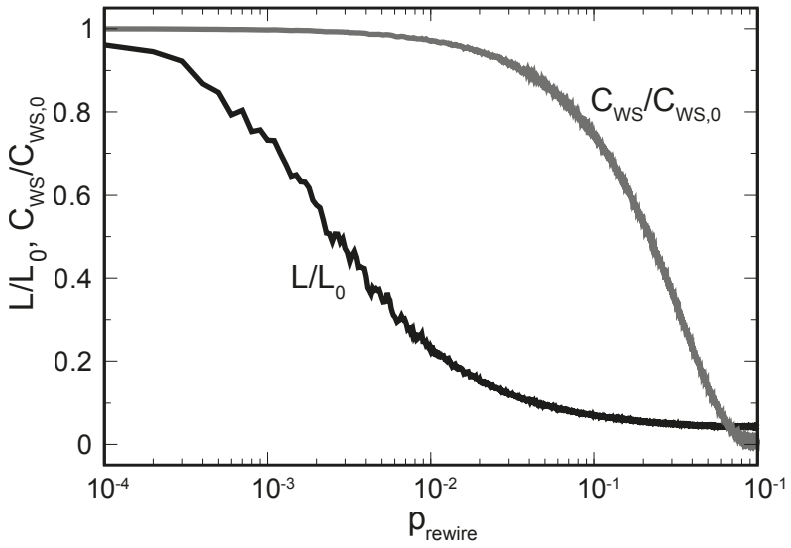

Figure 2.4: Normalized average path length L/L_0 and clustering coefficient $C_{ws}/C_{ws,0}$ for varying rewiring probability p_{rewire} in the Watts-Strogatz model - Data shown corresponds to an average over 50 realizations of the rewiring process described in the main text, starting from a ring regular network with size $Z = 10^3$, average connectivity $\langle k \rangle = 4$, average path length L_0 and clustering coefficient C_0.

Networks exhibiting these properties ($C_{WS} \gg C_{WS}^{random}$ and $L \gtrsim L_{random}$, where C_{WS}^{random} and L_{random} stand for the clustering coefficient and the average path length measured in a network with the same degree distribution and $p_{rewire} = 1$) are known as *small-world networks*, and the study by Watts and Strogatz (7) as well as other more recent studies (21, 22) have shown that many real world networks exhibit these characteristics, ranging from neuronal networks to power grids.

A slight departure from this method originates yet another type of networks, which are also frequently used in the literature. Also using as a starting point a regular ring network with Z nodes and E edges, this method (23) consists of randomly swapping the ends of *pairs* of links with probability p_{rewire}. This method ensures that the number of connections of each individual remains unaltered, contrary to the method adopted by Watts and Strogatz. When $p_{rewire} = 1$ in this case we obtain Homogeneous Random networks (**HoRand**), characterized by both small average path length and clustering coefficient.

2.4 Scale-Free networks

The 1990s were marked by still another advance in network theory: just one year after the work by Watts and Strogatz on small-world networks, in 1999, Barabási and Albert proposed a model (24) which, for the first time, did not simply *describe* other, novel (at that time), network characteristics, but succeeded in explaining *why* they exhibited those properties. On random networks, the only heterogeneous networks that had been studied so far, all nodes had approximately the same degree. However, in real networks we frequently encounter a small fraction of *hubs* – nodes with a large number of connections –, and a large number of nodes with just a few connections – the *leaves*. The algorithm for building *Scale-Free Barabási-Albert* networks (**BA**) starts from a small number m_0 of disconnected nodes, and new nodes and edges are added combining the following steps:

- *Growth*: In every fictitious time-step t, a new node is added to the network establishing links with m different nodes (with $m \leq m_0$) that were present in the network in time-step $t-1$. After t time-steps, the network has $Z = t + m_0$ nodes and mt edges.

- *Preferential Attachment*: each of the m links mentioned above is established preferentially to highly connected nodes; that is, the probability p that the new node connects with node i depends on its degree k_i, according to

$$p\left(k_i\right) = \frac{k_i^{\alpha}}{\sum_j k_j^{\alpha}} \tag{2.12}$$

  with $\alpha = 1.0$ (it has been shown, both by computer simulations (24) and analytically (25), that only linear preferential attachment ($\alpha = 1.0$) leads to a power-law degree distribution. Preferential attachment leads to the popular *rich get richer* effect: highly connected nodes will become more and more prone to receive more links.

When $\alpha = 0$ in equation 2.12, we have

$$p(k) = \frac{1}{m_0 + t - 1} = \text{const}, \tag{2.13}$$

that is, new links are established randomly, and the degree distribution of the emerging network does not follow a power-law but an exponential distribution. That is, when preferential attachment is replaced by random attachment the tail of the degree distribution of the emerging network with a given size will be much smaller than the

maximum connectivity observed in a scale-free **BA** network grown with the same parameters, and for this reason for exponential networks we cannot really refer to the existence of hubs (as nodes with a connectivity much larger than all the others in the network).

Many real world networks are conjectured to be scale-free, but results are many times still inconclusive. Very frequently, the data available corresponds to a sampling of the entire network, and from such sub-network it is not possible to affirm that the degree distribution of the total network is scale-free, even if the one of the sub-network is.

In order to determine analytically the expression for the degree distribution $D(k)$ and the exact scaling exponent γ of the power-law, Barabási and colleagues (24, 26) have adopted the continuum limit method, in which it is assumed that k is continuous[†]. In this way, the probability for preferential attachment $p\left(k_i\right)$, expressed in equation 2.12, can be interpreted as a continuous rate of change of k_i (from here on we will consider $\alpha = 1$ in equation 2.12). As Barabási and Albert show (24), the rate at which a node acquires links is given by

$$\frac{\partial k_i}{\partial t} = \frac{k_i}{2t} \Rightarrow k_i(t) = m\left(\frac{t}{t_i}\right)^{1/2} \tag{2.14}$$

From equation 2.14 Barabási and colleagues were able to determine analytically the value of γ:

$$D\left[k_i(t) < k\right] = D\left[t_i > \frac{m^2 t}{k^2}\right] = 1 - D\left(t_i \leq \frac{m^2 t}{k^2}\right) = 1 - \frac{m^2 t}{k^2}\left(t + m_0\right) \tag{2.15}$$

which for long time periods gives

$$D(k) = \frac{2m^2}{k^3}, \tag{2.16}$$

that is, $\gamma = 3$. Note that, in the limit of infinite size, in the continuum limit the average degree $\langle k \rangle$ is given by

$$\langle k \rangle = \int_{k_{min}}^{k_{max}} kD(k)dk = 2m^2 \int_{k_{min}}^{k_{max}} k^{1-\gamma}dk = 2m^2\left[\frac{k_{max}^{2-\gamma}}{2-\gamma} - \frac{k_{min}^{2-\gamma}}{2-\gamma}\right] \tag{2.17}$$

where k_{min} and k_{max} and the minimum and maximum degrees observed in the network, respectively. Given that $k_{max} \to \infty$ and $k_{min} = m$, we obtain

$$\langle k \rangle = -2m^{4-\gamma}\frac{1}{2-\gamma} \tag{2.18}$$

[†]Dorogovtsev, Mendes and Samukhin derive an exact solution to a more general network model, of which the Barabási-Albert model is a particular case, by solving the master equation of the system, in (27).

which for $\gamma = 3$ simplifies to

$$\langle k \rangle = 2m \tag{2.19}$$

The variance of the degree distribution $D(k)$ in the limit of infinite size is given by

$$\begin{aligned} \sigma_k^2 &= \int_{k_{min}}^{k_{max}} k^2 D(k) dk - \int_{k_{min}}^{k_{max}} k D(k) dk = \\ &= 2m^2 \left[\frac{k_{max}^{3-\gamma} - k_{min}^{3-\gamma}}{3-\gamma} - \frac{k_{max}^{2-\gamma} - k_{min}^{2-\gamma}}{2-\gamma} \right] \end{aligned} \tag{2.20}$$

Once again, given that $k_{max} \to \infty$ and $k_{min} = m$, we obtain

$$\sigma_k^2 = 2m^2 \left[\frac{1 - m^{3-\gamma}}{3-\gamma} + \frac{m}{2-\gamma} \right] \tag{2.21}$$

which diverges for $\gamma = 3$. That is, scale-free networks grown according to the Barabási-Albert model exhibit infinite variance. In fact, the term "scale-free" originates in the fact that these networks, contrary to the ones discussed so far, do not have a characteristic scale. While for previous networks we could state, for instance, that the average degree had a certain value plus or minus a given standard deviation, the same does not happen in this case because the second moment of its degree distribution, its variance, diverges. As such, the notion of average degree has to be taken with special care when considering these networks.

Another important property of scale-free networks is the very small average distance between any two nodes: it has been shown (28) that the average path length of (very large) random scale-free networks scales as $L \sim \ln \ln Z$, and because of such it is said that scale-free networks are *ultra-small* (in comparison to the small world networks discussed above, for which the average path length scales as $L \sim \ln Z$).

Despite its many advantages, this model also has some shortcomings. On the one hand, this model only accounts for degree distributions $D(k) \approx k^{-\gamma}$ with $\gamma = 3$, ignoring other possible γ values. In fact, several real networks whose degree distribution is candidate to be classified as scale-free have γ values in the interval $2 < \gamma < 3$. On the other hand, in the scale-free **BA** model newly added nodes never have the chance of obtaining a higher degree than those nodes that were already in the network by the time they arrived. This age effect does not always occur in real networks: for instance, Google appeared 7 years after the World Wide Web (WWW) was made public, and even so became the largest hub. To address these and other issues several other models were proposed in the literature shortly after the **BA** model. One of them is the *fitness model*

(29), also proposed by Barabási and colleagues: this consists of a slight modification of their original model to take into account the different capacity that nodes may have to acquire links. In this case, each newly added node i is attributed a fitness η_i extracted from a distribution $\rho(\eta)$. This η_i is constant in time and represents the capacity of an individual i to establish more or less links. As previously discussed for the **BA** model, each newly added node establishes m links to nodes already present in the network, and the probability of connecting to a node i is proportional to the product of his degree and fitness,

$$p_i = \frac{\eta_i k_i}{\sum_j \eta_j k_j} \tag{2.22}$$

With this generalized preferential attachment newer nodes in the network have now the possibility of surpassing older ones in the number of established connections. Also, with this generalization γ is now dependent of the fitness distribution chosen.

The models for growth of scale-free networks described so far lead naturally to a low clustering coefficient – the probability of building loops is very low. But real (social) networks usually exhibit sizable values of clustering, as shown in table 2.1. To account for this property, yet another model has been proposed in the literature, the *Minimal Model* (30): starting with a seed of m_0 fully connected nodes as described above, each newly added node establishes m (with $m \leq m_0$ and m even); each pair of links is established to the ends of a randomly chosen link already existing in the network. Although the preferential attachment mechanism is not imposed as a rule, it emerges naturally as in other duplication-based models (31, 32).

Table 2.2 compares the clustering coefficient C_{WS} and the average path length L of the network models discussed in this chapter, namely ring networks, lattices and homogeneous random (**HoRand**) as representative of homogeneous networks in which all nodes have the same number of connections; and small-world (**SW**), scale-free Barabási-Albert (**BA**), scale-free Minimal Model (**MM**) and exponential networks as representative of heterogeneous networks.

	Ring	**SW**	**HoRand**	**SF Bara**	**SF MM**	**Exponential**
C_{WS}	High	High	Low	Low	High	Low
L	High	Low	Low	Low	Low	Low

Table 2.2: Qualitative comparison of the values of clustering coefficient (C_{WS}) and average path length (L) of important homogeneous and heterogeneous network models that will be referred to later in this thesis.

3

Game Theory of Cooperation

3.1 Game Theory

Game Theory provides a convenient mathematical framework for the study of strategic situations, where the success of an individual depends on the decisions adopted by others. Individuals interact according to the rules of a given *game*, from which they obtain a certain gain (or loss) – denoted as *payoff* – dependent on the other players' actions – denoted as *strategies*. Individuals are typically assumed to be perfectly rational and aware of the structure of the game in which they participate. Rational individuals are expected to adopt strategies that maximize their payoff. Since everyone is equally rational, this can lead to situations in which there is a conflict between individual rationality and collective interest. These special cases are known as *social dilemmas*.

Game Theory established itself as a unique field in 1944, with the publication of (33); however, there are records of early discussions of game theoretical ideas that date as early as the beginning of the 1^{st} millennium. The Babylonian Talmud (0-500 AD) consisted of a compilation of Jewish laws and traditions; among these, the Talmud stated how the estate S of a recently deceased individual should be divided among the debts d_1, d_2 and d_3 that he had left to his three wives (with $d_1 + d_2 + d_3 > S$). An intuitive reasoning would suggest to distribute S equally among the three of them, or proportionally to the debts owed to each wife. However, the Talmud presented some different alternative solutions depending on the specific value of S which intrigued scholars for almost two millenia. In 1985 (34), Robert Aumann and Michael Mashler finally demonstrated that the intriguing solutions on the Talmud could be interpreted

as the anticipation of the modern game theory. More recent accounts of game theoretical elements comprise a letter written by James Waldergrave (a British ambassador in Austria and France) to Pierre-Remond de Montmort (a French mathematician) concerning the best strategical solution to the card game Le Her, which remounts to the 18^{th} century (35); as well as works by the French mathematicians Antoine Augustin Cournot (36) and Émile Borel (37).

In Physics, determining the motion of two point particles is conceptually a simple problem: depending on the system, either a classical or quantum mechanical approach leads to a correct and well-behaved analytical solution. Increasing the number of interacting particles increases the complexity of the problem [†]: several approximations can be adopted to restrict the motion of the particles (to a plane or a specific orbit, for instance), and often results can be obtained that rely on numerical simulations. But even in the restricted case the orbits are chaotic. Similarly, while games with $N = 2$ individuals have simple and well understood solutions, N-Person Games (with $N > 2$) lead to far more complex possibilities. We will address both cases on this thesis; furthermore, we will focus on games with only two, unconditional, strategies. In this chapter, we will start by over-viewing the main concepts of Game Theory: we discuss the fundamental concept of Nash equilibria (section 3.1.1), which allows us to compute the optimal strategies for rational individuals, and proceed to analyze the parameter space of symmetric 2-person social dilemmas with two strategies. Three social dilemmas can be defined: the *Prisoner's Dilemma*, the *Snowdrift Game*, and the *Stag-Hunt Game*. Subsequently, we address the issue of N-Person games, namely *Public Goods Games* (**PGGs**). Afterwards we shift our focus to Evolutionary Game Theory (**EGT**), introducing the concept of Evolutionary Stable Strategy (section 3.2.1) and analyzing the dynamics on both infinite (section 3.2.2) and finite (section 3.2.3) populations.

3.1.1 Nash Equilibria

In Game Theory, not only individuals are assumed to be perfectly rational, but each one is also aware that the others are rational and will adopt the same reasoning to evaluate

[†]Briefly, given that each particle is represented by six variables (three spatial and three momentum components), we face a $6N$ variables problem, where N stands for the number of particles. There is a total of ten independent first integrals (for the center of mass, linear momentum, angular momentum and energy), which for $N \geq 3$ is insufficient to reduce the number of variables in a way that the equation obtained could be solved directly.

what is their best move. The concept of *Nash equilibrium*, introduced by the American mathematician John Nash (38) (who was awarded the Nobel Prize for Economics in 1994 for his work on this subject) and of fundamental importance in Game Theory, states that a set of strategies is said to be a Nash equilibrium if no player can increase his/her payoff of an N-Person game by unilaterally changing his/her strategy. That is, each strategy in a Nash equilibrium is a best response to all the $N-1$ others in that equilibrium. Formalizing this concept for 2-person games with 2 strategies (a generalization for a higher number of strategies and/or players is straightforward), if player i (j) adopts strategy s_i (s_j), the solution $\left(s_i^*, s_j^*\right)$ is said to be a (weak) Nash equilibrium whenever

$$\Pi(s_i^*, s_j^*) \geq \Pi(s_i, s_j^*) \geq \Pi(s_i^*, s_j); \text{ with } s_i^* \neq s_i \text{ and } s_j^* \neq s_j \tag{3.1}$$

where $\Pi\left(s_i, s_j\right)$ represents the payoff obtained by individual i with strategy s_i when playing with individual j with strategy s_j. The weak Nash equilibrium becomes strict whenever the inequality in equation 3.1 becomes strict. Note that this concept is applicable both to pure strategies – in which an individual always adopts the same action – and to mixed strategies – in which individuals opt probabilistically among the set of available pure strategies. John Nash proved that, if we allow for individuals to adopt mixed strategies, then any game with a finite number of players and a finite set of pure strategies has at least one Nash equilibrium.

3.1.2 2-person Games

We consider games in which individuals may adopt either one of two possible pure strategies: to cooperate (***C***) or to defect (***D***) with all of their opponents. A cooperator is an individual who pays a certain cost, c, to provide a certain benefit, b, to another individual (with $b > c$). The payoffs for 2-person games with such strategies can be organized in the payoff matrix

$$\begin{array}{c} \\ \boldsymbol{C} \\ \boldsymbol{D} \end{array} \begin{array}{c} \begin{array}{cc} \boldsymbol{C} & \boldsymbol{D} \end{array} \\ \begin{pmatrix} (R,R) & (S,T) \\ (T,S) & (P,P) \end{pmatrix} \end{array} \tag{3.2}$$

The first element on each entry of the above payoff matrix represents the payoff obtained by the first player (the row player), while the second element stands for the payoff of the second player (the column player). The payoff matrix above represents a

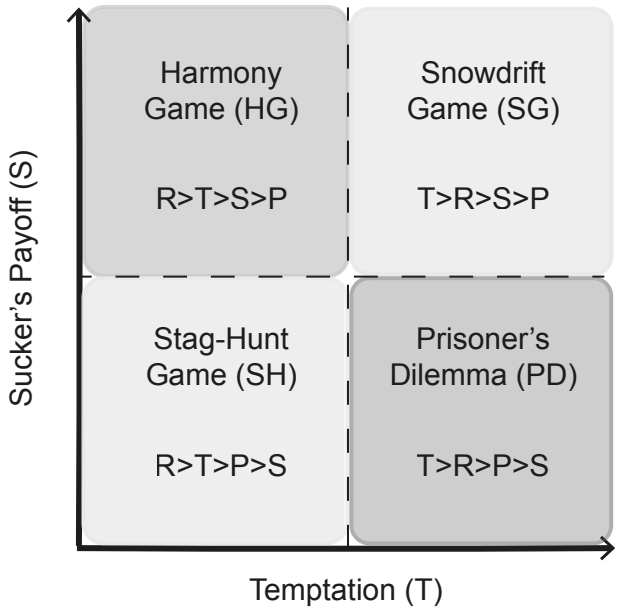

Figure 3.1: Parameter space for 2-Person games with 2 strategies. - Of the four regimes identified, all but the Harmony Game classify as social dilemmas.

symmetric game, for which the order of the players that adopt each strategy does not matter, and so we can adopt the simpler representation

$$\begin{array}{c} \\ \boldsymbol{C} \\ \boldsymbol{D} \end{array} \begin{array}{c} \begin{array}{cc} \boldsymbol{C} & \boldsymbol{D} \end{array} \\ \begin{pmatrix} R & S \\ T & P \end{pmatrix} \end{array} \tag{3.3}$$

in which we represent only the payoff of the row player. Mutual cooperation is awarded with a Reward (R), and mutual defection with a Punishment (P); if individuals opt for opposite strategies, the defector falls into the Temptation (T) to defect, while the cooperator receives the Sucker's Payoff (S). Assuming that $R > P$ we can define four different regimes according to the relative values of R, S, T and P, identified in figure 3.1. The *Harmony Game* (represented on the upper left panel) corresponds to a special case in which the only rational decision is to cooperate regardless of the partner's choice, and for that reason it is not classified as a social dilemma, since both players opting for $\boldsymbol{C}$ leads to the maximum collective return R instead of the alternative P. The remaining three are:

- **Prisoner's Dilemma (PD) ($T > R > P > S$)**
  This dilemma was originally introduced by Merrill Flood and Mervil Desher as

a model of cooperation and conflict in 1950, when working at RAND Corporation (**R**esearch **AN**d **D**evelopment), a non-profit research organization originally funded to work for the United States armed forces. The *Prisoner's Dilemma* denomination came shortly after, when Albert Tucker, a Canadian mathematician and colleague of theirs, devised a suitable metaphor involving prisoners and prison sentences. Two alleged criminals, recently caught by the police who does not have sufficient proofs to take them to court, are interrogated separately and each one is offered a deal: to testify against his partner and, if he remains silent, go free while the other receives the full charge, 1 year. If both remain silent, each serve 1 month in jail. While if both betray each other, each serves 3 months in jail. None of them can know what the other will choose, they decide simultaneously and independently. However, regardless of what the other decides, each individual gets a lighter conviction by betraying the other (by defecting, if we identify cooperation with remaining silent and not testifying against their partner). Alternatively, we can adopt a parametrization in terms of costs (c) and benefits (b), and setting $R = 1$ and $P = 0$ we obtain the payoff matrix

$$\begin{array}{c} \\ \boldsymbol{C} \\ \boldsymbol{D} \end{array} \begin{array}{c} \begin{array}{cc} \boldsymbol{C} & \boldsymbol{D} \end{array} \\ \begin{pmatrix} b-c & -c \\ b & 0 \end{pmatrix} \end{array}, b > c > 0 \tag{3.4}$$

leaving only one free parameter ($b-c=1$). Note, however, that this parametrization represents a special case: other values for R, S, T and P are possible as long as the inequality $T > R > P > S$ holds [†]. This same remark is valid for the payoff matrices 3.5 and 3.6 given that the corresponding inequalities are respected. The (***D,D***) pair is the only Nash equilibrium of this game, and because of this the Prisoner's Dilemma represents the essence of the conflict between individual and collective interest – although a rational player would always choose to defect regardless of his partner's option, both individuals would be better off by cooperating.

- **Snowdrift Game (SG) (**$T > R > S > P$**)**
  This game has been used in the study of the problem of evolution of coopera-

[†]If the players play the Prisoner's Dilemma more than once with each other, and are able to remember their past actions, one must also ensure that $2R > T + S$, to prevent that the individuals can obtain a greater reward from alternating between (***C***, ***D***) and (***D***, ***C***), than by mutual cooperation (***C***, ***C***). Iterated games will be further explored in section 3.3.2

tion since 1986, by the English economist Robert Sugden (39). However, the basic concepts that underly its formulation date back from the 1950s, when it was known as the *Chicken game* – from the 1955 film *Rebel without a cause*, in which two youths drive their cars towards a cliff: the one who first turns away is "chicken" but if none of them turns away they both end up dying (40). Also, in 1973, John Maynard Smith and George Price introduced this game in the study of the logic of animal conflicts, under the name of *Hawk-Dove game* (41). In its original formulation, two individuals are driving on a road which gets blocked by a snowdrift. To proceed their journey home (the benefit b), the snow must be removed (incurring in a cost c), which will happen if at least one of the drivers decides to cooperate and shovel the snow. Of course, if both shovel (cooperate) each one spends only half of the workload of shoveling the snow. This metaphor can be translated in the payoff matrix

$$\begin{array}{c} \\ \boldsymbol{C} \\ \boldsymbol{D} \end{array} \begin{array}{c} \begin{array}{cc} \boldsymbol{C} & \boldsymbol{D} \end{array} \\ \begin{pmatrix} b - c/2 & b - c \\ b & 0 \end{pmatrix} \end{array}, b > c > 0 \tag{3.5}$$

The pairs (***C***, ***D***) and (***D***, ***C***) are both Nash equilibria – intuitively, each individual is better off if the other one invests all the effort necessary for shoveling the snow without investing anything himself. A third Nash equilibrium exists if one considers mixed strategies, but in this thesis we will only study situations involving pure strategies.

- **Stag-Hunt Game (SH) (**$R > T > P > S$**)**
  The *Stag-Hunt* denomination comes from a metaphor described by Jean-Jacques Rousseau in (42, 43) concerning two individuals that go on a hunt. Each of them has two options: to hunt a stag, for which he needs the collaboration of his partner; or to hunt a hare, that he can hunt by himself (but is worth less than a stag). If, as a simplification, we assume that hunting a stag provides a reward b and hunting a hare simply provides a reward $\frac{b}{2}$, this metaphor can be translated by the payoff matrix

$$\begin{array}{c} \\ \boldsymbol{C} \\ \boldsymbol{D} \end{array} \begin{array}{c} \begin{array}{cc} \boldsymbol{C} & \boldsymbol{D} \end{array} \\ \begin{pmatrix} b - c & -c \\ b/2 - c & 0 \end{pmatrix} \end{array}, b > c > 0 \tag{3.6}$$

  where c represents the cost associated with the hunt. Of course, as in the previous cases, the values for each of the entries of the payoff matrix above can be any as

long as the inequalities $R > T > P > S$ are respected; the payoff matrix 3.6 corresponds to a simplification frequently found in the literature.

This dilemma, also known as *Coordination Game*, *Assurance Game* and *Trust Dilemma*, has two (pure strategy) Nash equilibria, (***C***, ***C***) and (***D***, ***D***).

3.1.3 *N*-Person games

Many real-life situations, however, involve decisions derived from groups composed by more than two individuals. Group hunting, the payment of taxes, the participation in open source projects, trying to solve the problem of global warming – are just a few of the many examples that can be given. This type of collective action problems – which abound, not only in humans (44, 45, 46), but also in other upper primates (47, 48) – is best described in the framework of N-Person games (44, 49, 50, 51, 52, 53), which provide a richer spectrum of evolutionary possibilities, but are also more complex to analyze, as recognized by the evolutionary biologist W. D. Hamilton:

> "*The theory of many person games may seem to stand to that of two-person games in relation of sea-sickness to a headache.*"
>
> – W. D. Hamilton in "Innate Social Aptitudes of Man: an Approach from Evolutionary Genetics" (1975)

There are many types of N-Person games (53). *Public Goods Games* (**PGGs**) are a special case of N-Person games. **PGGs** concern the provision of a certain benefit that will be available to all individuals of the group (48, 54) and which depends on how many cooperate towards its attainment.

A *public good* is a certain resource, a benefit, that is both *non-excludable* and *non-rival*: all can benefit from it, irrespectively of having contributed to its provision or not; and one individual benefiting from the public good does not exclude another from obtaining the same benefit.

Another special class of N-Person games is the *Tragedy of the Commons*, which owes this denomination to the homonym article by Garrett Hardin in 1968 (44). The Tragedy of the Commons addresses the problem of how a given common good should be explored by a group of individuals – each one obtains a benefit by using that common good, but if all use it to its maximum potential it will be overexploited and no one will be able to benefit from it anymore. One can benefit from public parks or public television without paying taxes (the most profitable situation), but if all adopt the same behavior that public service can no longer be provided – the result is the tragedy of the

commons. Note that on this case we are referring to common goods (that are available to all individuals), but these can be exhausted, that is, an individual benefiting from it can affect another individual benefiting or not (if not sufficient people pay the necessary taxes for the maintenance of public television and yet benefit with it, it cannot be further maintained). On this thesis we will focus solely on **PGGs**.

The generalization from 2-Person to N-Person games adds some new possible scenarios. While on 2-Person Games an individual is always aware of his partners' choice (to cooperate or to defect) after payoffs are attributed, in the latter it may happen that actions are not disclosed, and as such, defectors can exploit the public good without being noticed. Also, while in dyadic interactions the costs of the defection of an individual relies completely on his partner, on multi-person interactions that impact is shared through all the members of the group.

The mapping of the contributions of ***C****s* onto the public good is given by a *production function*; that is, a production function establishes the relationship between the level of contributions and the level of public good produced. Some examples of production functions are depicted in figure 3.2. Note that the production function can overlay with the fitness of a given strategy as a function of the number of cooperators in the group, but that is not always the case. In this thesis we will focus on the N-Person generalization of the Prisoner's Dilemma (**NPD**) and the N-Person generalization of the Snowdrift Game (**NSG**). The **NSG** is characterized by a benefit that once obtained is fixed, and so the production function corresponds to a step-function (Figure 3.2D). As for the **NPD**, it is characterized by a benefit proportional to the number of contributors – we will consider a linear production function (Figure 3.2A), but accelerating (Figure 3.2B, also known as increasing returns) or deccelerating (Figure 3.2C, also known as decreasing returns) production functions would also be possible choices. In the literature, most attention has been dedicated to collective social dilemmas characterized by linear production functions; however, it has been shown that in the real world non-linear dilemmas are more common, by far, than linear ones (55, 56, 57, 58). Importantly, the evolutionary dynamics of an N-Person social dilemma are significantly altered depending on the choice of the production function, as will be shown in chapters 4 and 5: one may pass from a scenario of ***D***-dominance, for a linear production function, to a scenario of coexistence of cooperators and defectors, depending on the particular details of a non-linear production function (59, 60).

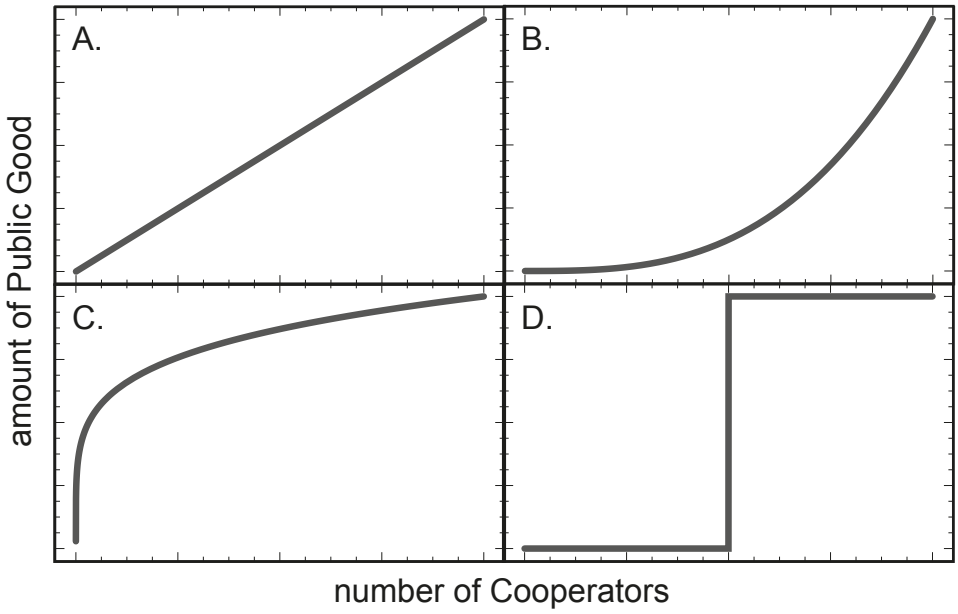

Figure 3.2: Production functions in *N*-person games - Production functions establish the relationship between the level of contributions and the level of public good obtained. We schematize the following examples of production functions: **A.** linear, in which all contributions have the same impact, **B.** accelerating, in which initial contributions have little effect but increasing contributions lead to increasing outcomes, **C.** decelerating, in which initial contributions have the greatest effect, and **D.** step function, in which the public good is only obtained after a certain minimum number of contributions is reached. Figure based on the one in (48), page 8.

3.2 Evolutionary Game Theory

Game Theory provides convenient tools to analyze strategic situations in which $N \geq 2$ perfectly rational individuals interact. Evolutionary Game Theory (**EGT**), which has its origins in the pioneer work of John Maynard Smith and George R. Price (41, 61) (who applied the notions of game theory to biology) is a dynamical description, contrary to the static description of Game Theory: it expands the description of Game Theory to a population, where the individuals interact according to the rules of the games previously described. The payoff the individuals obtain from all interactions is translated onto *individual fitness*. This, in a biological context, is associated with reproductive success: more successful individuals can, by reproduction, spread their strategy, which will increase its frequency in the population. Besides the biological interpretation, one

may also think in terms of cultural evolution in populations: more successful ideas or behaviors – *memes* – will be more imitated and consequently will spread in the population.

In the following sections, we will start by introducing the concept of Evolutionary Stable Strategy (**ESS**), an analogue of the Nash equilibrium for the Evolutionary Game Theory, and present the mathematical formalism for both infinite and finite well-mixed (**WM**) populations[†], for the simpler case of 2-person games. Chapters 4 and 5 will comprise the mathematical formalism for the corresponding N-person games.

3.2.1 Nash equilibrium revisited – ESS

The concept of Evolutionary Stable Strategy (**ESS**) was introduced in 1973 by John Maynard Smith and George R. Price (41) (however, the peer-reviewing of this paper took so long that John Maynard Smith decided to introduce this concept in an essay in (62) in 1972). A more detailed analysis was presented the year after in (63). While the concept of Nash equilibrium emerges as the consequence of individuals' perfect rationality and complete knowledge of the structure of the game in which they are participating, the motivation for the concept of **ESS** is quite different: it is a result of the application of the concepts of Game Theory to Biology, and players are assumed to not have any saying in their strategy, because strategies are interpreted as being inherited from one generation to the next, and hence an individual will play unconditionally his strategy against any opponent. Informally, a strategy is said to be **ESS** if, when adopted by a population, it cannot be invaded by another strategy, initially rare. Formalizing this concept mathematically, a strategy s^* is an **ESS** if it obeys either one of the following conditions,

$$\Pi\left(s^*, s^*\right) > \Pi\left(s, s^*\right) \tag{3.7a}$$

$$\Pi\left(s^*, s^*\right) = \Pi\left(s, s^*\right) \text{ and } \Pi\left(s^*, s\right) > \Pi\left(s, s\right) \tag{3.7b}$$

In equations 3.7, $\Pi\left(s^*, s\right)$ represents the payoff obtained by the individual adopting strategy s^* (the evolutionary stable strategy) when he plays with an individual adopting strategy s (where s^* and s represent distinct strategies).

[†]That is, populations in which each and every individual has the same probability of interacting with every other in the population; we may also refer to this class of populations as *structureless*, in relation with the absence of structure in the contacts between individuals.

Note that the first **ESS** condition corresponds to the definition of strict Nash equilibrium presented in equation 3.1 for the strict inequality. The second condition can be understood as follows: if $\Pi(s^*, s^*) = \Pi(s, s^*)$, then strategy s could invade the population of s^* players by random drift. But $\Pi(s^*, s) > \Pi(s, s)$ ensures that s^* players continue to be advantageous when playing against partners adopting s and hence the population will not be invaded.

Note that, while the Nash equilibrium corresponds to a set of strategies (the strategies of each of the N individuals playing the game), an **ESS** is a single strategy. Also, while all **ESS**s correspond to Nash equilibria, the reciprocal is not true: not all Nash equilibria are **ESSs**. For instance, when two individuals play a Snowdrift Game (section 3.1.2), both $(\boldsymbol{C}, \boldsymbol{D})$ and $(\boldsymbol{D}, \boldsymbol{C})$ are Nash equilibria. However, since in the Snowdrift game we have $T > R > S > P$, no pure strategy can be an **ESS**; that is, if all the population adopted cooperation (defection) as strategy, an individual that switched to defection (cooperation) would obtain a higher fitness than the rest of the individuals in the population and would be able to spread his strategy.

3.2.2 Infinite, Well-Mixed Populations

As previously stated, we consider two types of pure strategies: individuals that always *cooperate* (**C**), and individuals that always *defect* (**D**). Let us denote the fraction of ***C*s** (***D*s**) in the population by x_C (x_D). Individuals interact following the payoff matrix 3.3, and we assume that their average payoff reflects their fitness, associated with reproductive or social success. The fitness f_C (f_D) of a $\boldsymbol{C}$ ($\boldsymbol{D}$) can therefore be written as

$$f_C(x_C, x_D) = x_C R + x_D S \tag{3.8a}$$

$$f_D(x_C, x_D) = x_C T + x_D P \tag{3.8b}$$

That is, the fitness of each individual is frequency-dependent. The evolution of strategies is modeled by the *replicator dynamics* (64, 65): a strategy spreads in the population when its fitness is larger than the average fitness of the population. This is translated into the following set of ordinary differential equations

$$\dot{x_C} = x_C \left(f_C(x_C, x_D) - \bar{f}(x_C, x_D) \right) \tag{3.9a}$$

$$\dot{x_D} = x_D \left(f_D(x_C, x_D) - \bar{f}(x_C, x_D) \right) \tag{3.9b}$$

that describe how the frequency of individuals adopting each strategy varies over time, where $\bar{f}(x_C, x_D) = x_C f_C(x_C, x_D) + x_D f_D(x_C, x_D)$ represents the average fitness of the population. Noting that $1 - x_D = x_C \equiv x$, this set can be simplified into the single ordinary differential equation

$$\dot{x} = x(1-x)(f_C(x) - f_D(x)) \tag{3.10}$$

We shall also refer to the right-hand side of the replicator equation 3.10 by *gradient of selection* $g(x) \equiv \dot{x} = x(1-x)(f_C(x) - f_D(x))$. The sign of $\dot{x}$, which is solely determined by the fitness difference $f_C(x) - f_D(x)$, indicates the direction of selection: whenever $\dot{x} > 0$ ($\dot{x} < 0$) selection favors cooperation (defection). In a biological context, the replicator equation 3.10 translates the idea that individuals reproduce proportional to their fitness. In a cultural context it may be interpreted as ideas or behaviors with higher fitness being more imitated. Equation 3.10 has two trivial equilibria, $x^*_{triv} = 0$ and $x^*_{triv} = 1$, but depending on the details of the game one further interior equilibria $x^*_{int} \in]0, 1[$ can exist,

$$x^*_{int} = \frac{P - S}{R - S - T + P}. \tag{3.11}$$

Depending on the values of R, S, T and P, one can distinguish four evolutionary scenarios, schematized in Figure 3.3 according to the profile of the gradient of selection $g(x)$:

- ***C*-dominance (panel A)**: It is characterized by $R > T$ and $S > P$ - cooperators always have a higher fitness regardless of their initial fraction on the population, and so the population will evolve towards the fully cooperative state. As discussed for the Harmony Game, this is the best scenario possible for cooperators, and does not pose a social dilemma. No interior root exists.

- **Coexistence (panel B)**: In this case $T > R$ and $S > P$, the interior fixed point x^*_{int} is stable, while the trivial solutions are unstable. The direction of selection depends on the initial fraction x of cooperators in the population: for $x < x^*_{int}$ ($x > x^*_{int}$) the fraction of cooperators increases (decreases), as the population evolves towards the stable interior root.

- **Coordination (panel C)**: In opposition to the coexistence scenario, coordination is characterized by $R > T$ and $P > S$ – the interior root x^*_{int} is unstable, and selection will act in order to push the fraction of cooperators towards one of the monomorphic states depending on the initial composition of the population.

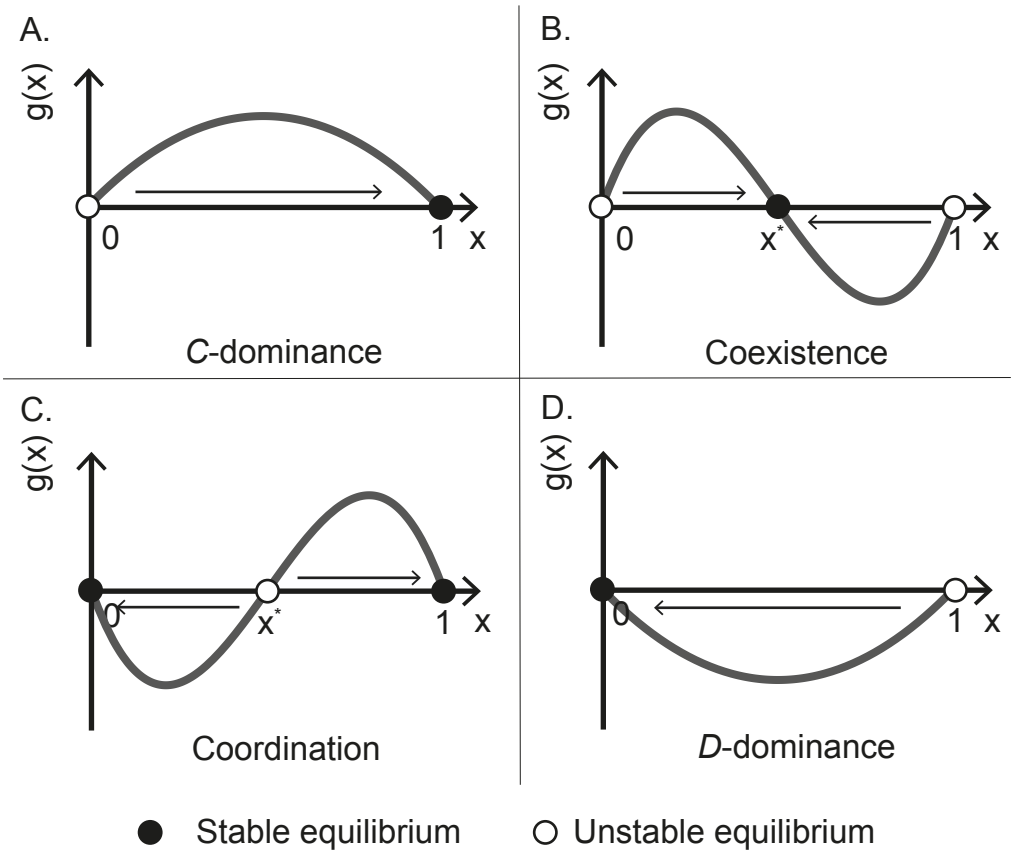

Figure 3.3: Possible evolutionary scenarios for 2-person games with 2 strategies - Panels **A.** to **D.** show typical shapes of the replicator equation for 2-person games with 2 strategies, which depends on the fitness difference $f_C(x) - f_D(x)$. Solid (open) circles represent stable (unstable) equilibria; arrows indicate direction of selection.

- ***D*-dominance (panel D)**: Opposite to the ***C***-dominance scenario, it is characterized by $T > R$ and $P > S$ – defectors always have a higher fitness than the cooperators regardless of the initial composition of the population. No interior root exists: for the trivial solutions, $x^*_{triv} = 0$ is a stable fixed point, while $x^*_{triv} = 1$ is unstable.

3.2.3 Finite, Well-Mixed Populations

Assuming that a population is infinite is always an approximation, and in many cases a very unrealistic one. To describe the evolutionary dynamics of the propagation of

strategies in a finite population, it is necessary to take into account stochastic effects. All finite populations are subject to fluctuations, which cannot be described in a deterministic formulation. The assumption behind the replicator equation 3.10, $\dot{x} = x(1-x)\left(f_C(x) - f_D(x)\right)$, is either that individuals reproduce at a rate proportional to their fitness (in the biological context), or that individuals imitate actions or behaviors that exhibit a higher fitness, with a probability proportional to the fitness difference (in the cultural context). The detailed way in which we model these assumptions in finite populations (which we will call *update methods*) can have decisive consequences in the evolutionary dynamics of the population, even though in the limit of an infinitely large population those detailed update methods can converge to the replicator dynamics previously discussed.

In the next sections, we will adopt the formulation of stochastic processes for the modeling of evolution of cooperation in finite populations. In particular, we will adopt the formalism of *Markov processes*, processes in which the state of the system at time $t+1$ only depends of its state at time t (and not of all the previous history of the system starting from its initial configuration). Afterwards, we will discuss some detailed update methods that in the limit of infinitely large populations lead to the replicator dynamics (but which exhibit very distinct dynamics for finite populations), and we will end by discussing some mechanisms that promote the emergence and evolution of cooperation.

3.2.3.1 Markov Processes

EGT in finite populations was pioneered by Young (66) and by Kandori, Mailath and Rob (67).The fraction of ***C*s** ceases to be a continuous variable, and varies in steps of j/Z, where j represents the number of ***C*s** in the population and Z the population size. Fitnesses are now given by

$$f_C(j) = \frac{j-1}{Z-1}R + \frac{Z-j}{Z-1}S \tag{3.12a}$$

$$f_D(j) = \frac{j}{Z-1}T + \frac{Z-j-1}{Z-1}P \tag{3.12b}$$

where we exclude self-interactions[†]. We will assume that evolution occurs in the absence of mutations, and that it satisfies the *Markov property*, that is, it is *memoryless*: the state of the system at time $t+1$ only depends of its state at time t, and not on past states. Formally, a stochastic process is identified as a *Markov process* if, for any a successive times (that is, $t_1 < t_2 < ... < t_a$), it obeys the property (68)

$$P\left(x_a, t_a | x_1, t_1; x_2, t_2; ...; x_{a-1}, , t_{a-1}\right) = P\left(x_a, t_a | x_{a-1}, t_{a-1}\right) \tag{3.13}$$

where x_a represents the state of the system at instant t_a. That is, the probability of encountering the system in state x_a at time t_a does not depend on the whole history of the system, $P\left(x_a, t_a | x_1, t_1; x_2, t_2; ...; x_{a-1}, t_{a-1}\right)$, but only on the previous state x_{a-1} at time t_{a-1}.

Once we consider evolutionary dynamics on finite populations, it is necessary to adopt an update mechanism that models the transitions between different states of the population. We will represent by $\mathcal{T}^{+n}(j)$ $(\mathcal{T}^{-n}(j))$ the probability that at time $t+1$ the population will have $j+n$ $(j-n)$ Cooperators, given that it has j Cooperators at time t. All transition probabilities can be generally summarized in the stochastic transition matrix

$$\boldsymbol{\mathcal{T}} = \begin{bmatrix} \mathcal{T}^{0}(0) & \mathcal{T}^{+1}(0) & \mathcal{T}^{+2}(0) & \cdots & \mathcal{T}^{+Z}(0) \\ \mathcal{T}^{-1}(1) & \mathcal{T}^{0}(1) & \mathcal{T}^{+1}(1) & \cdots & \mathcal{T}^{+Z}(1) \\ \mathcal{T}^{-2}(2) & \mathcal{T}^{-1}(2) & \mathcal{T}^{0}(2) & \cdots & \mathcal{T}^{+Z}(2) \\ \vdots & \vdots & \vdots & \ddots & \vdots \\ \mathcal{T}^{-Z}(Z) & \mathcal{T}^{-(Z-1)}(Z) & \mathcal{T}^{-(Z-2)}(Z) & \cdots & \mathcal{T}^{0}(Z) \end{bmatrix} \tag{3.14}$$

From the transition matrix we can compute the *stationary distribution* – the fraction of time the system spends on each state, or alternatively the probability of encountering the system in state j at any time. The stationary distribution $\boldsymbol{\pi}$ can be defined as a vector which is not altered by the application of the transition matrix $\boldsymbol{\mathcal{T}}$, that is, it satisfies the equation $\boldsymbol{\pi}\boldsymbol{\mathcal{T}} = \boldsymbol{\pi}$. In other words, $\boldsymbol{\pi}$ corresponds to the left eigenvector of the transition matrix $\boldsymbol{\mathcal{T}}$ with eigenvalue 1 (69) (which is the highest eigenvalue, since $\boldsymbol{\mathcal{T}}$ is a stochastic matrix).[‡]

[†]Since we assume $R > P$, self-interactions would introduce a built-in advantage for cooperators. Self-interactions are also unrealistic in most real world scenarios, and for these reasons we opt to exclude them in this thesis.

[‡]If $\boldsymbol{\mathcal{T}}$ is a symmetric matrix, left and right eigenvectors are equal; however, $\boldsymbol{\mathcal{T}}$ will not be symmetrical for any of the update methods considered here.

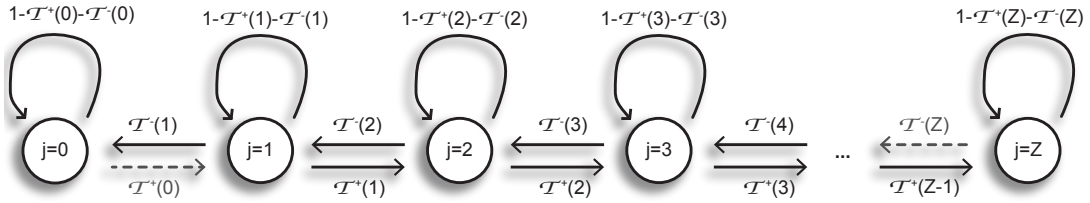

Figure 3.4: Markovian birth-death process - Markov chain describing the evolutionary dynamics of a birth-death process in a population with j cooperators. Dashed curves represent transitions only possible for innovative update methods. For non-innovative update methods, $j = 0$ and $j = Z$ represent absorbing states.

In the transition matrix 3.14 one assumes that all transitions from any state to any other state are possible from t to $t + 1$. For that to occur, one may for instance consider that all individuals may revise their strategy in each instant. A well-known example is the *Wright-Fisher process*, with roots in population genetics (70, 71). In each generation (1 generation = Z strategy revisions) each individual reproduces proportionally to his/her fitness, and from the offspring pool Z individuals are randomly chosen to form the next generation.

The analytical study of the general matrix 3.14 is very complex. For the sake of simplicity we adopt a *birth-death process*: at each time-step in discrete time only one individual may revise his/her strategy. In this case, the transition matrix $\mathfrak{T}$ is tri-diagonal: it is only possible to vary the number of cooperators by one, $\mathfrak{T}^{\pm 1}(j)$ (to simplify notation, from here on we assume $\mathfrak{T}^{\pm 1}(j) \equiv \mathfrak{T}^{\pm}(j)$). The Markov chain schematized in figure 3.4 represents the possible transitions for birth-death processes, in a population of size Z with j cooperators. Depending on the details of the update method adopted, individuals may either be able to adopt a strategy if it has already been adopted by one of the members of the population (*non-innovative* update methods), or have access to the whole set of strategies allowed by the rules of the game even if no individual in the population is currently adopting one of them (*innovative* update methods). In the latter case, the dashed transitions signaled in figure 3.4 can happen (that is, their probability can be different from zero): when the population is in a monomorphic state (either all ***Cs*** or all ***Ds***) an individual revising his strategy can change to a different one. Some examples of innovative update methods are the *Best-Response* (72, 73) and the *Reinforcement Learning* (74). For non-innovative update methods, the dashed transitions shown in figure 3.4 cannot occur, and this class of update methods will be the focus of our research for the remainder of this thesis.

For non-innovative update mechanisms, $j = 0$ and $j = Z$ are *absorbing states*, that is, states that when reached it is impossible to move out. In these cases, it may be relevant to compute the *fixation probability* ϕ_j: the probability that j cooperators invade a population in which the remaining $Z - j$ individuals are defectors. It is given by

$$\phi_j = \frac{\sum_{i=0}^{j-1} \prod_{m=1}^{i} \lambda_m}{\sum_{i=0}^{Z-1} \prod_{m=1}^{i} \lambda_m} \tag{3.15}$$

where $\lambda_j = \mathcal{T}^-(j)/\mathcal{T}^+(j)$. The scenario $\mathcal{T}^-(j) = \mathcal{T}^+(j)$ corresponds to *neutral selection*, for which $\lambda_j = 1$ and the fixation probability is simply $\phi_j = j/Z$. In the case of non-innovative update mechanisms, for which $j = 0$ and $j = Z$ are absorbing states, it may be useful to compute the fraction of time the system spends in eventual internal stable equilibria. This cannot be obtained with the stationary distribution $\boldsymbol{\pi}$ (since it will simply reflect the fact that the system converges in either one of the absorbing states); but such difficulty can be overcome by introducing a small mutation rate μ. In each state a randomly chosen individual may either mutate to the other strategy with probability μ or follow the standard update update mechanism with probability $1 - \mu$. The *quasi-stationary* distribution $\boldsymbol{\pi_\mu}$ satisfies the condition $\boldsymbol{\pi_\mu \mathcal{T}_\mu = \pi_\mu}$, and the transition probabilities $\mathcal{T}_\mu$ of the transition matrix $\boldsymbol{\mathcal{T}_\mu}$ are now given by

$$\mathcal{T}_\mu^+(j) = (1 - \mu)\,\mathcal{T}^+(j) + \mu \frac{Z - j}{Z} \tag{3.16a}$$

$$\mathcal{T}_\mu^-(j) = (1 - \mu)\,\mathcal{T}^-(j) + \mu \frac{j}{Z} \tag{3.16b}$$

where $\frac{j}{Z}$ (conversely, $\frac{Z-j}{Z}$) represents the probability of selecting a cooperator (defector), and $\mathcal{T}^{\pm}(j)$ represent the usual transition probabilities obtained according to the preferred update mechanism. This is the only context where we consider the occurrence of mutations; in the remainder of this chapter and in the following ones, we consider $\mu = 0$ unless explicitly stated otherwise.

The Master Equation of the system is written as

$$\begin{aligned} P^{t+1}(j) - P^t(j) = P^t(j-1)\mathcal{T}^+(j-1) + \\ + P^t(j+1)\mathcal{T}^-(j+1) - P^t(j)\mathcal{T}^+(j) - P^t(j)\mathcal{T}^-(j) \end{aligned} \tag{3.17}$$

where $P^t(j)$ represents the probability of the population to be in configuration j at

time t, or, equivalently,

$$\begin{aligned}\rho\left(x,\tau+\frac{1}{Z}\right)-\rho\left(x,\tau\right)=\rho\left(x-\frac{1}{Z},\tau\right)\mathcal{T}^{+}\left(x-\frac{1}{Z}\right)+\\+\rho\left(x+\frac{1}{Z},\tau\right)\mathcal{T}^{-}\left(x+\frac{1}{Z}\right)-\rho\left(x,\tau\right)\mathcal{T}^{-}\left(x\right)-\rho\left(x,\tau\right)\mathcal{T}^{+}\left(x\right)\end{aligned} \tag{3.18}$$

where we have replaced $x=\frac{j}{Z}$, $\tau=\frac{t}{Z}$ and $\rho\left(x,\tau\right)=ZP^{t}\left(j\right)$ for $Z\gg1$. We can perform a Kramers-Moyal expansion of the Master Equation 3.17 by expanding it in a Taylor series at x and τ, yielding

$$\rho\left(x,\tau+\frac{1}{Z}\right)\approx\rho\left(x,\tau\right)+\frac{\partial}{\partial\tau}\rho\left(x,\tau\right)\frac{1}{Z}+\frac{\partial^{2}}{\partial\tau^{2}}\rho\left(x,\tau\right)\frac{1}{2Z^{2}}, \tag{3.19a}$$

$$\rho\left(x\pm\frac{1}{Z},\tau\right)\approx\rho\left(x,\tau\right)\pm\frac{\partial}{\partial x}\rho\left(x,\tau\right)\frac{1}{Z}+\frac{\partial^{2}}{\partial x^{2}}\rho\left(x,\tau\right)\frac{1}{2Z^{2}}, \tag{3.19b}$$

$$\mathcal{T}^{\pm}\left(x\mp\frac{1}{Z}\right)\approx\mathcal{T}^{\pm}\left(x\right)\mp\frac{\partial}{\partial x}\mathcal{T}^{\pm}\left(x\right)\frac{1}{Z}+\frac{\partial^{2}}{\partial x^{2}}\mathcal{T}^{\pm}\left(x\right)\frac{1}{2Z^{2}}. \tag{3.19c}$$

If we plug these expansions in equation 3.17 and neglect the terms of order higher than $1/Z^{2}$, we obtain the Fokker-Planck equation of the population (of course, we could preserve all the terms of the Taylor series of each of the expansions performed, but in that case we would still be handling the Master Equation itself, which would be equally hard to analyze). Considering the terms in $1/Z$ we obtain

$$\begin{aligned}\frac{1}{Z}\frac{\partial}{\partial\tau}\rho\left(x,\tau\right)=-\rho\left(x,\tau\right)\frac{\partial}{\partial x}\mathcal{T}^{+}(x)-\left(\frac{\partial}{\partial x}\rho\left(x,\tau\right)\right)\mathcal{T}^{+}+\rho\left(x,\tau\right)\frac{\partial}{\partial x}\mathcal{T}^{-}(x)+\\+\left(\frac{\partial}{\partial x}\rho\left(x,\tau\right)\right)\mathcal{T}^{-}(x)=-\frac{\partial}{\partial x}\left[\mathcal{T}^{+}(x)-\mathcal{T}^{-}(x)\right]\rho\left(x,\tau\right),\end{aligned} \tag{3.20}$$

and grouping the terms in $1/Z^{2}$ yields

$$\begin{aligned}&\left(\frac{\partial}{\partial x}\rho\left(x,\tau\right)\right)\left(\frac{\partial}{\partial x}\mathcal{T}^{+}\left(x\right)\right)+\frac{1}{2}\rho\left(x,\tau\right)\frac{\partial^{2}}{\partial x^{2}}\mathcal{T}^{+}\left(x\right)+\frac{1}{2}\mathcal{T}^{+}\left(x\right)\frac{\partial^{2}}{\partial x^{2}}\rho\left(x,\tau\right)+\\&+\left(\frac{\partial}{\partial x}\rho\left(x,\tau\right)\right)\left(\frac{\partial}{\partial x}\mathcal{T}^{-}\left(x\right)\right)+\frac{1}{2}\rho\left(x,\tau\right)\frac{\partial^{2}}{\partial x^{2}}\mathcal{T}^{-}\left(x\right)+\frac{1}{2}\mathcal{T}^{-}\left(x\right)\frac{\partial^{2}}{\partial x^{2}}\rho\left(x,\tau\right)=\\&=\frac{1}{2}\frac{\partial^{2}}{\partial x^{2}}\left[\mathcal{T}^{+}\left(x\right)+\mathcal{T}^{-}\left(x\right)\right]\rho\left(x,\tau\right).\end{aligned} \tag{3.21}$$

Equations 3.20 and 3.21 lead to the Fokker-Planck equation

$$\frac{\partial}{\partial \tau}\rho\left(x,\tau\right)=-\frac{\partial}{\partial x}a(x)\rho\left(x,\tau\right)+\frac{1}{2}\frac{\partial^{2}}{\partial x^{2}}b^{2}(x)\rho\left(x,\tau\right) \tag{3.22}$$

where

$$a\left(x\right)=\mathcal{T}^{+}\left(x\right)-\mathcal{T}^{-}\left(x\right) \tag{3.23}$$

and

$$b^{2}\left(x\right)=\frac{\mathcal{T}^{+}\left(x\right)+\mathcal{T}^{-}\left(x\right)}{Z}. \tag{3.24}$$

It has been shown (68, 75) that the Fokker-Planck equation can be equivalently described by a stochastic differential equation – a *Langevin equation*. In this particular case, assuming the noise is microscopically uncorrelated, we can adopt the Itô interpretation, which after a proper transformation of the coefficients $a(x)$ and $b(x)$ (68) yields

$$\dot{x}=a(x)+b(x)\xi \tag{3.25}$$

where ξ stands for (uncorrelated) Gaussian noise. The coefficient $a(x)$ is known as the *drift* term, while $b(x)$ is known as the *diffusion* term. Note that for non-innovative update mechanisms we have $\mathcal{T}^{+}(0)=\mathcal{T}^{-}(0)=0$ and, conversely, $\mathcal{T}^{+}(Z)=\mathcal{T}^{-}(Z)=0$, which yields $b(x)=0$ at the absorbing states ($x=0$ and $x=1$).

For $Z\rightarrow\infty$ we get $b(x)\rightarrow 0$ and therefore only the $a(x)$ term determines the dynamics. In this case we have the deterministic equation

$$\dot{x}=\mathcal{T}^{+}(x)-\mathcal{T}^{-}(x) \tag{3.26}$$

The difference $\mathcal{T}^{+}(x)-\mathcal{T}^{-}(x)$ represents the *gradient of selection*, which in the limit of large Z is equivalent to the replicator equation 3.10 for infinite populations.

3.2.3.2 Update mechanisms

In order to fully define the Markov chain introduced above, we must introduce a local update mechanism that allows us to obtain an expression for $\mathcal{T}^{\pm}(j)$. One commonly used in the literature is the *replicator analogue for finite populations* (64, 76), in which individuals only imitate others if they are more successful than themselves. Two individuals, A and B (with strategies s_{A} and s_{B}, and fitnesses $f_{s_{A}}$ and $f_{s_{B}}$ respectively) are randomly chosen from the population. Given that $s_{A}\neq s_{B}$ ($s_{A},s_{B}\in\{\boldsymbol{C},\boldsymbol{D}\}$), A imitates B if and only if $f_{s_{B}}(j)>f_{s_{A}}(j)$, with a probability given by

$$p_{RD}(j)=\frac{f_{s_{B}}(j)-f_{s_{A}}(j)}{G(j)} \tag{3.27}$$

$G(j)$ stands for the adequate normalization factor: taking s_A (s_B) as the strategy of individual A (B) – $s_i = 1$ if cooperator, $s_i = 0$ if defector – $G(j)$ consists of the difference between the maximum fitness possible when adopting s_B, and the minimum fitness possible when adopting s_A, when there are j cooperators in the population. The transition probabilities are in this case given by

$$\mathcal{T}^+(j) = \begin{cases} \frac{Z-j}{Z}\frac{j}{Z-1}\frac{f_C(j)-f_D(j)}{G(j)} & \text{if } f_C(j) > f_D(j) \\ 0 & \text{otherwise} \end{cases} \tag{3.28a}$$

$$\mathcal{T}^-(j) = \begin{cases} \frac{j}{Z}\frac{Z-j}{Z-1}\frac{f_D(j)-f_C(j)}{G(j)} & \text{if } f_D(j) > f_C(j) \\ 0 & \text{otherwise} \end{cases} \tag{3.28b}$$

In equation 3.28a for the transition probability $\mathcal{T}^+$, the term $\frac{Z-j}{Z}$ corresponds to the probability of selecting a defector among the Z individuals in the population, and the term $\frac{j}{Z-1}$ corresponds to the probability of subsequently selecting a cooperator to be imitated, among the $Z-1$ individuals that are left in the population (selection is made without replacement). Conversely, in equation 3.28b for the transition probability $\mathcal{T}^-$, the term $\frac{j}{Z}$ corresponds to the probability of selecting a cooperator from the population, and the term $\frac{Z-j}{Z-1}$ corresponds to the probability of subsequently selecting a defector from the $Z-1$ remaining individuals.

Note that this update mechanism does not leave room for errors in strategy adoption: an individual only evaluates the possibility of imitating a partner if he is more successful than him.

To account for errors in the update process a non-linear alternative to the mechanism described above, widely used in the literature, is the *Fermi process* (77, 78, 79): a randomly chosen individual A, with strategy s_A, imitates a randomly chosen partner B, with strategy s_B ($s_A \neq s_B$), with a probability p_{Fermi} given by the Fermi probability distribution from statistical physics

$$p_{Fermi}(j) = \frac{1}{1 + e^{-\beta(f_{s_B}(j) - f_{s_A}(j))}}, \tag{3.29}$$

where β stands for the intensity of selection regulating the accuracy of the imitation process, and f_{s_i} the fitness associated with individual i adopting strategy s_i. Figure 3.5 shows how this probability function varies with fitness difference for several β values. For $\beta \to \infty$ we obtain pure copying dynamics, commonly used in studies of cultural

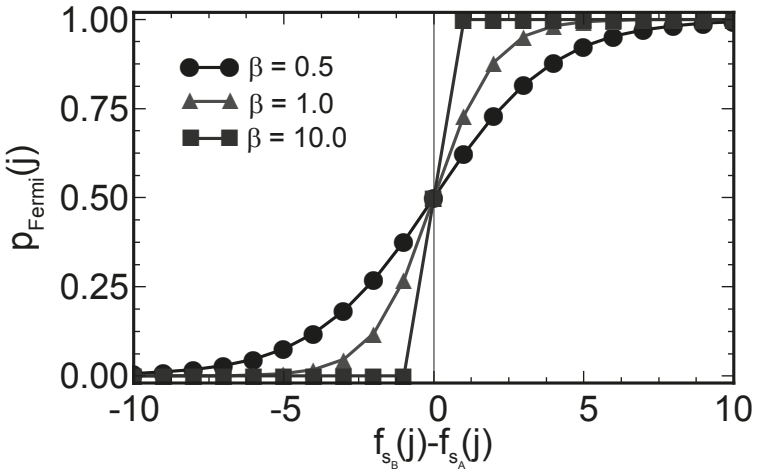

Figure 3.5: Probability function p_{Fermi} for the Fermi Imitation update method - We plot the probability p_{Fermi} that an individual A imitates the strategy of a randomly chosen player B, $p_{Fermi}(j)$, as a function of their fitness difference $f_{s_B}(j) - f_{s_A}(j)$ for different values of β. The parameter β regulates the intensity of selection: note how $p_{Fermi}(j)$ approaches a step-function for increasing β.

evolution, whereas in the limit of weak selection $\beta \to 0$ evolution proceeds by random drift.

The transition probabilities $\mathcal{T}^{\pm}(j)$ are given by

$$\mathcal{T}^{\pm}(j) = \frac{j}{Z}\frac{Z-j}{Z-1}\left[1 + e^{\mp\beta(f_C(j)-f_D(j))}\right]^{-1} \tag{3.30}$$

The first and second terms have a similar interpretation: $\frac{j}{Z}$ corresponds to the probability of selecting a cooperator, and $\frac{Z-j}{Z-1}$ to the probability of selecting a defector. The last term corresponds to the probability of a cooperator imitating a defector, or vice-versa. The balance of transition probabilities, $G(j) = \mathcal{T}^{+}(j) - \mathcal{T}^{-}(j)$, can be written as

$$G(j) \equiv \mathcal{T}^{+}(j) - \mathcal{T}^{-}(j) = \frac{j}{Z}\frac{Z-j}{Z-1}\tanh\left[\frac{\beta}{2}(f_C(j) - f_D(j))\right] \tag{3.31}$$

Note that, in the limit of weak selection ($\beta \to 0$) we may rewrite equation 3.31 as

$$G(j) \simeq \frac{j}{Z}\frac{Z-j}{Z-1}\frac{\beta}{2}\left(f_C(j) - f_D(j)\right) \tag{3.32}$$

which for large populations is equivalent to the replicator equation 3.10 with a different timescale. The sign of $G(j)$ informs about the preferred direction of selection: when $G(j) > 0$ ($G(j) < 0$) selection favors cooperators (defectors), and the number of ***C*s** will

most likely increase (decrease). The case $G(j) = 0$ corresponds to the case of neutral selection.

For the particular case of the Fermi process the general formula for the fixation probability 3.15 can be simplified to

$$\phi_j = \frac{\sum_{i=0}^{j-1} \exp\left[-\beta i(i+1)u - 2\beta iv\right]}{\sum_{i=0}^{Z-1} \exp\left[-\beta i(i+1)u - 2\beta iv\right]} \tag{3.33}$$

where $2u = R - S - T + P$ and $2v = -R + SZ - PZ + P$. When the entries of the payoff matrix satisfy the condition $R + P - S - T = 0$, equation 3.33 can be further simplified to

$$\phi_j = \frac{1 - e^{-\beta vj}}{1 - e^{-\beta vZ}} \tag{3.34}$$

This case is known as *equal gains from switching* (80) - the change in fitness an individual obtains from switching strategy is the same regardless of his opponent's strategy.

3.3 Rules for the evolution of cooperation

According to Darwin's perspective in his Theory of Natural Selection, the individuals that are better adapted to their surroundings survive longer, which is translated in a higher reproductive fitness - their genes are passed on to the next generation. This *survival of the fittest* can be interpreted as a competition between egoistic individuals. How to explain the pervasiveness of cooperation in Nature, if cooperating implies incurring in a cost to the cooperative individual, thereby decreasing his fitness? Darwin himself was puzzled by this (apparent) paradox:

> *If it could be proved that any part of the structure of any one species had been formed for the exclusive good of another species, it would annihilate my theory, for such could not have been produced through natural selection.*
>
> - Charles Darwin in "On the Origin of Species" (1859)

However, cooperation remained as a secondary aspect in his work, a problem that would be solved later on. In the 1950s, with the advent of Game Theory and the formulation of the first social dilemma - the Prisoner's Dilemma - the paradox remained: if rational individuals, interested solely in maximizing their own gains, always opt for

defection, how do we explain the pervasiveness of cooperation in Nature? Two problems can be identified in this reasoning. One, is that individuals need not be perfectly rational: several recent experiments have shown that humans' decisions in economic experiments are not perfectly rational - that is, individuals do not aim exclusively at maximizing their fitness. On the other hand, there are other social dilemmas besides the **PD** - such as the Stag-Hunt (**SH**) and the Snowdrift Game (**SG**) - that are less strict for cooperation. In the case of the **SG**, it is possible to observe a coexistence of cooperators and defectors, and in the case of the **SH**, depending on the initial composition it is even possible for the population to evolve towards a fully cooperative state. However, these dilemmas emerged some decades later than the **PD**, so for quite some time social dilemmas found in Nature were generally identified with the **PD** (48, 81). Since cooperation was observed in all those examples, some mechanism had to be responsible for its existence.

During the last decades several mechanisms have been proposed to account for the existence of cooperation, and all of them rely on the same property - to promote positive assortment between cooperators. This positive assortment can be caused by genetic relatedness between individuals, repeated interactions between them, localized interactions, etc. It is however important to note that the problem of cooperation is not the same for all of the social dilemmas, and depending on the particular case at study it may be possible to explain coexistence levels of cooperation and defection without resorting to any of these mechanisms. The mechanisms we list below - *kin selection* (section 3.3.1), *direct* and *indirect reciprocity* (sections 3.3.2 and 3.3.3 respectively), and *network reciprocity*) (section 3.3.4) can explain the emergence of cooperation in the context of the **PD** (in which case a rational player would never cooperate), and promote higher levels of cooperation in other social dilemmas such as the **SG** and the **SH** (although this is debatable in some cases (64)). Also, we schematize these mechanisms for the evolution of cooperation in figure 3.6.

3.3.1 Kin Selection

The first mechanism proposed to explain the existence of cooperation accounts for the occurrence of cooperative acts between genetically related individuals, and is known as *kin-selection* (83).

In the 1930, the English(-born) geneticist J. B. S. Haldane said "I would lay down my life for two brothers of eight cousins", a famous affirmation that was in the origin of

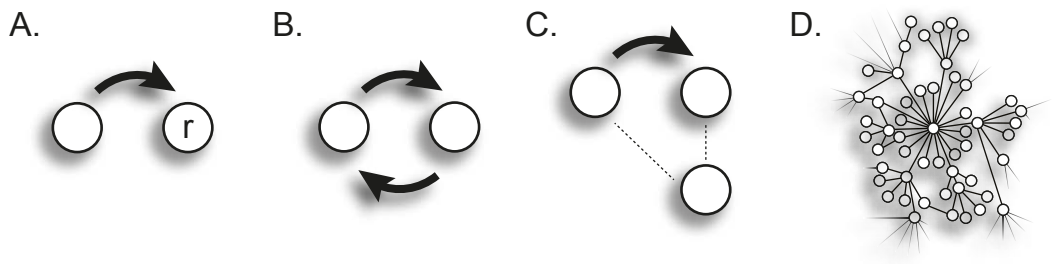

Figure 3.6: Mechanisms for the promotion of the emergence and evolution of cooperation - **A.** Kin selection, which accounts for the occurrence of cooperative acts between genetically related individuals, where r represents the degree of genetic relatedness between donor and recipient; **B.** direct reciprocity, which assumes repeated encounters between the same individuals; **C.** indirect reciprocity, which is based on *reputation*, and in which two individuals are not supposed to interact more than once; **D.** network reciprocity, in which interactions are localized. This figure is inspired in, and is similar to, the one that can be found in (82).

what is now known as Hamilton's law, $r > c/b$, where r represents the degree of genetic relatedness between donor (who provides the effort c) and recipient (who receives the benefit b). For instance, because brothers share on average half of their genetic material, their coefficient of genetic relatedness is $r = \frac{1}{2}$ (homozygotic twins are an exception, as for them we have $r = 1$). Cooperation is explained as the consequence of an egoistical motivation: in an extreme situation in which one could sacrifice his/her life to save the life of one or more family members, by saving two brothers one would guarantee that on average all his genes would pass on to the next generation.

One example that is found in nature is food sharing in vampire bats (84, 85). Vampire bats feed mostly on blood, and can die if they do not have a blood meal for two consecutive days. It has been shown that vampire bats regurgitate blood to feed other vampire bats of their group if for some reason they were unable to go hunting on that night, and it has also been shown that the majority of food sharing instances observed were among relatives, supporting the kin selection theory. However, a small fraction of the instances observed occurred between non-related individuals, a fact that requires further explanation.

3.3.2 Direct Reciprocity

The small fraction of occurrences of food sharing between non-related vampire bats mentioned in the previous section requires further explanations - because kin selection requires donor and recipient to be genetically related, this mechanism only covers a small fraction of cooperative acts in nature. The *direct reciprocity* mechanism (86) does not require genetic relatedness but assumes repeated encounters; it can be resumed by the popular saying "You scratch my back and I'll scratch yours".

Let us suppose that individuals play an iterated Prisoner's Dilemma game, the harshest social dilemma of cooperation. If the participants are aware of the number of encounters beforehand, it is still impossible for cooperation to emerge: in the last encounter rational players opt to defect, as there is no room for future reciprocation, and such reasoning is repeated backwards for all previous encounters. However, not knowing the number of encounters beforehand introduces a possibility for cooperation to emerge.

In 1980, in order to understand what would be the best strategy to play an iterated Prisoner's Dilemma game, Robert Axelrod held a computational tournament for which he asked anyone interested to submit a strategy they thought could win this tournament (87); these strategies would then play against each other following the rules of the Prisoner's Dilemma game. The payoff each strategy accumulated over all interactions would be a measure of its success. Note that in the context of an iterated game, *strategy* refers, not to the action taken in a single encounter (to cooperate or to defect), but to the set of rules an individual uses to decide if he cooperates or defects in each encounter, taking into account information from the previous round(s). The winning strategy was the simplest in the competition: the Tit-for-Tat (**TFT**) strategy, which consisted of only two lines of Fortran programming, submitted by the Russian-born mathematician Anatol Rapoport. This strategy starts by cooperating, and then repeats its opponent's previous move; in essence, **TFT** transforms the iterated Prisoner's Dilemma in an iterated coordination game (48). This strategy was then characterized by being nice (as it would always start by cooperating), and forgiving (it would reciprocate a defection, but as soon as its opponent resumes to cooperation he would start cooperating too). This strategy proved to be extremely robust to others, winning a second tournament that was also held during the 1980s.

However, these tournaments did not allow for occasional errors in decision making, to which **TFT** is particularly vulnerable: in a pair of individuals using the **TFT** strategy, if by mistake one defects when he was supposed to cooperate, this initiates a wave of

retaliation that only ceases with the occurrence of another error (87, 88). It was then shown on computer tournaments where occasional mutations were allowed to occur that another strategy emerged as the most successful: Win-Stay-Lose-Shift (**WSLS**) (89), which takes into account the previous move of both players (and not only the previous move of the opponent, as does **TFT**). With the **WSLS** strategy (also known as Pavlov strategy because of its reflex-like response to payoff), a player cooperates if and only if both players opted for the same alternative in the previous move, or in other words: if with the previous move he obtained either R or T as payoff, he repeats it; otherwise, he switches.

3.3.3 Indirect Reciprocity

Repeated interactions between the same two individuals are frequent in the animal world, but not so much between humans - or at least not anymore. More and more frequently, we interact with individuals whom we have not met before and probably will not meet again in the future (90), as is the case in online auctions and other electronic transactions (91, 92). The *indirect reciprocity* (93) mechanism explains the emergence of cooperation in populations where any two individuals are supposed to interact only once (repeated interactions are excluded to avoid instances of direct reciprocity). Compared with direct reciprocity, it can be translated in the saying "You scratch my back and I'll scratch someone else's" (54), and is based on *reputation*.

Let us suppose the following scenario, illustrated in figure 3.6C: an individual A helps an individual B, and this interaction is observed by other individuals in the population (the *observers*). How should one judge the action of individual A, that is, how should we formulate an individual's reputation and which actions should increase or decrease his reputation? One could adopt an image scoring system (93) in which the assessment of each action as positive or negative would increase or decrease an individual's reputation by one point. Or, more simply, one can allow the reputation of an individual to be affected only by his last action, and judge the world in "black and white", that is, judge them as "good" or "bad" (94). Returning to the example illustrated in Figure 3.6C, an individual C will decide either or not to cooperate with individual A by recurring to *i)* an *assessment rule* or *social norm*, and *ii)* an *action rule*. The moral assessment uses the available information to decide on the donor's reputation; depending on the information used to reach this decision, assessment rules may be classified either as 1^{st} order (take into account the donor's action, if he cooperated or not), 2^{nd}

Donor's action	Recipient's reputation	New reputation of the donor
Cooperated	Good	Good
Cooperated	Bad	Bad
Defected	Good	Good
Defected	Bad	Bad

Table 3.1: Example of a 2^{nd} order social norm, in which both the donor's action and the recipient's reputation are taken into account to decide on the reputation of the donor after the action. Taking into account all the possibilities of "good" and "bad" in the rightmost column, there are $2^{2^2} = 16$ possible 2^{nd} order social norms.

order (take into account the donor's action and the recipient's reputation), and so on. There are 2^{2^n} possible social norms of order n - one example of a social norm of order $n = 2$ is represented in table 3.1. Associated with a social norm, individuals resort also to an action rule, which tells them if they should cooperate or not with a given individual taking into account his reputation.

Although some examples are known in the animal world of the use of reputation (95, 96), this mechanism is found almost only among humans. Because it is necessary to track one's own interactions, but also all the other individuals interactions, this mechanism is very demanding at the cognitive level (97), as summarized by the American evolutionary biologist David Haig:

> "*For direct reciprocity you need a face. For indirect reciprocity you need a name.*"
>
> - David Haig as cited by Martin Nowak in "SuperCooperators" (2011)

3.3.4 Network Reciprocity

All previous mechanisms assume that populations are well-mixed. This assumption may hold on small communities, on which everyone knows and interacts with everyone else, but it is not realistic for larger populations: in this latter case, different individuals interact with different sub-sets of partners. This interaction structure can be conveniently modeled with the use of *networks*: individuals are assigned to nodes, and edges between them represent the possibility of interaction.

The introduction of structure in the population - a mechanism later coined *network reciprocity* - has a significant impact on the fitness of individuals, as exemplified in

figure 3.7: while in well-mixed populations (panel A) all cooperators have the same fitness, because all have the same number of interactions with partners of either strategy (the same happening with all defectors), in structured populations (panel B) fitness becomes context dependent: the fitness of two individuals with the same strategy is no longer the same, but depends of their position on the network, on their number of connections to individuals playing either cooperate or defect, and in some cases it may even depend on the social context of their neighbors as well as occurs in N-Person games (with $N > 2$) played in networks (we will discuss this aspect in detail in chapter 4). In 1992, Nowak and May (98) considered for the first time population structure in the studies of emergence and evolution of cooperation in the Prisoner's Dilemma game, adopting a spatial grid as a model of the underlying network of contacts in the population. The authors showed that, compared with the well-mixed case in which defection would dominate entirely, the spatial grid could generate chaotically changing spatial patterns, in which both ***C****s* and ***D****s* would coexist indefinitely.

This pioneer work was rapidly followed by hundreds of articles investigating what would be the impact of regular structures on other social dilemmas (surprisingly, it was shown that it can produce a slight inhibition of the level of cooperation in the 2-person Snowdrift Game (64)), and later on what is the impact of other, more complex population structures on the evolution of cooperation.

The introduction of population structure has two main implications: the introduction of *local interactions* (already discussed), and *local dispersal* - that is, whenever a strategy reproduces it can only occupy its closest neighborhood. To analytically describe the evolution of cooperation (or any other dynamical process) in a structured population is very difficult: one has to describe not only the global fraction of ***C****s* (and ***D****s*) in the population, but also where each of them is located. Sometimes, a mean-field approach is adopted to compute individuals' fitness (assuming that the probability of encountering a strategy in an individual's neighborhood is simply given by its global prevalence in the population), but this approach amounts to simply neglecting population structure and the existence of spatial correlations. Although difficult, it is possible to retain more information about the spatial configuration of the system if, instead of describing it as a well-mixed population of *individuals*, we describe it as a well-mixed population of *pairs of individuals*, in which pairs are independent of each other. This is the approach adopted by *pair approximation* (99), a method that originates in physics and is now widely applied in the description of the evolution of several dynamical pro-

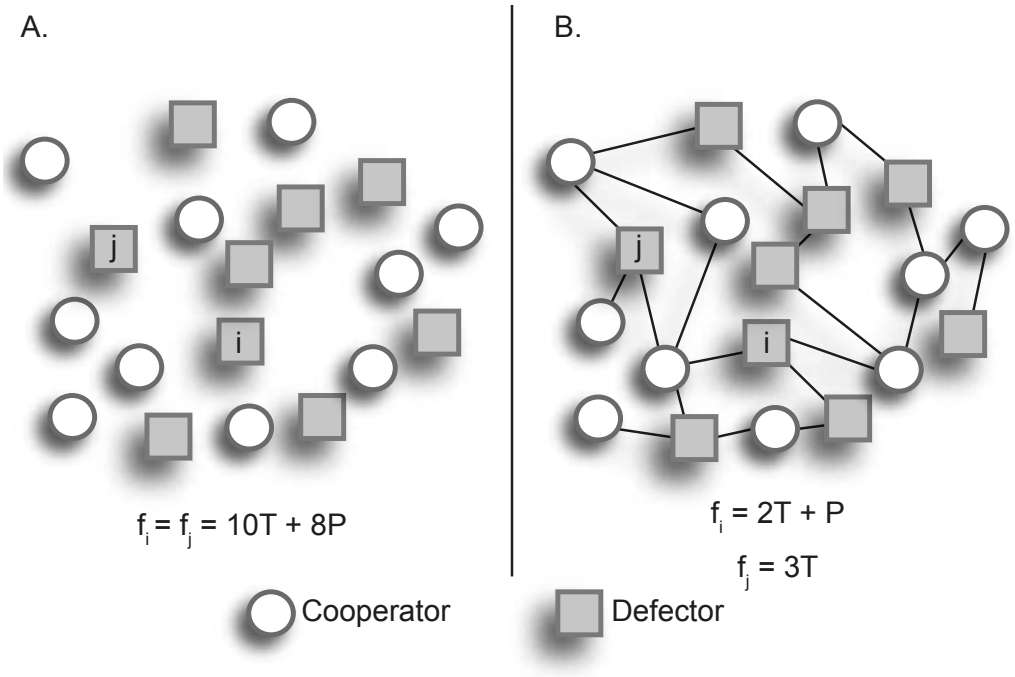

Figure 3.7: Impact of structured populations on individual fitness - **A.** In well-mixed populations, all individuals with the same strategy (as individuals i and j, for example) have the same fitness. **B.** The introduction of structure in a population leads to localized interactions: now individuals i and j have different fitnesses, constrained by their social context, despite the fact that they play the same strategy.

cesses on structured populations, from epidemics spreading to opinion dynamics and the propagation of cooperative strategies.

Let us briefly describe this formalism in the context of social dilemmas with two (unconditional) strategies. Besides the global fraction of ***Cs*** (p_C) and ***Ds*** (p_D), the system is now also described by the densities of pairs of strategies, namely **CC** pairs (p_{CC}), **CD** pairs (p_{CD}), **DC** pairs (p_{DC}) and **DD** pairs (p_{DD}). These variables are subject to the restrictions $p_C + p_D = 1$, $p_{CC} + p_{CD} + p_{DC} + p_{DD} = 1$ and $p_{CD} = p_{DC}$.

The last condition means that, when counting pairs of strategies, their spatial orientation (left-right versus right-left, or top-bottom versus bottom-top, in the spatial lattice) is equivalent. With these quantities, one can also determine the *local densities* $q_{C|C} = \frac{p_{CC}}{p_C}$, $q_{C|D} = \frac{p_{CD}}{p_D}$ and $q_{D|D} = \frac{p_{DD}}{p_D}$.

$q_{s_i|s_j}$ represents the probability of a s_i strategist being connected with a s_j strategist. Because of the restrictions imposed by the equations introduced above, in the

specific case of games with only two strategies the system can be described by only two quantities (p_C and p_{CC}, or p_C and $q_{C|C}$, for instance).

Depending on the social dilemma considered, and on the particular update method adopted (which affects the transition probabilities from a state with j cooperators to a state with $j \pm 1$ cooperators), these calculations can be far from trivial. Also, note that pair approximation considers that pairs of individuals are independent of each other, which amounts to say that if individual A is connected to B, and individual B is connected to individual C, any influence that A may exert on C is neglected in the context of pair approximation. In mathematical terms, this means that $q_{s_i|s_j s_k} \approx q_{s_i|s_j}$. This is a strong assumption, and one that not always holds - given their social proximity, in many dynamical processes A is expected to be positively correlated with C. This is particularly evident when the system is close to a transition - from full cooperation to full defection or vice-versa. In such cases, the (few) cooperators that survive are able to do so by forming clusters, in which they reinforce cooperation and escape exploitation by defectors. However, such clusters cannot be described by pair approximation, and therefore its predictions fail in such regimes. Also important is the computation of fitnesses in N-Person games, which requires studying configurations that span beyond the first neighborhood of an individual - this particular aspect will be further discussed in chapters 4 and 5. Also, we will shown in chapter 6 that for different dynamical processes belonging to different universality classes the pairwise interactions between individuals give rise to spatial correlations that extend beyond individuals' closest neighbors, a scenario that cannot be described by the pair approximation method.

Pair approximation can be extended to study the frequency of larger motifs - triplet approximation, quadruplet approximation or, more generally, n-point approximation - but note that the number of variables one needs to keep track of in each of these cases is much larger, which leads to cumbersome or even impossible calculations.

Modeling games on networks introduces yet another degree of freedom. Should the fitness of individuals be computed as the payoff accumulated from all the games in which they participate, or correspond to an *average* of the payoff obtained in each of those games? Note that in equations 3.8 for infinite **WM** populations, and in equations 3.12 for finite **WM** populations, we associate the fitness of individuals to the average payoff obtained from all interactions in which an individual engages. In fact, in homogeneous networks performing such normalization amounts to a rescaling of the intensity of selection in the evolutionary dynamics. If we consider the particular case

of 2-person games, the fitness of a cooperator (f_C) and of a defector (f_D), each with n_C cooperator neighbors and $\langle k \rangle - n_C$ defector neighbors is given by

$$f_C^{NORM} = \frac{n_C}{\langle k \rangle} R + \frac{\langle k \rangle - n_C}{\langle k \rangle} S \Rightarrow f_C^{NORM} = \frac{1}{\langle k \rangle} \underbrace{\left(n_C R + \left(\langle k \rangle - n_C\right) S\right)}_{\text{accumulated payoff, } f_C^{ACC}} \tag{3.35a}$$

$$f_D^{NORM} = \frac{n_C}{\langle k \rangle} T + \frac{\langle k \rangle - n_C}{\langle k \rangle} P \Rightarrow f_D^{NORM} = \frac{1}{\langle k \rangle} \underbrace{\left(n_C T + \left(\langle k \rangle - n_C\right) P\right)}_{\text{accumulated payoff, } f_D^{ACC}} \tag{3.35b}$$

For the Fermi Imitation update rule, we may write

$$p_{Fermi} = \frac{1}{1 + e^{-\beta\left(f_C^{NORM} - f_D^{NORM}\right)}} = \frac{1}{1 + e^{-\frac{\beta}{\langle k \rangle}\left(f_C^{ACC} - f_D^{ACC}\right)}} \tag{3.36}$$

That is, the intensity of selection is rescaled by the average connectivity $\langle k \rangle$ of the network (the number of games in which an individual participates, in the case of 2-person games), which is reflected in the evolutionary times but not on the overall dynamics.

On the contrary, on heterogeneous networks different nodes have different number of connections. Depending on the network class and on its degree distribution, the difference in the number of neighbors of different nodes can be overwhelming (as is the case in Scale-Free **BA** networks, for instance). In this case, although one can opt to attribute individual fitness to the average payoff obtained by an individual in all games in which he participates, that would amount to treating all individuals as equivalent. One of the main advantages of the introduction of this type of networks in the study of the problem of the emergence and evolution of cooperation is to be able to model the (real) fact that different individuals may have different roles in the society, and interact more frequently than others. For these reasons, we opt to associate individual fitness, in networks, to the payoff individuals *accumulate* in all their interactions. In chapters 4 and 5 we will discuss in more detail how N-Person games should be formulated in networks.

Network reciprocity is a recent and rapidly expanding area of research, in which this thesis is included.

4

Collective Prisoner's Dilemma

4.1 Introduction

> *We must abandon the conceit that individual, isolate, private actions are the answer. They can and do help. But they won't take us far enough without collective action.*
>
> – Al Gore, on his acceptance speech of the Nobel Peace Prize in 2007

The declarations of the American environmental activist Al Gore testify the collective nature of the global warming problem (100) – a problem that involves all individuals in the planet without exception (101).

The global warming problem is just one example of collective action problems which in Evolutionary Game Theory (**EGT**) are best dealt-with in the framework of N-Person games (section 3.1.3). Other problems that are contingent of the simultaneous decisions of several individuals are the payment of taxes and social welfare; the participation in open source projects; group hunting; and the sharing of common resources among countries, to mention a few examples.

In this chapter, we will focus on the framework of Public Goods Games (**PGGs**), and we will consider the most used metaphor to study **PGGs** – the N-Person generalization of the Prisoner's Dilemma. This collective social dilemma emerges as the most suitable metaphor for problems in which the outcome obtained is proportional to the number of contributors in the group. We will start by presenting the model and highlighting its relationship with its 2-person counterpart, the Prisoner's Dilemma, in section 4.3. We will discuss the evolutionary dynamics of the **NPD** on infinite and finite well-mixed

(**WM**) populations; the mathematical formalism introduced here will also be useful for the next chapter (chapter 5). Then, in section 4.4 we will investigate how Public Goods Games should be defined in social networks, that is, how the social neighborhood of an individual defines the number of games in which he engages, and then we proceed to evaluate the impact of the introduction of population structures of different degree distributions and average connectivity in the evolutionary dynamics of the **NPD**. Up to now, individuals have been treated as equivalent in all respects (102, 103), in sharp contrast with real-life situations, where diversity is ubiquitous. We introduce social diversity by means of heterogeneous networks and show that cooperation is promoted by the diversity associated with the number and size of the public goods game in which each individual participates. Furthermore, we find that levels of cooperation are even more pronounced when social diversity is also reflected in the cooperators' individual contribution (section 4.5). In this work we use a modified version of the traditional contributive paradigm that takes into account the underlying population structure. Finally, we present a detailed analytical study to account for the mechanism responsible for the impressive results obtained with the new contributive scheme, in section 4.8

4.2 The Model

We start by presenting and discussing the **NPD** with the traditional contributive scheme. Let us consider a population composed of individuals behaving either as unconditional cooperators (***C**s*) or defectors (***D**s*). Each ***C*** contributes to a common pool with a certain cost c, while ***D**s* do not contribute; the total contribution is multiplied by an enhancement factor r $(r > 0)$ and equally distributed among all individuals in the group (of size N). The gain obtained by an individual i adopting strategy s_i $(s_i \in \{\boldsymbol{C}, \boldsymbol{D}\})$ in a single group interaction is identified as the individuals' *payoff*, Π_{s_i}. The payoff of ***C**s* (Π_C) and ***D**s* (Π_D) can then be written as

$$\Pi_D\left(n_C\right) = \frac{crn_C}{N} = \eta c n_C \tag{4.1a}$$

$$\Pi_C\left(n_C\right) = \Pi_D\left(n_C\right) - c \tag{4.1b}$$

where n_C is the number of cooperators in the group of size N, and $\eta = r/N$ is the renormalized enhancement factor. Note that in this case the amount of public good that is produced is linear on the number of contributors in the group, which corresponds to the linear production function shown in figure 3.2A and discussed in section 3.1.3.

A direct relationship can be established between the 2-person Prisoner's Dilemma (**PD**) and the equations 4.1 above for the **NPD**. If for a moment we assume that in a group of size N interactions are pairwise (instead of a single group interaction as we have been discussing for the **NPD**) and fitnesses are computed following the general payoff matrix 3.3 formulated in terms of the general gains R, S, T and P, the fitness of a cooperator (f_C) and a defector (f_D) corresponds to[†]

$$f_C = (n_C - 1)\,R + (N - n_C)\,S \tag{4.2a}$$

$$f_D = n_C T + (N - n_C - 1)\,P \tag{4.2b}$$

where n_C is the number of cooperators in the group of size N. We can rewrite equations 4.2 as

$$f_C = (n_C - 1)\,\beta + (N - 1)\,\gamma \tag{4.3a}$$

$$f_D = n_C \beta \tag{4.3b}$$

with

$$\beta = \frac{P\,(N - n_C - 1)}{n_C} + T \tag{4.4a}$$

$$\gamma = \frac{P\left(N - N n_C + n_C^2 - 1\right) + n_C\left((n_C - 1)\,R + NS + T - n_C\,(S + T)\right)}{n_C\,(N - 1)} \tag{4.4b}$$

With this formulation, the transformation between the 2-person Prisoner's Dilemma and the **NPD** is straightforward, and corresponds to

$$\beta \to \frac{r}{N} c \tag{4.5a}$$

$$\gamma \to \frac{N - r}{N(N-1)c} \tag{4.5b}$$

So, with the formulation of the **NPD** presented in equations 4.1, we may affirm that in **WM** populations the **NPD** is a *compound game*, that is, one in which a group interaction may be formulated as a succession of 2-person interactions. However, as will become clear in the next section, this does not hold for structured populations.

[†]The deduction that follows is based on the one in (104).

4.3 The *N*-Person Prisoner's Dilemma in Well-Mixed Populations

4.3.1 Infinite Populations

An individual's *fitness* corresponds to the payoff obtained in all games in which that individual participates. In an infinite well-mixed (**WM**) population fitness is obtained by summing the average payoffs obtained over all the possible groups of size N that can be formed with n_C cooperators. The random selection of N individuals leads to groups whose composition follows a binomial distribution, and therefore the average fitness of ***C*s** (f_C) and ***D*s** (f_D) can be written as

$$f_C(x) = \sum_{n_C=0}^{N-1} \binom{N-1}{n_C} x^{n_C}(1-x)^{N-1-n_C}\Pi_C(n_C+1) \tag{4.6a}$$

$$f_D(x) = \sum_{n_C=0}^{N-1} \binom{N-1}{n_C} x^{n_C}(1-x)^{N-1-n_C}\Pi_D(n_C) \tag{4.6b}$$

where x stands for the fraction of cooperators in the population (and $(1-x)$ is the fraction of defectors). In this case (of an infinite **WM** population), the evolutionary success of each strategy is dictated by the replicator equation 3.10, $\dot{x} = x(1-x)\left(f_C(x) - f_D(x)\right)$. The direction of evolution (that is, the sign of $\dot{x}$) is determined by the fitness difference $f_C(x) - f_D(x)$, which for equations 4.1 and 4.6 reads

$$\begin{aligned} f_C(x) - f_D(x) = \\ &= \sum_{n_C=0}^{N-1} \binom{N-1}{n_C} x^{n_C}(1-x)^{N-1-n_C}\left[\Pi_C\left(n_C+1\right) - \Pi_D\left(n_C\right)\right] = \\ &= \sum_{n_C=0}^{N-1} \binom{N-1}{n_C} x^{n_C}(1-x)^{N-1-n_C}(\eta-1)c = \\ &= (\eta-1)c \sum_{n_C=0}^{N-1} \binom{N-1}{n_C} x^{n_C}(1-x)^{N-1-n_C} \end{aligned} \tag{4.7}$$

That is, $f_C(x) - f_D(x) < 0$ whenever $\eta < 1$, and in this case cooperation is disadvantageous (conversely, cooperators are in advantage with respect to defectors whenever $\eta > 1$). This result is independent of the group size N. For $\eta = 1$ we have neutral

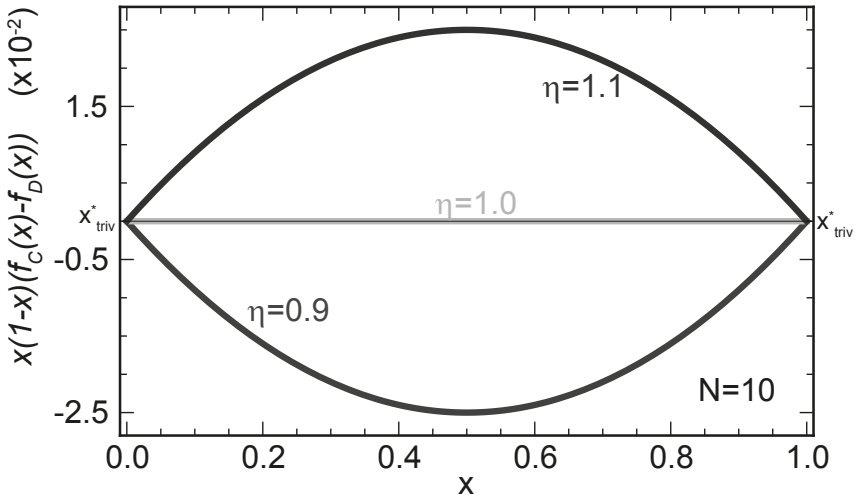

Figure 4.1: Evolutionary Dynamics of the *N*-Person Prisoner's Dilemma in Infinite Well-Mixed Populations - Profile of the replicator equation $\dot{x} = x(1-x)\left(f_C(x) - f_D(x)\right)$ for increasing renormalized enhancement factor $\eta = r/N$. Cooperators are disadvantageous for $\eta < 1$, and the trivial root $x^*_{triv} = 0$ is stable ($x^*_{triv} = 1$ is unstable). Conversely, cooperators are in advantage with respect to defectors whenever $\eta > 1$, and the stability of the trivial roots x^*_{triv} is exchanged. This latter case $(\eta > 1)$ does not represent a social dilemma. Parameters: $N = 10$, $c = 1.0$.

selection, as $f_C(x) = f_D(x) \; \forall \; x \; [0, 1]$. These three distinct scenarios are illustrated in figure 4.1 for a group size of $N = 10$.

4.3.2 Finite Populations

In finite **WM** populations of size Z, the above binomial sampling (equations 4.6) is replaced by a hyper-geometrical sampling (without replacement),

$$f_C(j) = \binom{Z-1}{N-1}^{-1} \sum_{n_C=0}^{N-1} \binom{j-1}{n_C} \binom{Z-j}{N-n_C-1} \Pi_C(n_C+1) \tag{4.8a}$$

$$f_D(j) = \binom{Z-1}{N-1}^{-1} \sum_{n_C=0}^{N-1} \binom{j}{n_C} \binom{Z-j-1}{N-n_C-1} \Pi_D(n_C) \tag{4.8b}$$

where j stands for the number of cooperators in the population. In this case, we may write (105)

$$
\begin{aligned}
&f_C(j) - f_D(j) = \\
&= \binom{Z-1}{N-1}^{-1} \sum_{n_C=0}^{N-1} \left\{ \binom{j-1}{n_C} \binom{Z-j}{N-n_C-1} \Pi_C(n_C+1) - \binom{j}{n_C} \binom{Z-j-1}{N-n_C-1} \Pi_D(n_C) \right\} \\
&= \binom{Z-1}{N-1}^{-1} \sum_{n_C=0}^{N-1} \left\{ \binom{j-1}{n_C} \binom{Z-j}{N-n_C-1} [\eta c(n_C+1) - c] \binom{j}{n_C} \binom{Z-j-1}{N-n_C-1} \eta n_C c \right\} \\
&= c(\eta-1) + \eta c \binom{Z-1}{N-1}^{-1} \sum_{n_C=0}^{N-1} n_C \left\{ \binom{j-1}{n_C} \binom{Z-j}{N-n_C-1} - \binom{j}{n_C} \binom{Z-j-1}{N-n_C-1} \right\}
\end{aligned}
\tag{4.9}
$$

We can simplify the notation by replacing $\tilde{x} = x - 1$ (105), in which case we obtain

$$
f_C(j) - f_D(j) = c \left[(\eta-1) + \eta \binom{\tilde{Z}}{\tilde{N}} \sum_{n_C=0}^{\tilde{N}} n_C \left\{ \binom{\tilde{j}}{\tilde{N}-n_C} - \binom{j}{n_C} \binom{\tilde{Z}-j}{\tilde{N}-j} \right\} \right] \tag{4.10}
$$

And in this case the sum simplifies to

$$
\begin{aligned}
f_C(j) - f_D(j) &= c \left[(\eta-1) + \eta \left(\frac{\tilde{N}}{\tilde{Z}} \right) \left(\tilde{j} - j \right) \right] = c \left[(\eta-1) - \eta \frac{\tilde{N}}{\tilde{Z}} \right] = \\
&= c \left[\eta \left(1 - \frac{N-1}{Z-1} \right) - 1 \right],
\end{aligned}
\tag{4.11}
$$

that is, the fitness difference $f_C(j) - f_D(j)$ in finite populations is independent of the number of cooperators in the population, but depends on both the population size Z and the group size N. For $Z > N$ the evolutionary dynamics is qualitatively equivalent to that observed in infinite **WM** populations. Whenever group size is equal to population size ($Z = N$), we obtain simply $f_C(j) - f_D(j) = -c$: cooperators are disadvantageous irrespective of the value of the renormalized enhancement factor η. Note that this contrasts with the dynamics described for infinite **WM** populations, in which case cooperation is advantageous whenever $\eta > 1$.

4.4 How public are Public Goods Games?

To model N-Person games on structured populations requires knowing how the underlying network of contacts determines the pattern of interactions and which games

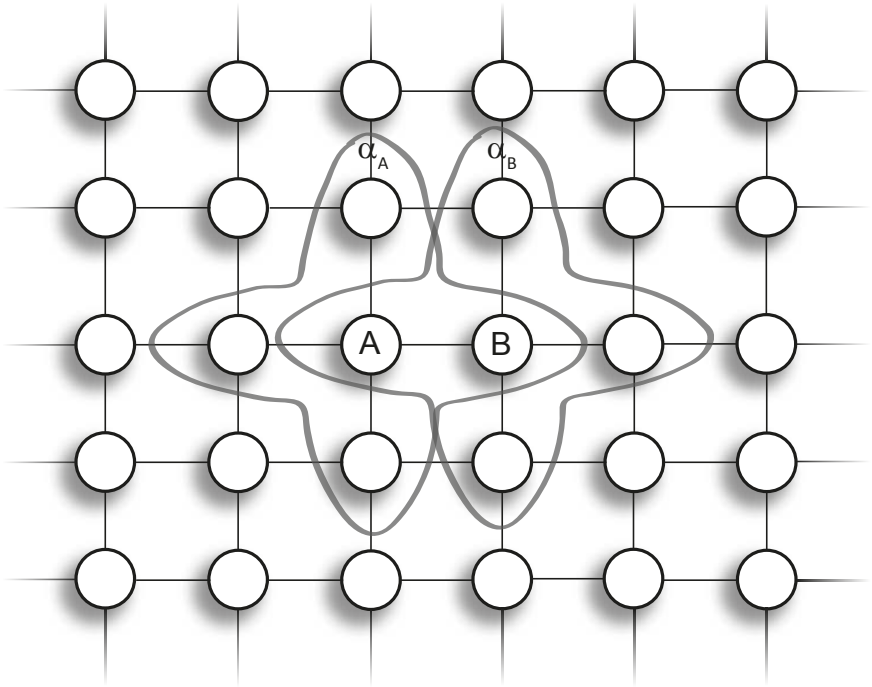

Figure 4.2: Pattern of interactions in *N*-Person games modeled on structured populations - Above we schematize the social neighborhood of two connected individuals, A and B. The games centered on themselves (α_A and α_B respectively) are not enough to determine their individual fitness; instead, we consider all the $k_i + 1$ games in which an individual i participates: those centered on the individual i plus those centered on each of his k_i neighbors.

determine an individual's fitness. Figure 4.2 represents a small part of a square lattice with an average degree $\langle k \rangle = 4$ where two neighboring individuals, A and B, and the games centered on each of them are highlighted. A given individual not only participates in the game centered on himself/herself and involving his/her neighbors, but also in the games centered in his/her neighbors. In this case, in order to compute the fitness of an individual i in an N-Person game we take into account $k_i + 1$ games, where k_i represents the number of neighbors of individual i: the game centered on the individual plus the games centered on each of his neighbors. Thus, in N-Person games it seems evident that not only the social context of an individual is important for his fitness (as occurs for 2-person games) but also his neighbors' social context.

However, previous works on spatial N-Person games (103) consider (for computational efficiency) only the game centered on an individual, arguing that such sim-

plification does not significantly alter the evolutionary dynamics and the final average levels of cooperation. We investigate to which extent this simplification is valid, by simulating the **NPD** on ring regular, homogeneous random (**HoRand**) and scale-free Barabási-Albert (**BA**) networks (see Methods – section 4.10 – for details) when individual fitness is computed taking into account:

- only the game α_i centered on each individual i (which we denote as $f_i^1 = \Pi_{s_i}(n_C)$, with $s_i \in \{\boldsymbol{C}, \boldsymbol{D}\}$),
- the game α_i centered on individual i plus the games centered on each of his k_i neighbors ($f_i^{k+1} = f_i^1 + \sum_j f_j^1$ where the index j refers to the k_i neighbors of individual i, and f_j^1 represents the gain that individual i obtains when participating in the game centered on individual j).

The initial state of the population will correspond to a random distribution of 50% of ***C**s* and ***D**s* in the nodes of the network. In each time-step of the evolution of the population, all individuals evaluate their individual fitness, by assessing all games in which they participate in. Also, each individual is given the opportunity to revise his or her strategy. A strategy revision occurs according to the following method: an individual A randomly chooses a neighbor B, whom he will imitate only if he is more successful than him, with a probability proportional to the fitness difference $f_B - f_A$, and given by equation 3.27. We evaluate the impact of population structure, and the method adopted for computing individuals' fitness, by studying the final average fraction of cooperators when the population reaches a stationary state (that is, a state for which the global composition of the population in terms of the number of ***C**s* and ***D**s* is not significantly altered in time). Please see Methods (section 4.10) for details.

Figure 4.3 shows the final average fraction of cooperators in the population as a function of the renormalized enhancement factor $\eta = \frac{r}{\langle k \rangle + 1}$ assuming both f_i^1 (figure 4.3A) and f_i^{k+1} (figure 4.3B). The vertical dashed line indicates the sharp transition from full defection to full cooperation that occurs in well-mixed populations, described in section 4.3. Regardless of computing individual fitness as f_i^1 of f_i^{k+1}, network reciprocity (82, 98, 106) leads to an enhancement on the levels of cooperation obtained when compared with the **WM** scenario. When individual fitness is given by f_i^1 (figure 4.3A), the transition from full defection to full cooperation begins at $\eta \approx 0.7$ regardless of the population structure (ring regular, **HoRand** and scale-free **BA**). Note that in this case individuals participate in just one game regardless of the population structure and on how many neighbors they have. The only aspect that differs from

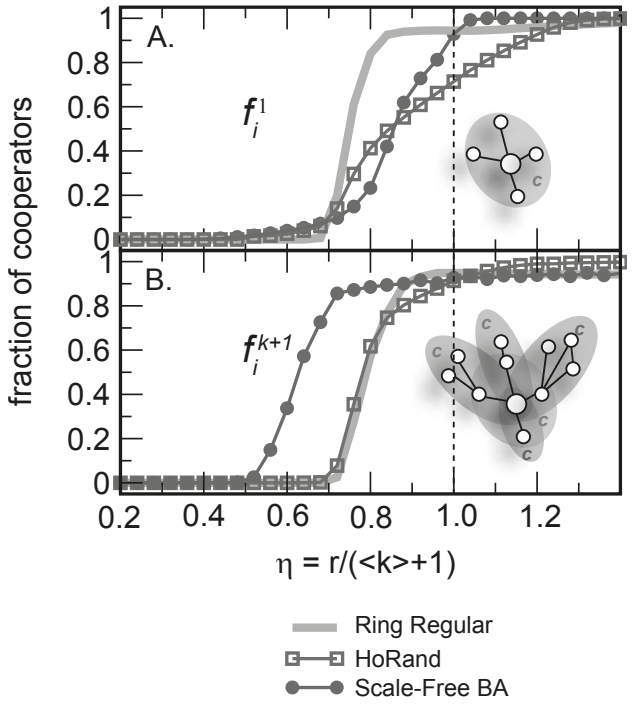

Figure 4.3: How Public are Public Goods Games? - Final average fraction of cooperators as a function of the renormalized enhancement factor $\eta = \frac{r}{\langle k \rangle + 1}$ for the **NPD** on networked populations, when for determining individual fitness we consider: **A.** only the group centered on the individual $\left(f_i^1\right)$, **B.** the game centered on him plus the ones centered on each of his k first neighbors $\left(f_i^{k+1}\right)$. Note the significant improvement on the average level of cooperation obtained for scale-free networks from panel A to panel B. Parameters: $Z = 10^3$, $\langle k \rangle = 4$, $c = 1.0$.

homogeneous to heterogeneous populations when individual fitness is computed as f_i^1 is the group size of the Public Good Game in which individuals participate. In scale-free **BA** populations there is a marked heterogeneity in the size of **PGGs**, but this does not seem enough to promote higher average levels of cooperation in comparison with homogeneous populations.

When individual fitness is computed using f_i^{k+1}, the qualitative behavior in homogeneous populations remains approximately the same but the same does not occur in scale-free **BA** populations. In the latter, the departure from full defection to full cooperation starts at approximately $\eta \approx 0.5$ – as opposed to the value $\eta \approx 0.7$ for homogeneous populations. Note that the behavior of the curve for scale-free **BA** pop-

ulations in figure 4.3B is quite different from the curves for ring regular and **HoRand** populations in the same panel. This is due to the introduction of two levels of social diversity:

- Diversity in the size of the **PGGs**, and
- Diversity in the number of **PGGs** in which different individuals engage.

Comparing the results presented in figure 4.3A with those from figure 4.3B for the scale-free **BA** networks, we can say that allowing for different individuals to interact a different number of times promotes a significant enhancement of cooperation levels.

Although not relevant for the present analysis, another aspect worth noticing is the impact of computing individual fitness using f_i^1 of f_i^{k+1} when individuals are part of ring regular and **HoRand** networks. In both networks, all individuals participate in the same number of games: with f_i^1 they participate only in one game, while with f_i^{k+1} they participate in $\langle k \rangle + 1$ games. What differs is how neighborhoods are organized: ring regular networks are characterized by a much larger clustering coefficient than **HoRand** networks ($C_{WS}^{RING} = 0.5$ and $C_{WS}^{HORAND} \approx 0$ for $\langle k \rangle = 4$). It appears that this difference is most significant for f_i^1 (coexistence levels register a large fraction of cooperators in ring regular than in **HoRand** networks), and this disparity disappears when all $\langle k \rangle + 1$ games are taken into account. Further ahead in this chapter we will analyze in more detail the impact of clustering on the final average cooperation levels.

In sum, we conclude that, not only the simplification of computing individual fitness as f_i^1 is only qualitatively valid for homogeneous populations, but also that the diversity in the number and size of **PGGs** an individual engages in scale-free **BA** networks promote higher average levels of cooperation for a larger range of η values. On the following sections, we will always assume that individual fitness is computed as f_i^{k+1}, unless explicitly stated otherwise.

4.5 Act of giving is more important than the amount given

We have so far assumed that the contribution of each individual i that is a cooperator to the common pool of the **PGG** is proportional to $k + 1$, that is, a ***C*** individual invests always the same cost c in each game, independently of the number of games in which he/she participates. This implies arbitrarily large resources for highly connected ***C****s*, a scenario that is somewhat unrealistic – social rules often provide a more egalitarian

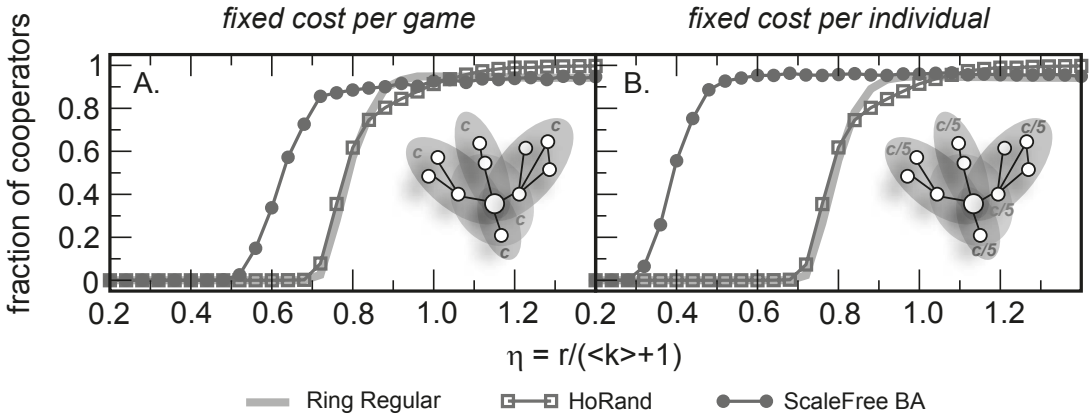

Figure 4.4: Contributive paradigms on the networked *N*-Person Prisoner's Dilemma - Final average fraction of cooperators as a function of the renormalized enhancement factor $\eta = \frac{r}{\langle k \rangle + 1}$ on ring regular, HoRand and scale-free Barabási-Albert populations, when we consider the following contributive schemes: **A.** *fixed cost per game*, **B.** *fixed cost per individual*. Parameters: $Z = 10^3$, $\langle k \rangle = 4$, $c = 1.0$.

contribution from individuals (107). We now consider the extreme opposite limit, in which all ***C*s** contribute the same overall cost, equally shared between all games in which each individual participates. In other words, in this new contributive paradigm, which we shall denominate as *fixed cost per individual* (as opposed to the conventional one, introduced in the previous section, which we denominate as *fixed cost per game*), a cooperator A with k_A neighbors invests $c/(k_A + 1)$ in each game in which he/she participates. Generically the payoff of an individual B with strategy s_B (1 if ***C***, 0 if ***D***) associated with the **PGG** centered in an individual A, $\Pi_{B,A}$, is given by

$$\Pi_{B,A} = \frac{r}{k_A + 1} \sum_{i=0}^{k_A} \frac{c}{k_i + 1} s_i - \frac{c}{k_B + 1} s_B \tag{4.12}$$

where $i = 0$ is the index referring to for individual A, s_i is the strategy of the neighbor i of A, and k_i is his/her degree. In this limit, a new level of diversity is introduced: that of individual contributions to each game. Real-world situations will naturally fall somewhere between these two limits, as individuals learn to cooperate (or defect) in better ways (43).

Figure 4.4 shows the final average levels of cooperation obtained on ring regular, **HoRand** and scale-free **BA** populations for both the *fixed cost per game* and *fixed cost per individual* contributive paradigms. Figures 4.4A and 4.4B show that the results for

homogeneous networks are independent of the contributive paradigm adopted: as all individuals participate in the same number of games, of equal size, the contributions of ***C**s* is simply rescaled to $\frac{c}{\langle k \rangle + 1}$, and this affects in equal manner all individuals in the population. Under the *fixed cost per individual* paradigm, the contributions are lower and therefore the final outcome for all members in a group will be proportionally lower, but since for strategy revision the only aspect that matters if the fitness difference between the potential role model and the focal player, this rescaling only affects the evolutionary time towards the stationary state.

Regarding the scale-free **BA** networks (figures 4.4A and 4.4B), the *fixed cost per individual* paradigm promotes an impressive boost in cooperation. In this case, the marked heterogeneous nature of the underlying network of contacts introduces three distinct levels of social diversity: besides the diversity in the number and size of **PGGs** an individual engages, the contribution of a cooperator to a **PGG** is also determined by his social context. Because each individual i that is a cooperator now contributes with $\frac{c}{k_i+1}$ to each game (where k_i represents the number of neighbors of individual i), diversity resulting from heterogeneous networks determines a richer spectrum of individual fitness. In a single **PGG**, the fitness difference between a ***C*** and a ***D*** is no longer constant and proportional to the cost c, as on homogeneous networks, but now depends on the social context of the individual.

In fact, heterogeneity gives a natural advantage on hubs, as will be shown in detail in section 4.8: under the *fixed cost per individual* contributive paradigm, the relative fitness of a cooperator increases with its connectivity, and consequently hubs are those that turn most quickly into cooperation. In practice, ***C**s* survive extinction for values of $\eta = \frac{r}{\langle k \rangle + 1}$ of about 0.25. Because $\langle k \rangle = 4$, $\eta = 0.25$ implies that $r = 1.25$, much lower than the size $N = 3$ of the smallest group in the entire population[†]. Note that, in those games for which $\eta_k = \frac{r}{k+1} > 1$ (the smallest groups), the social dilemma is relaxed, because in this case it is better to play ***C*** than ***D***. As figure 4.4B shows, cooperation prevails despite $\eta_k < 1$ in every **PGG** played. In fact, the impact of diversity is preserved even when the social dilemma is transformed such that defection is always preferred, irrespective of η.

It still remains to explain how a ***D*** individual on a large hub can be taken over by a ***C***. This will be explained in detail in section 4.8; briefly, what occurs is that ***D**s* are

[†]Because we are studying scale-free **BA** networks with average connectivity $\langle k \rangle = 4$, the lower number of connections of a given node that is registered in the network is $k_i = 2$, which corresponds to a group size of $N = 3$.

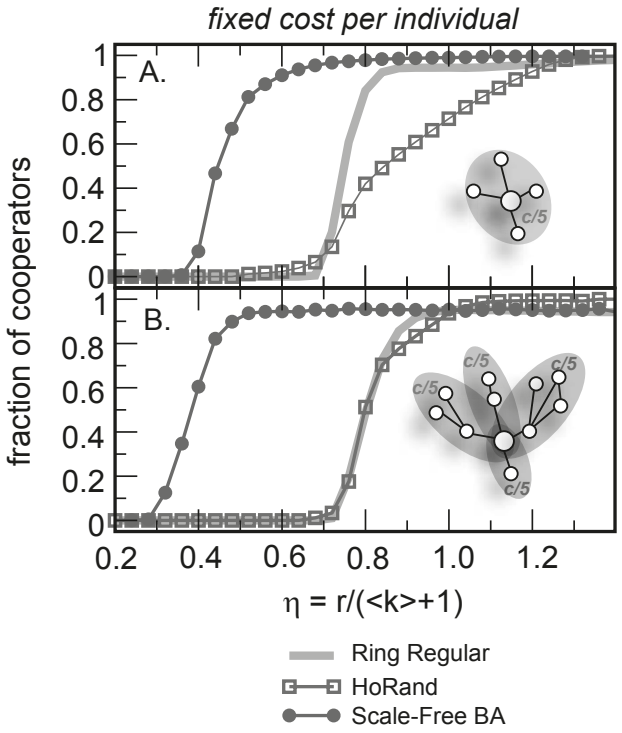

Figure 4.5: Extended study of the *fixed cost per individual* contributive paradigm in the *N*-Person Prisoner's Dilemma - In order to understand the origin of the boost in cooperation documented in figure 4.4 for the *fixed cost per individual* contributive paradigm, we analyze the extreme situations when **A.** only the game centered on the individual is taken into account for his fitness $\left(f_i^1\right)$, **B.** all but the game centered on himself are taken into account to compute his fitness $\left(f_i^{k+1} - f_i^1\right)$. Parameters: $Z = 10^3$, $\langle k \rangle = 4$, $c = 1.0$.

victims of their own success: successful ***D****s* breed ***D****s* in their neighborhood, inducing a negative feedback mechanism that reduces their fitness. Consequently, they become vulnerable to nearby cooperators. Once invaded by a ***C***, a hub will remain ***C***, as by placing ***C****s* on nearby sites, successful ***C****s* increase their fitness. The role of the ***C****s* is therefore crucial and twofold: they efficiently disseminate the cooperator strategy across social networks, whereas they get a stronghold on hubs by minimizing the potential loss from exploitation by free-riding ***D****s*. It is noteworthy that the results shown in figure 4.4B, in which selection is strong, are robust with respect to the detailed evolutionary dynamics (if we use the Fermi Imitation update method (77, 78, 79) instead of the replicator analogue in finite populations), to the updating strategy (synchronous versus asynchronous) and even to errors (mutations cannot destroy ***C***-dominance).

In order to understand the origin of such a boost in cooperation, we extend our study of the *fixed cost per individual* contributive paradigm. In figure 4.5 we present the results obtained in the extreme cases when individuals participate only in the games centered on themselves (figure 4.5A) and when individuals participate only in the games centered on their neighbors (figure 4.5B). In scale-free **BA** networks, while in the former case the transition from full defection to full cooperation occurs at approximately $\eta \approx 0.4$, in the latter case it occurs for $\eta \approx 0.3$. In face of these results, we affirm that a significant contribution for the evolution of cooperation comes from individuals playing the games of others.

Although it is difficult to apply analytical methods to complex networks (and for that reason all our results have so far relied on computational simulations), it is still possible to have an analytical insight on what is the reason behind this significant boost in cooperation. In section 4.8 we provide some analytical basis to the mechanism responsible for the cooperators advantage towards defectors.

4.6 Economical Perspective

In a more economical perspective, figure 4.6 shows the fraction of the population that holds a given fraction of the total wealth both for ring regular and scale-free **BA** networks, when every individual in the population is a cooperator. We consider both the *fixed cost per game* and the *fixed cost per individual* contributive paradigms.

On regular networks the wealth distribution is egalitarian, regardless of the contributive paradigm considered, as represented by the thick black bar in figure 4.6. In scale-free **BA** networks, on the other hand, the wealth distribution follows a power-law, also regardless of the contributive scheme, as represented by the gray bars for the *fixed cost per game* contributive paradigm, and by the open squares for the *fixed cost per individual* contributive paradigm.

As discussed in detail in section 4.4 and figure 4.2, the income of an individual depends not only on her number of social ties but also on the connectivity of her neighbors. In this sense, heterogeneous graphs lead to the appearance of several classes of individuals, both in what concerns the number of games in which they participate and also in what concerns their wealth. Let us then consider, for simplicity, that according to their number k_i of social ties in a (heterogeneous) network individuals can either belong to the

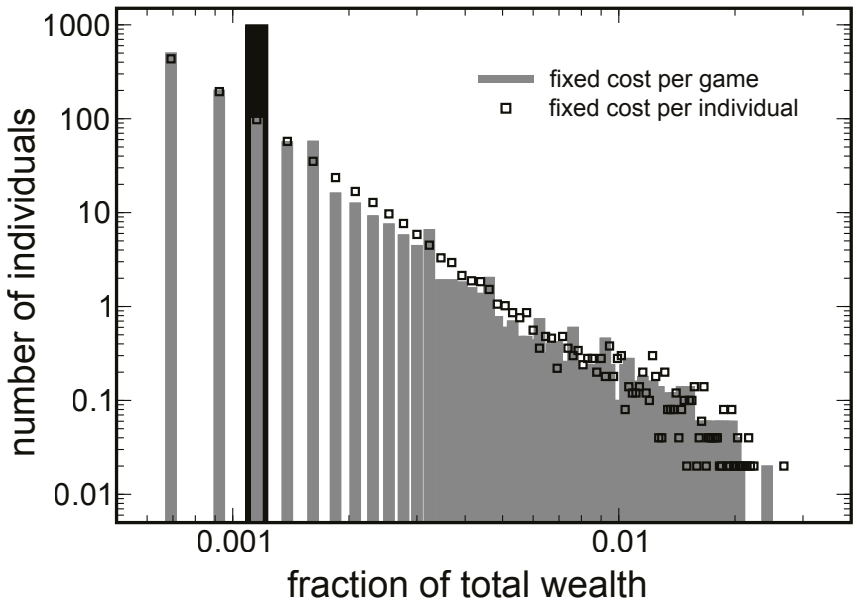

Figure 4.6: Wealth distribution on the *N*-Person Prisoner's Dilemma - On scale-free **BA** networks, the wealth (fitness) distribution follows a power-law, both when each individual invests a fixed cost per game (gray bars) or when he/she spends an overall fixed cost (open squares). These behaviors contrast with the egalitarian wealth distribution characteristic of homogeneous graphs (thick black bar). Parameters. $Z = 10^3$, $\langle k \rangle = 4$, $r = 5.0$ (that is, $\eta = 1.0$).

- **Low-Degree** class, whenever $k_i < \langle k \rangle$;
- **Medium-Degree** class, whenever $\langle k \rangle \leq k_i < \frac{k_{max}}{3}$, and
- **High-Degree** class, whenever $\frac{k_{max}}{3} \leq k_i \leq k_{max}$.

where k_{max} stands for the value of the largest connectivity observed in a given network.

Furthermore, based on their personal wealth (fitness) we distinguish individuals according to the following rules:

- **Lower-Class**, when $f_i < \frac{f_{total}}{3}$;
- **Middle-Class**, when $\frac{1}{3} f_{total} \leq f_i < \frac{2}{3} f_{total}$, and
- **Upper-Class**, when $\frac{2}{3} f_{total} \leq f_i \leq f_{total}$,

where f_{total} is the total wealth of the population at a given time of the evolutionary process.

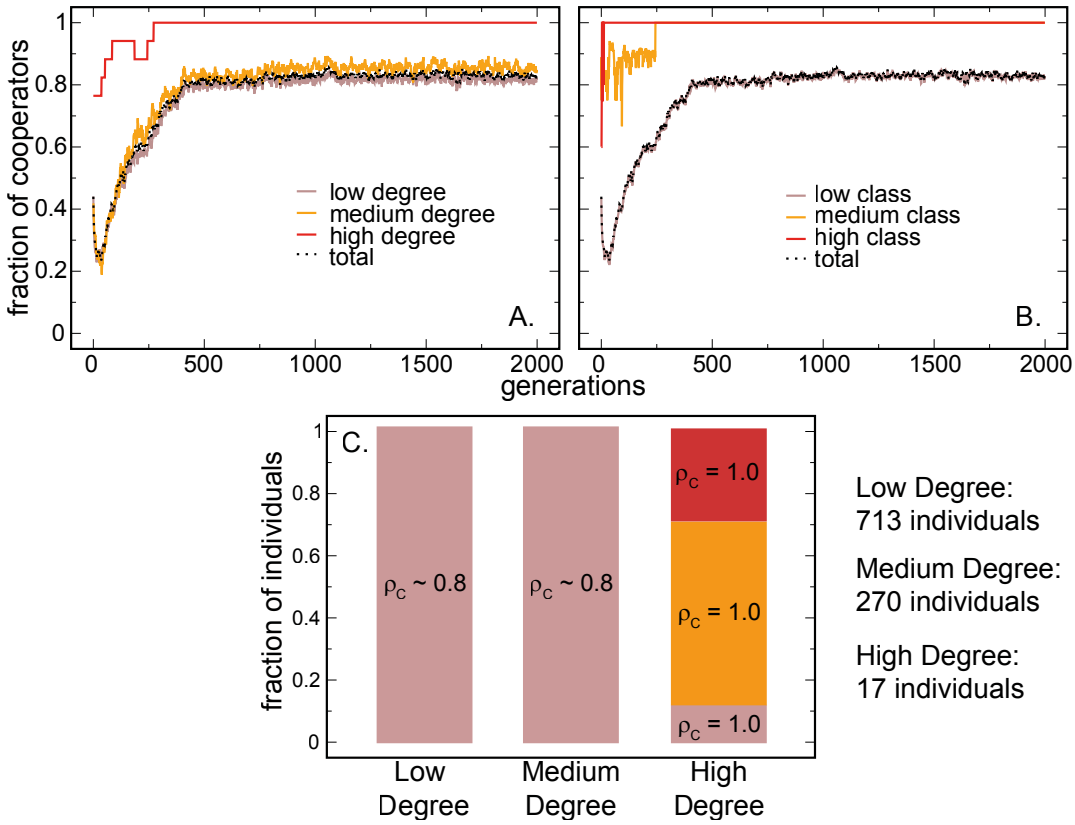

Figure 4.7: Time-dependence of the fraction of cooperators on scale-free Barabási-Albert populations for the *N*-Person Prisoner's Dilemma - Representative run of the time-evolution of cooperators on scale-free Barabási-Albert networks, classified according to: **A.** degree, **B.** wealth, and **C.** both degree and wealth combined (at the end of the 2 x 10^3 generations). In panel **C.**, ρ_C represents the fraction of cooperators that are classified as having a Low, Medium or High Degree, respectively, and can be observed in the final generations represented in panel **A**. Parameters: $Z = 10^3$, $\langle k \rangle = 4$, $r = 1.7$ (that is, $\eta = 0.34$).

In figure 4.7 we show the evolution in time (generations, taking into account that 1 generation corresponds to Z strategy revisions in a synchronous update) of the fraction of cooperators in the population when adopting the *fixed cost per individual* paradigm. Individuals are classified according to both their connectivity and relative fitness, as discussed above. The time-dependent curves in figure 4.7 provide a representative *run* for a multiplication factor $r = 1.7$, that is, $\eta = 0.34$ ($\langle k \rangle = 4$). For this value of η, cooperators dominate the population but are unable to wipe out defectors.

In figure 4.7A, it is clear that individuals of **High-Degree** quickly become cooperators and remain so for the rest of the evolutionary process. On the contrary, in the first generations **Low-Degree** and **Medium-Degree** classes start by adopting defector strategies, but the more individuals adopt the ***D*** strategy, the more vulnerable they become to the influential role played by ***C*** hubs (**High-Degree** individuals). Consequently, the situation quickly reverts to a scenario where the majority of individuals of **Low-Degree** and **Medium-Degree** are cooperators.

This analysis is complemented by figure 4.7B, which shows that high levels of wealth (fitness) – **Upper-Class** – are associated with ***C****s*. Moreover, no ***D****s* survive in the **Middle-Class**, being all relegated to the **Lower-Class**.

Finally, figure 4.7C combines the information provided separately in panels A and B, correlating fitness, degree and strategy. Only individuals of **High-Degree** classes can achieve the **Upper-Class** in terms of wealth. On the other hand, the presence of ***D****s* in the population, both in the **Lower-Degree** and **Medium-Degree** classes, renders some **High-Degree** individuals unable to join the rest of the "hubs" in the upper class. The survival of ***D****s* is therefore detrimental to the overall wealth of the population and, individually, ***D****s* fare pretty badly in strongly heterogeneous communities, down to small values of the enhancement factor r. Diversity provides indeed a powerful mechanism to promote cooperation.

4.7 Dependence on population size and average connectivity

We now investigate how the results discussed above depend on both population size Z and average connectivity $\langle k \rangle$. To this end we carried out simulations for $Z = 500, 1000$ and 5000 (for fixed average connectivity $\langle k \rangle = 4$), and for several average connectivities between $\langle k \rangle = 4$ and $\langle k \rangle = 70$ for fixed $Z = 1000$. Results for fixed $\langle k \rangle = 4$ are shown in Figures 4.8 and 4.9, whereas results for fixed Z and varying $\langle k \rangle$ are shown in Figure 4.10.

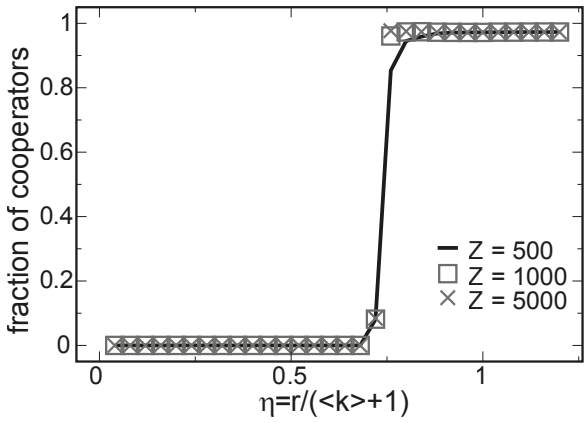

Figure 4.8: Dependence of the average level of cooperation on the population size for the *N*-Person Prisoner's Dilemma – ring regular networks. - Final average fraction of cooperators as a function of the renormalized enhancement factor $\eta = \frac{r}{\langle k \rangle + 1}$ on ring regular networks. Results show that evolution of cooperation is independent of population size for fixed average connectivity $\langle k \rangle$. Note that, for regular networks, the results do not depend on the cost paradigm: *fixed cost per game*, or *fixed cost per individual*. Parameters: $\langle k \rangle = 4$, $c = 1.0$

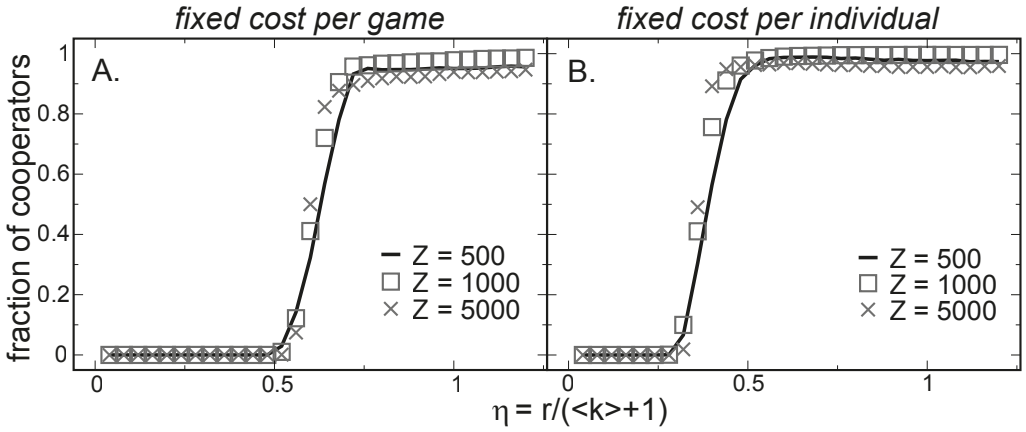

Figure 4.9: Dependence of the average level of cooperation on the population size for the *N*-Person Prisoner's Dilemma – scale-free Barabási-Albert networks - Final average fraction of cooperators as a function of the renormalized enhancement factor $\eta = \frac{r}{\langle k \rangle + 1}$ on scale-free **BA** networks. The results show that the evolution of cooperation is independent of population size for fixed average connectivity. Parameters: $\langle k \rangle = 4$, $c = 1.0$.

Figures 4.8 and 4.9 evidence the negligible dependence of our results on the overall population size. We have checked that, for small $\langle k \rangle$, the results are valid down to population sizes of $Z \approx 250$, below which the results are less smooth, given the increasing role of finite-size fluctuations on the evolutionary dynamics. Note that the results for regular networks presented in figure 4.8 are independent of the contributive paradigm chosen.

Concerning the dependence of the results on the average connectivity $\langle k \rangle$, several factors work against cooperative behavior when the average number of social ties $\langle k \rangle$ increases. The increase of the average size of the groups $(\langle k \rangle + 1)$ induces an overall scaling of the value of the multiplication factor r: since in figure 4.8 we plot the fraction of cooperators as a function of the renormalized enhancement factor $\eta = \frac{r}{\langle k \rangle + 1}$, this scaling is automatically included, which means that the remaining differences between curves are due to other factors.

The results of figure 4.10 show that, irrespective of the cost paradigm, the critical value of η above which cooperators no longer get extinct does not qualitatively change with the average connectivity and is equivalent to an overall rescaling of r. This reflects the important role played by the average group size $(\langle k \rangle + 1)$.

Furthermore, increasing $\langle k \rangle$ towards a fully-connected network corresponds to the limit case of having a **PGG** with the size of the whole (finite) population. In this limit, the presence of a single defector will always lead to the demise of cooperation, independently of the value of r (with $r > 0$). For instance, figure 4.10A shows that, on regular networks, $\langle k \rangle = 16$ is enough to reduce significantly the final number of cooperators, even when $\eta < 1$.

Similarly to simple 2-player games, spatially constrained populations are only able to sustain sizable levels of cooperative behavior on sparse graphs (98, 103, 106) – lack of diversity makes survival of cooperation contingent on the feasibility of cooperators to form tight communities. With increasing connectivity, these tight communities become increasingly vulnerable to exploitation, favoring defectors. Figure 4.10B shows the significant boost in cooperation obtained for scale-free **BA** networks when compared to regular networks. In this case, the cooperation level decreases with average connectivity $\langle k \rangle$. The results of figure 4.10 correspond to the situation of a fixed investment per individual, but the conclusions remain qualitatively independent of the investment scheme adopted.

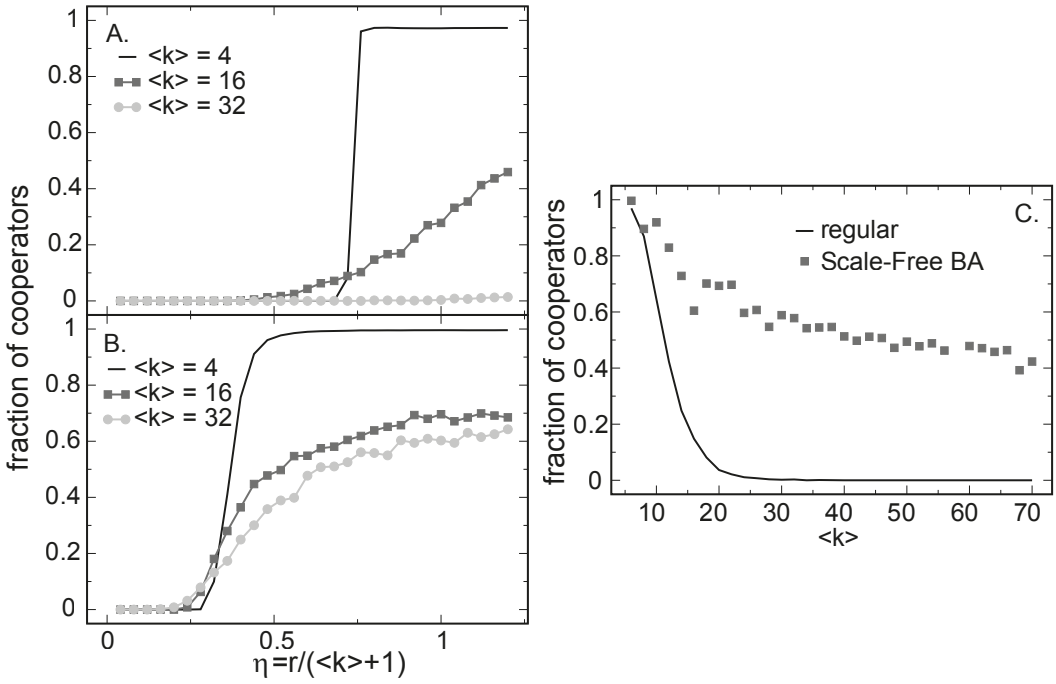

Figure 4.10: Evolution of cooperation under the *N*-Person Prisoner's Dilemma in populations with different average connectivity $\langle k \rangle$ - In panels **A.** and **B.** we represent the final average fraction of cooperators as a function of the renormalized enhancement factor $\eta = \frac{r}{\langle k \rangle + 1}$ for ring regular (panel A) and scale-free Barabási-Albert (panel B) networks. In panel **C.** we plot the final fraction of cooperators (for fixed $\eta = 0.8$ in a region of coexistence of defectors and cooperators – see figure 4.9). With increasing average degree z, results for the **NPD** on networks follow a trend similar to that obtained for simple 2-player games on networks (65) as one would expect. As $\langle k \rangle$ becomes sizable cooperation will inevitably collapse as average group size increases and the overall degree of heterogeneity (on scale-free networks) also decreases. Parameters: $Z = 10^3$, $c = 1.0$.

4.8 Cooperators (and Defectors) on the Star(s)

Structured populations pose some difficulties to any attempt of a simple analytical analysis. As discussed in section 4.4, local interactions lead to a marked diversity in the fitness of individuals adopting the same strategy, as it becomes strongly dependent of the individuals' neighborhood and of their position on the network. This strongly differs from the **WM** scenario, in which everyone is a neighbor of everyone else (a **WM** population can be modeled as a complete network).

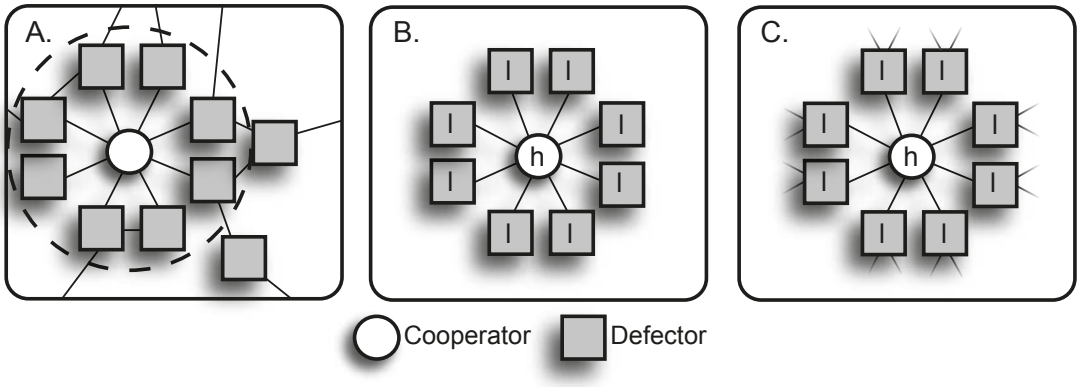

Figure 4.11: The star and generalized star graphs. - We shall employ the simple star graph depicted in panel **B.**, in this case with 1 center (h) and 8 leaves (l), as the simplest abstraction of the sub-graph selected in panel **A.**. In general, we will consider a star of size N, with 1 center (h) and $N-1$ leaves (l). In panel **C.** we generalize the star such that every leaf has $n-1$ links. As a simplification, the overall structure exhibits no loops.

Furthermore, in the particular case of the scale-free **BA** networks considered in sections 4.4 and 4.5, all individuals have at least 2 neighbors. This particularity is a consequence of the method used to create the networks (the Barabási-Albert Method described in section 2.4), for which we have $\langle k \rangle = 2m$. This feature determines the occurrence of short closed loops, for example triangles, which are responsible for the small yet non-zero value of the cluster coefficient exhibited by these networks, as depicted in figure 4.11. This makes it difficult to use the pair-approximation approach (section 3.3.4).

Despite these difficulties, it is possible to obtain some simple mathematical relations that shed a light into the mechanism responsible for the enormous boost of cooperation shown in the previous sections. We start by resorting to the simplest possible (and most disadvantageous) situation for a cooperator, that of a single ***C*** in a population of ***D*s**. Moreover, we shall start by neglecting the connections of the neighbors of this ***C*** to other ***D*s**, which naturally leads to a star-graph, figure 4.11B. To the extent that the single ***C*** may have a larger fitness than any of her ***D***-neighbors, the ***C***-strategy will spread. The fact that on a star there are only two types of nodes – *center* and *leaves* – and no loops clearly simplifies the mathematical analysis.

4.8.1 The Single Star

Let us then consider a star of size N: one center (h), and $N-1$ leaves (l) – with the single ***C*** located on the center (figure 4.11B). In such scenario (if the ***C*** is placed on a leaf her fitness will never exceed that of a ***D*** in the center), the fitnesses of the ***C*** in the center ($f_{C,h}$) and a ***D*** on a leaf ($f_{D,l}$) are given by

$$f_{C,h} = \underbrace{\frac{rc}{N^2}}_{\text{game centered on } h} + \underbrace{(N-1)\frac{r}{2}\frac{c}{N}}_{\text{games centered on the leaves } l} - c \tag{4.13a}$$

$$f_{D,l} = \underbrace{\frac{rc}{N^2}}_{\text{game centered on } h} + \underbrace{\frac{rc}{2N}}_{\text{game centered on } l} \tag{4.13b}$$

Note that the ***C***-hub participates in a total of N games – the one centered on himself/herself, and the $N-1$ centered in each of his/her ***D*** neighbors. The contribution of the ***C***-hub to each of the games is therefore c/N, according to the *fixed cost per individual* contributive paradigm. In equations 4.13, the first term corresponds to the payoff obtained by each of the players of the game centered on the ***C***-hub, while the second term corresponds to the payoff obtained by each of the players of the games centered on the leaves of the star. From the expressions above, the ***C***-strategy will spread whenever its fitness is higher than that of the ***D*** strategists on the leaves, that is,

$$f_{C,h} - f_D, l > 0 \Rightarrow r > \frac{2}{1-2/N} \tag{4.14}$$

Not only it is possible for a single ***C*** to become advantageous, but also the critical value of the enhancement factor r above which it can occur decreases with increasing number of leaves. The likelihood of the ***C***-strategy to spread increases with the connectivity of the node on which the ***C*** is located.

Clearly, the star is a gross simplification of a realistic population structure; a useful, yet simple, structure, is the generalized star depicted in figure 4.11C, in which every leaf has $n-1$ external links to other ***D***-neighbors. In this case, the fitnesses of the ***C***-center ($f_{C,h}$) and the ***D*** leaves ($f_{D,l}$) are given by

$$f_{C,h} = \underbrace{\frac{rc}{N^2}}_{\text{game centered on } h} + \underbrace{(N-1)\frac{rc}{nN}}_{\text{games centered on the leaves } l} - c \tag{4.15a}$$

$$f_{D,l} = \underbrace{\frac{rc}{N^2}}_{\text{game centered on } h} + \underbrace{\frac{rc}{nN}}_{\text{game centered on } l} \tag{4.15b}$$

Note that in this generalized configuration the ***D***-leaves now participate, each of them, in a total of n games, but of these only the game centered on themselves and the game centered on the ***C***-hub provide a positive gain (these are the only ones for which the ***C***-hub contributes). Taking into account equations 4.15, in this case, the ***C***-strategy can spread whenever

$$f_{C,h} - f_{D,l} > 0 \Rightarrow r > \frac{n}{1-2/N} \tag{4.16}$$

which is a decreasing function of N, for a fixed n value. Invasion is easier the larger the difference (diversity) between the connectivities of the center and of the leaves. When $n = N$, we obtain the limit of a "homogeneous generalized star", in which we may write for the critical threshold

$$r > \frac{N}{1-2/N} \tag{4.17}$$

Scale-free **BA** networks are characterized by having a majority of nodes with a few connections, whereas a minority of nodes – the *hubs* – have a high number of connections and ensure the overall connectivity of the network. Naturally, most of the hubs connect to nodes of low connectivity, which provides excellent conditions for a ***C*** on a hub to spread to other nodes.

4.8.2 The Double Star

The above analysis considered the spread of the ***C***-strategy starting from a highly connected node. But how does a ***C*** individual invade a hub in the first place? To answer this question let us consider to the double-star graph, depicted in figure 4.12, and once again analyze the most disadvantageous configuration for a ***C*** individual. We have two centers (hubs h_1 and h_2) with $N-2$ and $M-2$ leaves respectively, and one link connecting the two centers. Note that the size of the groups centered on h_1 and h_2 must obey $N > 2$ and $M > 2$ respectively. However, this condition is met even for the low average degrees ($\langle k \rangle = 4$) studied in sections 4.4 and 4.5: in this case, the lowest connected individuals have 2 neighbors and the group size is 3. Each of the $N-2$ leaves has $n-2$ external links, whereas each of the $M-2$ leaves has $q-2$ external links. In this case, the fitness obtained by the cooperator on the left center (f_{C,h_1}) is given by

$$f_{C,h_1} = \underbrace{\frac{rc}{N^2}}_{\text{game centered on } h_1} + \underbrace{(N-2)\frac{rc}{nN}}_{\text{games centered on the leaves } l_1} + \underbrace{\frac{rc}{MN}}_{\text{game centered on } h_2} - c, \tag{4.18}$$

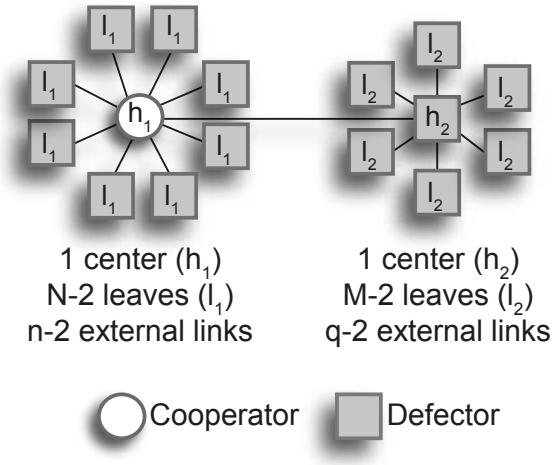

Figure 4.12: The generalized double star graph - A. We have 2 centers (h_1 and h_2), the left one with $N-2$ leaves and the right one with $M-2$ leaves. Each l_1 has $n-2$ external links (no loops) whereas each l_2 has $q-2$ external links.

the fitness of the defector on the right center (f_{D,h_2}) is

$$f_{D,h_2} = \underbrace{\frac{rc}{MN}}_{\text{game centered on } h_2} + \underbrace{\frac{rc}{N^2}}_{\text{game centered on } h_1}, \tag{4.19}$$

and the fitness of the defector on the leaves of the left center (f_{D,l_1}) is

$$f_{D,l_1} = \underbrace{\frac{rc}{N^2}}_{\text{game centered on } h_1} + \underbrace{\frac{rc}{nN}}_{\text{game centered on } l_1} \tag{4.20}$$

In this case the condition for the ***C***-hub to spread his/her strategy to h_2 is given by the difference of the fitnesses in equations 4.18 and 4.19, that is,

$$f_{C,h_1} - f_{D,h_2} > 0 \Rightarrow r > \frac{nN}{N-2} \equiv \alpha, \tag{4.21}$$

given that $N > 2$, whereas the condition for spreading to the leaves l_1 of h_1 is given by the difference of the fitnesses in equations 4.18 and 4.20, that is,

$$f_{C,h_1} - f_{D,l_1} > 0 \Rightarrow r > \frac{nMN}{n + M(N-3)} \equiv \gamma \tag{4.22}$$

for $N > 3$. Given that

$$\alpha - \gamma = \frac{nN(n-M)}{(N-2)(n+M(N-3))}, \tag{4.23}$$

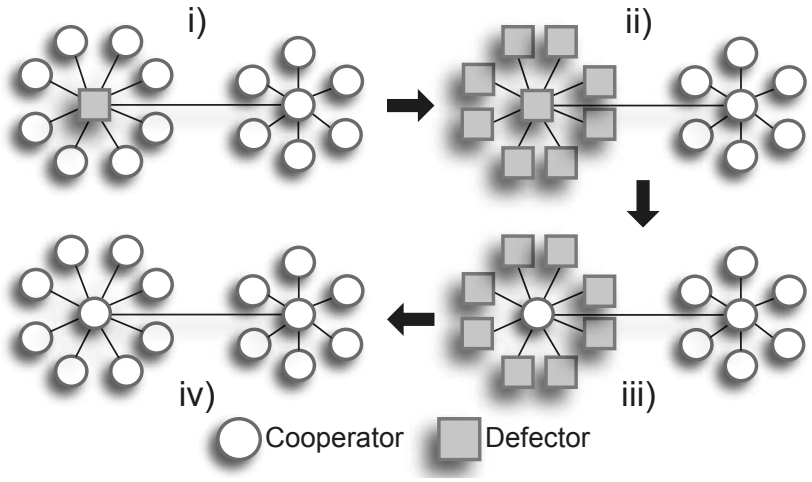

Figure 4.13: The demise of a successful *D* - We consider the simple double star construction, with two centers (hubs h_1 and h_2); the center h_1 has $N-2$ leaves l_1, while the center h_2 has $M-2$ leaves l_2. As a simplification, we neglect any external links of the leaves l_1 and l_2. The first configuration corresponds to a single ***D*** in a sea of ***C*s**. Whenever the ***D***-fitness is larger than the fitness of any of the ***C*s**, the ***D***-strategy will spread. We show that such spreading occurs preferentially to the leaves, which contributes to reduce the fitness of the ***D***-center, making it vulnerable to a take over by the central ***C***. Such negative feedback mechanism of the ***D*s** leads to their own demise.

we have $\alpha < \gamma$ whenever $M > n$, and in these conditions it is easier for the ***C*** on h_1 to invade h_2 than the leaves of h_1. In fact, the invasion of h_2 depends only on the number of leaves of h_1 and of their connectivity: the larger the leaf-connectivity the harder it will be to invade h_2, whereas the larger the connectivity of h_1, the easier it will be to invade h_2. In particular, note that the invasion condition does not depend on the connectivity of h_2. In other words, even on "generalized" double-stars ***C*s** will manage to expand to the extent that $r > \gamma$.

4.8.3 The Demise of a Successful D

Last but not least we show how ***C*s** can resist invasion by ***D*s** in the double-star construction – a crucial mechanism to the survival of cooperation (108). To this end, we introduce a defector in a population of cooperators, and make use of the double star graph to show how strategies propagate and how cooperation can become advantageous, as illustrated in figure 4.13. As a simplification, we resort to the simple double

star graph, in which we neglect the external links of any of the ***D*** leaves l_1 or l_2 of both centers. This allows for a significant simplification of the expressions obtained (as we do not need to take into account the connectivities of the leaves), but the conclusions that we draw here remain valid if we performed the more general calculations.

Figure 4.13 – from configuration i) to configuration ii):

The ***D*** strategy of the hub h_1 may, according to the fitnesses difference, spread either to the right hub h_2 or to any of the leaves l_1. According to the configuration **i)** depicted in figure 4.13, the fitness of the ***C*** individual on the right hub (f_{C,h_2}), the fitness of the ***D***-hub h_1 (f_{D,h_1}), and the fitness of any of the ***C*** leaves l_1 (f_{C,l_1}) are given by

$$f_{C,h_2} = \underbrace{\frac{r}{M}\left(\frac{c}{M} + (M-2)\,\frac{c}{2}\right)}_{\text{game centered on } h_2} + \underbrace{(M-2)\,\frac{r}{2}\left(\frac{c}{2} + \frac{c}{M}\right)}_{\text{games centered on leaves } l_2} + \underbrace{\frac{r}{N}\left(\frac{c}{M} + (N-2)\,\frac{c}{2}\right)}_{\text{game centered on } h_1} - c \tag{4.24a}$$

$$f_{D,h_1} = \underbrace{\frac{r}{N}\left(\frac{c}{M} + (N-2)\,\frac{c}{2}\right)}_{\text{game centered on } h_1} + \underbrace{(N-2)\,\frac{rc}{4}}_{\text{games centered on leaves}} + \underbrace{\frac{r}{M}\left(\frac{c}{M} + (M-2)\,\frac{c}{2}\right)}_{\text{game centered on } h_2} \tag{4.24b}$$

$$f_{C,l_1} = \underbrace{\frac{rc}{4}}_{\text{game centered on } l_1} + \underbrace{\frac{r}{N}\left((N-2)\,\frac{c}{2} + \frac{c}{M}\right)}_{\text{game centered on } h_1} - c \tag{4.24c}$$

Whether a single ***D*** is the fittest individual in the double star will depend on the balance between N and M. Indeed, we obtain

$$f_{C,h_2} > f_{D,h_1} \Leftrightarrow r > \frac{4M}{M^2 - 4 - M(N-2)} \tag{4.25}$$

given that $N > 2$, and to the extent that r satisfies the inequality above, the ***C***-center will have a larger fitness that the ***D***-center and consequently will spread the ***C***-strategy onto the ***D***-star.

Another interesting condition is the one equating the fitness of both centers if, instead of a neighborhood with ***C***s only, the ***D***-center has only $n \leq N-2$ ***C*** neighbors. We may write

$$f_{C,h_2} > f^k_{D,h_1} \Leftrightarrow r > \frac{4M}{M^2 - 4 - Mn} \tag{4.26}$$

where f^k_{D,h_1} represents the fitness of the ***D***-center h_1 when he has only $n \leq N-2$ ***C*** neighbors.

Let us imagine, however, that we start with $m = N - 2$ and (for example) r is such that $f_{C,h_2} < f_{D,h_1}$. In this case the ***D*** strategy will spread. However, unlike the symmetric situation discussed before, here we get

$$[f_{D,h_1} - f_{C,l_1}] - [f_{D,h_1} - f_{C,h_2}] = \frac{rc}{4M^2}\left[4 + M(M^2 + M - 8)\right] > 0 \tag{4.27}$$

for $M > 2$. Consequently, it is more likely that ***D*** will spread to l_1 than to h_2, given that each player will imitate her neighbor with a probability proportional to the fitness difference. This means the neighborhood of h_1 will turn into ***D*** before h_2, creating the configuration **ii)** in figure 4.13 (in practice, it need not reach configuration **ii)** as whenever $f_{C,h_2} > f_{D,h_1^m}$ the ***C***-center may actually invade the ***D***-center).

In other words, ***Ds*** are *victims of their own success*, as they efficiently spread their strategy to the "weak" neighbors, reducing their own fitness and becoming prone to be taken over by the ***C***-center (108).

Figure 4.13 – from configuration ii) to configuration iii):

At this stage (configuration **ii)**) in figure 4.13), the fitnesses of both the ***D***-center (f_{D,h_1}) and the ***C***-center (f_{C,h_2}) are

$$f_{D,h_1} = \underbrace{\frac{rc}{NM}}_{\text{game centered on } h_1} + \underbrace{\frac{r}{M}\left(\frac{c}{M} + (M-2)\frac{c}{2}\right)}_{\text{game centered on } h_2} \tag{4.28a}$$

$$f_{C,h_2} = \underbrace{\frac{r}{M}\left(\frac{c}{M} + (M-2)\frac{c}{2}\right)}_{\text{game centered on } h_2} + \underbrace{\frac{rc}{NM}}_{\text{game centered on } h_1} + \underbrace{(M-2)\frac{r}{2}\left(\frac{c}{2} + \frac{c}{M}\right)}_{\text{games centered on leaves } l_2} - c \tag{4.28b}$$

such that h_2 easily becomes advantageous with respect to h_1 ($M > 2$)

$$f_{C,h_2} > f_{D,h_1} \Leftrightarrow r > \frac{4M}{M^2 - 4} \tag{4.29}$$

In other words, evolutionary dynamics leads the population into the configuration **iii)** in figure 4.13 (or, even better, the ***D***-center will be taken over by the ***C***-center before all ***Cs*** on the leaves of the left turn into ***Ds***).

Figure 4.13 – from configuration iii) to configuration iv):

At this stage we return to a configuration similar to the one of figure 4.12, but more beneficial for ***Cs***. The fitness of the ***C***-hub on the left center (f_{C,h_1}) and the fitness of

any of the ***D*** strategists on the leaves l_1 (f_{D,l_1}) are given, respectively, by

$$f_{C,h_1} = \underbrace{\frac{r}{N}\left(\frac{c}{N}+\frac{c}{M}\right)}_{\text{game centered on } h_1} + \underbrace{(N-2)\frac{rc}{2N}}_{\text{games centered on leaves } l_1} + \underbrace{\frac{r}{M}\left(\frac{c}{N}+\frac{c}{M}+(M-2)\frac{c}{2}\right)}_{\text{game centered on } h_2} - c \tag{4.30a}$$

$$f_{D,l_1} = \underbrace{\frac{rc}{2N}}_{\text{game centered on } l_1} + \underbrace{\frac{r}{N}\left(\frac{c}{N}+\frac{c}{M}\right)}_{\text{game centered on } h_1} \tag{4.30b}$$

The spreading of the ***C***-strategy to the leaves will take place whenever $(\{M,N\}>2)$

$$r > \frac{2M^2N}{2(M+N)+2MN(M-1)-3M^2} \tag{4.31}$$

which clearly favors invasion of the leaves, even for small N and M.

In practice, simulation results show that ***Cs*** will tend to dominate the population: in figure 4.14 we show representative runs of the **NPD** on the simple double star, highlighting the main transitions. We start with a defector in a population of cooperators, attributing the defector both to the largest center and the smallest center (figure 4.14A). We track the fraction of ***Cs*** on the leaves of both centers, and show how in both cases the double star evolves until it is composed solely by ***Cs***. We also study the evolution of the simple double star when a single cooperator is placed in a population of defectors, with the ***C*** located both in the largest center and in the smallest center (figure 4.14B) – also in this case the cooperative strategy is able to invade the whole simple double star.

As first noted in the beginning of this section, this analytical study is valid only in the limit of the non-existence of triangles (loops) in the population. Scale-free **BA** networks are characterized by a very small clustering coefficient (see section 2.4) and therefore the results obtained in their context can be explained qualitatively by these simple mathematical relations. But what would happen to the final average levels of cooperation if clustering was significant? Are topological clusters beneficial or not for cooperation in the framework of the **NPD**?

In figure 4.15 we compare the final fraction of cooperators obtained in scale-free networks grown according to the Barabási-Albert model (**BA**) and the Minimal Model (**MM**). The latter are characterized by a very large clustering coefficient (see section 2.4), of approximately 0.7 for $\langle k\rangle = 4$. The results show that clustering is beneficial for cooperation in the **NPD** regardless of the particular contributive paradigm

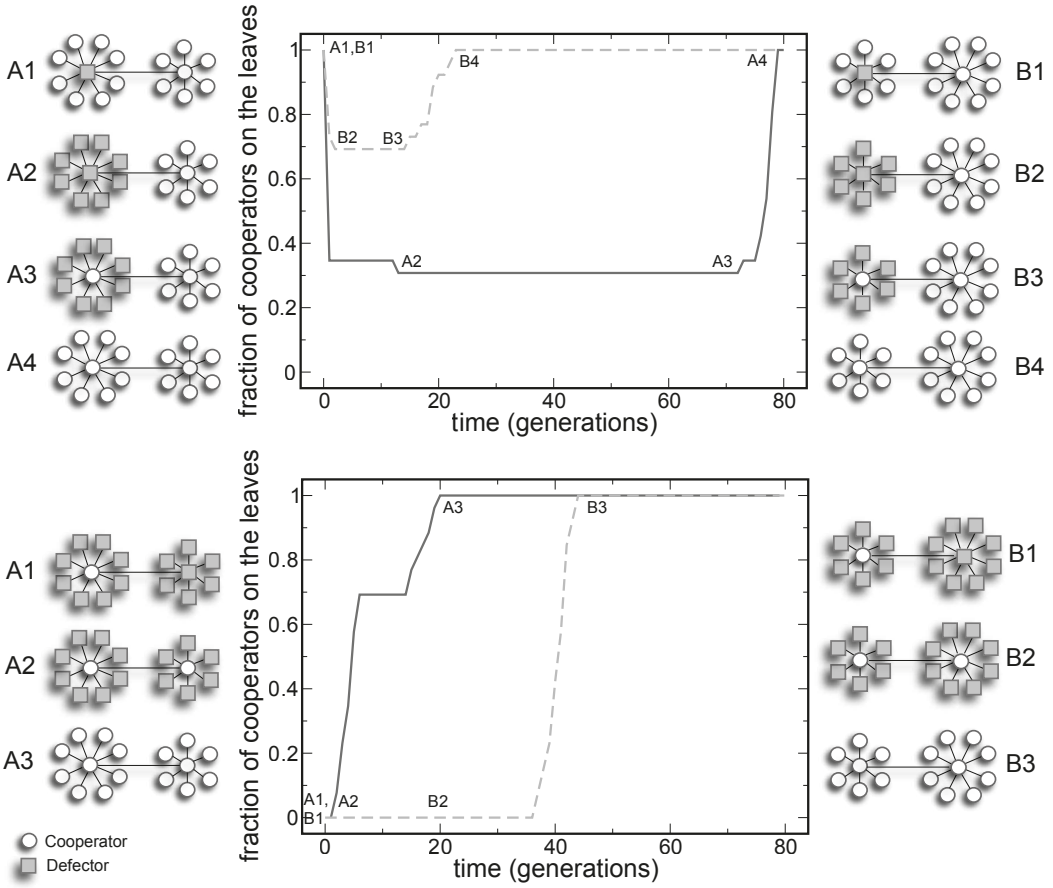

Figure 4.14: The *N*-Person Prisoner's Dilemma on double stars - Panels **A.** and **B.** provide a typical scenario for time evolution of the fraction of ***C****s* on the leaves of double-star graphs. **A.** We start with a single ***D*** both in the largest center and in the smallest center (A1 and B1). The overall behavior shows that the ***D*** invades the leaves of her star (A2 and B2), after which is invaded by the ***C*** in the center of the second star (A3 and B3). Subsequently, the remaining defectors on the leaves are invaded by ***C****s* (A4 and B4) (see figure 4.13). As expected, the relative connectivity of both centers (***C*** and ***D***) determines the overall time required for invasion (full line: $r = 1.3$, $N = 20$, and $M = 10$; dashed line: $r = 1.3$, $N = 10$ and $M = 20$). **B.** We start with a single ***C*** located in one of the centers in a population of ***D****s* (A1 and B1), with $r = 2.8$ ($r > \gamma > \alpha$, see equations 4.21 and 4.22). The ***C***-center starts by invading the ***D***-center (A2 and B2), after which the ***C***-strategy spreads to all leaves (A3 and B3). Given that the ability of the ***C***-center to invade the ***D***-center increases with the ***C***-center connectivity, $N > M$ leads to a faster invasion than $N < M$.

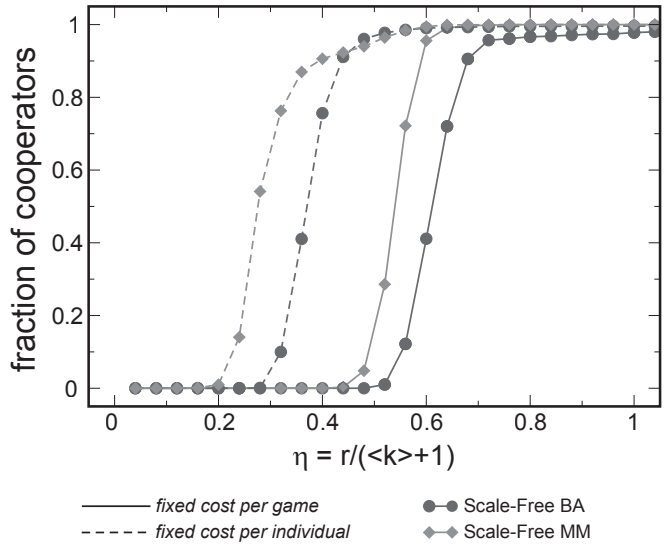

Figure 4.15: Evolution of cooperation under the *N*-Person Prisoner's Dilemma in scale-free networks grown according to the Barabási-Albert model and the Minimal Model - Final average fraction of cooperators as a function of the renormalized enhancement factor $\eta = \frac{r}{\langle k \rangle + 1}$ on scale-free networks grown according to the Barabási-Albert model (curves with filled circles) and the Minimal Model (curves with filled diamonds). Both contributive paradigms are considered: *fixed cost per game* (full curves) and *fixed cost per individual* (dashed curves). Parameters: $Z = 10^3$, $\langle k \rangle = 4$, $c = 1.0$.

considered: not only the time for ***C***-dominance decreases, but also the critical values of r above which ***C****s* dominate also decreases, a feature which is difficult to capture analytically. This can be understood by the fact that a high level of clustering allows cooperators to interact more with other cooperator neighbors while escaping the exploitation of defectors. This effect is also visible in other social dilemmas, as will be discussed in detail in the following chapters. This said, these results show that our (brief) mathematical analysis explains the cooperation levels obtained in the "worst" scenario for the *fixed cost per individual* paradigm.

4.9 Discussion

In this study, any contribution has been identified with cooperation. In communities under the influence of social norms, individual contributions will be easily classified as acts of cooperation (or not). In this context, our results suggest the possibility that

successful communities are those in which the act of giving is more important than the amount given. This may be of particular relevance whenever the survival of the community is at stake, in which case any help is necessary (107, 109).

However, it is important to note that our model has some limitations. One of them is the fact that the production function associated with this **PGG** is linear on the number of cooperators, a configuration that is not usual in many real world situations. In several cases, and in particular in the case of the climate change problem, a minimum effort or a minimum number of cooperators in a group is required for the public good to be achieved. Furthermore, this model does not encompass the role of *risk*, that is, individuals do not have the perception of the gravity of the problem they are tackling. In order to take these factors into account, in (110) we devise a new analytical model for a non-linear N-Person game in which a minimum number of cooperators is required for the public good to be achieved, and individuals have the perception of the risk associated with the task they are facing.

4.10 Methods

4.10.1 Population structure

For this study we consider two network classes, depicted in figure 2.3. On the one hand, following previous studies we consider one dimensional lattices (figure 2.3A), suitable for the modeling of communities in which all individuals (nodes) are topologically equivalent. In particular, we consider ring regular and homogeneous random (**HoRand**) networks. On the other hand, we adopt scale-free networks (figure 2.3C), grown following the model proposed by Barabási and Albert based on growth and preferential attachment ((24) and section 2.4 of this thesis), to model more realistic social structures. To investigate the role of significant clustering coefficient in the cooperation levels in the **NPD**, we also resort to scale-free networks grown according to the Minimal Model (**MM**) ((30) and section 2.4). In all simulations, networks remain fixed throughout evolution.

4.10.2 Evolution

In each game round, each and every individual assesses his/her individual fitness, by accumulating the payoff obtained from all the games he/she participates in. All strategies are updated synchronously following the finite population analogue of the replica-

tor dynamics discussed in Section 3.2.3.2: an individual A with strategy s_A imitates a randomly chosen neighbor B with strategy s_B ($s_A \neq s_B$) if and only if the fitness of B is higher than the fitness of A ($f_{s_B} > f_{s_A}$) and with a probability given by

$$p = \frac{f_{s_B} - f_{s_A}}{G} \tag{4.32}$$

where G represents the adequate normalization factor. G corresponds to the difference between the maximum possible fitness that can be obtained with strategy s_B $\left(f_{s_B}^{MAX}\right)$ and the minimum possible fitness that can be obtained with strategy s_A $\left(f_{s_A}^{MIN}\right)$, that is,

$$G = f_{s_B}^{MAX} - f_{s_A}^{MIN} \tag{4.33}$$

Both $f_{s_B}^{MAX}$ and $f_{s_A}^{MIN}$ depend on the social context of individuals B and A, respectively. In the context of the **NPD**, the maximum fitness for both strategies (**C** and **D**) is obtained when all the game partners of all games in which an individual participates in are ***C****s*; conversely, the minimum fitness for both strategies is obtained when all the game partners of that individual are ***D****s*.

The results are robust with respect to the detailed evolutionary dynamics (if we use the Fermi Imitation update method (77, 78, 79) instead of the replicator analogue in finite populations), to the updating strategy (synchronous versus asynchronous) and even to errors (mutations cannot destroy ***C***-dominance).

4.10.3 Simulations

Results were obtained for populations of size $Z = 10^3$ (figures 4.8 and 4.9 also include results for $Z = 5$ x 10^2 and $Z = 5$ x 10^3), and average connectivity $\langle k \rangle = 4$ (figure 4.10 also includes results for increasing average connectivity). Each equilibrium fraction of cooperators was obtained by averaging more than 2000 generations after a transient period of 10^5 generations. We started with 50% of ***C****s* randomly distributed on the network. Each data point in figures 4.3, 4.4, 4.8, 4.9, and 4.10 correspond to an average over 10^3 simulations: 10^2 runs for 10 different realizations of the same class of network.

5

Escaping the Snowdrift

5.1 Introduction

In the previous chapter we have focused on the most popular metaphor of collective action (48), the N-Person version of the Prisoner's Dilemma (**NPD**). The **NPD** model is suitable for situations in which the public good depends of, and is proportional to, the contribution of every single individual: the higher the number of contributors, the larger and better the final public good.

However, there are several day-life situations in which individuals are supposed to contribute to a public good which, once obtained, is constant and independent of the number of contributors. In these cases, the game metaphor that best describes this type of situations is the N-Person generalization of the Snowdrift Game (**NSG**) (111, 112). The **NSG** consists of the popular 2-person Snowdrift Game (**SG**) (39), also known as Chicken Game (40) or Hawk-Dove Game (61), now applied to a group of N individuals. A classic metaphor that illustrates this dilemma assumes N travelers trapped in a train blocked by a snowdrift, as illustrated in figure 5.1. Each individual can choose whether or not to cooperate by shoveling the snow: those who cooperate divide the workload, while everyone collects the benefit of resuming their journey home. It may also happen that the benefit is only obtained when a minimum threshold of individuals cooperates (105, 112, 113): in line with the previous example, the timely removal of the snow may require the combination of efforts from several individuals.

There are several examples of **NSG** games in the everyday life. When lions or lionesses gather to hunt a prey (114), sometimes not all of them participate in the hunting – yet, all have access to the same benefit. Whether the benefit is (equally) shared

Figure 5.1: The *N*-Person Snowdrift Game metaphor - The metaphor for the **NSG** assumes N travelers trapped in a train by a snowdrift. Each faces the decision whether or not to help shoveling the snow, such that the more individuals shovel, the less effort each one has to invest in order to surpass (in the illustrated example) a blocked rail. Moreover, as is often the case in collective dilemmas, the benefit of resuming the trip may only be obtained when a minimum number of individuals decide to cooperate.[†]

among all group members depends on of what is the benefit. Or take for instance the construction of a church by a group of colonizers who arrived to some newfound land. The effort of a single individual is not enough to build it up, and the more individuals contribute, the less effort each one has to invest.

Another example is "minga", an old tradition of community work in Latin America. One of its most common goals is the moving of entire houses, for reasons that span from religiosity to practical (like the acquisition of a new land or the necessity to be closer to a certain road). All the members of the community are invited to participate in these tasks, which sometimes even require carrying the houses across the sea. Of course one single individual could not complete this task, and the more individuals cooperate for the completion of this enterprise, the less effort each one has to invest.

[†]We thank António Araújo (email: ant.arj@gmail.com) for heartedly embracing the project of illustrating the **NSG**, resulting in this exceptional artwork.

The benefit, the same for all members of the community, would of course depend on the goal of the task.

Here, we study how an underlying network of contacts affects the evolutionary dynamics of collective action modeled in terms of the **NSG**. We analyze the impact of different types of networks in the global, population-wide dynamics of cooperators and defectors. We show that homogeneous social structures enhance the chances of coordinating towards stable levels of cooperation, while heterogeneous network structures create multiple internal equilibria, departing significantly from the reference scenario of a well-mixed (**WM**), structureless population. Contrary to the approach adopted in the previous chapter, where we analyzed the final average levels of cooperation obtained when starting from a population where cooperators and defectors were equally represented and randomly distributed in the population, here our study will be more general. We compute a numerical analogue of the right-hand side of the replicator equation $\dot{x} = x(1-x)\left(f_C(x) - f_D(x)\right)$, the *gradient of selection*, for structured populations, which provides a general view of how population structure affects the global game played in the population along time, regardless of the initial condition chosen.

We will start by presenting the model and its properties on both infinite well-mixed populations (section 5.3.1) and finite well-mixed populations (section 5.3.2). Then we proceed to introduce the gradient of selection in structured populations, and analyze in detail how the underlying network of contacts of the population affects the evolutionary dynamics of the **NSG**.

5.2 The Model

We consider a population of individuals behaving either as unconditional cooperators (***C**s*) or defectors (***D**s*). The threshold Q (with $1 \leq Q \leq N$) defines a minimum number of ***C**s* required in a group of size N to obtain the collective benefit, so as to encompass several situations in which the contribution of a single individual ($Q = 1$) is not enough to achieve the common goal. The payoffs of ***C**s* (Π_C) and ***D**s* (Π_D) resulting from a single group interaction can hence be written as

$$\Pi_C(n_C) = \mathrm{H}\left(n_C - Q\right)\left(c\left(\frac{1}{Q} - \frac{1}{n_C}\right) + b\right) - \frac{c}{Q} \tag{5.1a}$$

$$\Pi_D\left(n_C\right) = \mathrm{H}\left(n_C - Q\right) b \tag{5.1b}$$

respectively, where n_C is the number of ***C**s* in the group (of size N), c is the total cost involved in achieving b, the common benefit obtained by each individual of the group, regardless of her strategy, when $n_C \geq Q$ (we shall take $b = 1$). $\mathrm{H}(x-a)$ is the Heaviside step function which is 1 whenever $x \geq a$ and 0 otherwise.

Whenever $n_C < Q$, we obtain simply $\Pi_C(n_C) = -\frac{c}{Q}$ (which represents the maximum effort each cooperator can invest in a game) and $\Pi_D(n_C) = 0$. When $n_C \geq Q$, we obtain $\Pi_C(n_C) = b - \frac{c}{n_C}$ and $\Pi_D(n_C) = b$: all players obtain the benefit b, and to the cooperators is discounted the effort invested in each game, which consists of the cost c normalized by the number of cooperators in the group, n_C. As usual in N-Person games, $n_C = 0$ means that no cost is invested and no benefit is obtained. Note that the payoff functions $\Pi_C(n_C)$ and $\Pi_D(n_C)$ are non-linear (section 3.1.3), a fact that will originate richer evolutionary dynamics than those discussed in the previous chapter.

5.3 The *N*-Person Snowdrift Game in Well-Mixed Populations

5.3.1 Infinite Populations

Case $Q = 1$

We start by taking $Q = 1$ – that is, we start by considering the situation in which the effort of a single cooperator is sufficient to ensure the collective benefit. We define *individual fitness* as the gain an individual accumulates from all games in which he participates. The random selection of N individuals from an infinite population leads to groups whose composition follows a binomial distribution. The average fitness of ***C**s* (f_C) and ***D**s* (f_D) is given by equations 4.6 (105, 112, 115), which we reproduce here:

$$f_C(x) = \sum_{n_C=0}^{N-1} \binom{N-1}{n_C} x^{n_C}(1-x)^{N-1-n_C}\Pi_C(n_C+1) \tag{5.2a}$$

$$f_D(x) = \sum_{n_C=0}^{N-1} \binom{N-1}{n_C} x^{n_C}(1-x)^{N-1-n_C}\Pi_D(n_C) \tag{5.2b}$$

where x represents the fraction of cooperators in the population (and $(1-x)$ the fraction of defectors). The replicator equation 3.10, $\dot{x} = x(1-x)\left(f_C(x) - f_D(x)\right)$, allows us to follow the time evolution of ***C**s* in the population. In particular, the sign of the so-called *gradient of selection* (here denoted by $g(x)$ with $g(x) \equiv \dot{x}$) indicates which strategy

increases in abundance. To determine the interior fixed points x^* of the replicator equation 3.10 is equivalent to solve $f_C(x^*) - f_D(x^*) = 0$, that is,

$$\begin{aligned}
&f_C(x^*) - f_D(x^*) = 0 \Leftrightarrow \\
&\Leftrightarrow \sum_{n_C=0}^{N-1} \binom{N-1}{n_C} x^{*n_C} (1-x^*)^{N-n_C-1} \{\Pi_C(n_C+1) - \Pi_D(n_C)\} = 0 \Leftrightarrow \\
&\Leftrightarrow (1-x^*)^{N-1}(b-c) - \sum_{n_C=1}^{N-1} \binom{N-1}{n_C} x^{*n_C} (1-x^*)^{N-n_C-1} \frac{c}{n_C+1} = 0 \Leftrightarrow \\
&\Leftrightarrow \sum_{n_C=1}^{N-1} \frac{1}{n_C+1} \binom{N-1}{n_C} \left(\frac{x^*}{1-x^*}\right)^{n_C} = \frac{b-c}{c}
\end{aligned} \tag{5.3}$$

To solve equation 5.3, we will now rely on a couple of mathematical relations, to obtain the equation for the internal equilibria x^* of the **NSG** on infinite **WM** populations

$$\int_0^x (1+y)^N dy = \frac{1}{N+1}\left[(1+y)^{N+1}\right]_0^x \tag{5.4}$$

On the other hand, by applying the binomial theorem $(1+y)^N = \sum_{i=0}^N \binom{N}{i} y^i$, one may also write

$$\int_0^x (1+y)^N dy = \int_0^x \left[\sum_{i=0}^N \binom{N}{i} y^i\right] dy = \sum_{i=0}^N \binom{N}{i} \int_0^x y^i dy = \sum_{i=0}^N \binom{N}{i} \left[\frac{y^{i+1}}{i+1}\right]_0^x \tag{5.5}$$

by noticing that it is possible to invert the order between the integration and the summation. Therefore, joining equations 5.4 and 5.5 we have

$$\sum_{i=0}^N \binom{N}{i} \frac{x^{i+1}}{i+1} = \frac{1}{N+1}\left[(1+x)^{N+1} - 1\right] \tag{5.6}$$

which can be used to solve equation 5.3. Namely, we can write

$$\sum_{i=0}^N \binom{N}{i} \frac{x^{i+1}}{i+1} = x\left[\sum_{i=1}^N \binom{N}{i} \frac{x^i}{i+1} + 1\right] \Rightarrow \sum_{i=1}^N \binom{N}{i} \frac{x^i}{i+1} = \frac{(1+x)^{N+1}-1}{x(N+1)} - 1 \tag{5.7}$$

If we consider the auxiliary variable $A = \frac{x^*}{1-x^*}$ to rewrite equation 5.3 in terms of the variable A, we obtain

$$\sum_{j=1}^{N-1} \binom{N-1}{j} \frac{A^j}{j+1} = \frac{b-c}{c} \tag{5.8}$$

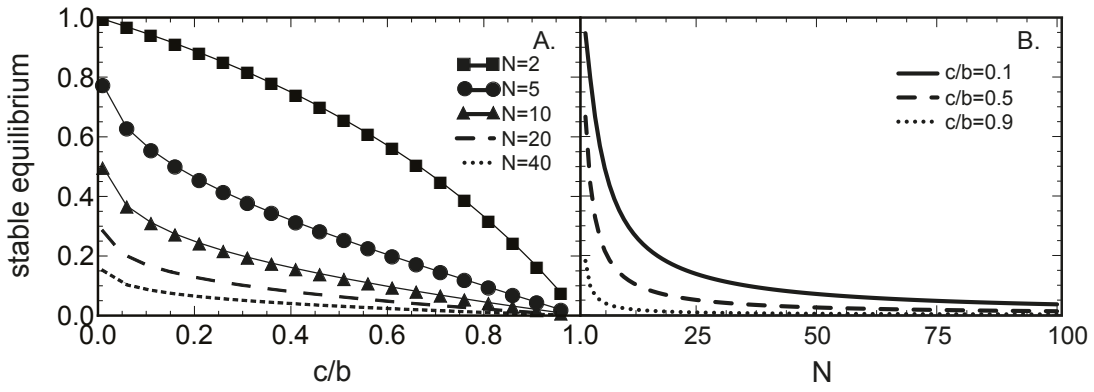

Figure 5.2: Internal equilibria of the *N*-Person Snowdrift Game in infinite well-mixed populations. - Internal equilibria of the N-Person Snowdrift Game as a function of **A.** cost-benefit ratio c/b (for different values of the group size N), and **B.** group size N (for different values of c/b).

And finally, from equations 5.6 and 5.8, after some algebraic manipulation we obtain

$$\frac{c}{b}(1-x^*)^N + Nx^*(1-x^*)^{N-1} - \frac{c}{b} = 0 \tag{5.9}$$

Equation 5.9 can be solved analytically for $N \leq 4$ (111); for $N = 2$ we recover the conventional result for the 2-person **SG** in infinite **WM** populations, $x^* = \frac{b-c}{b-c/2}$. For $N > 4$ equation 5.9 can be solved numerically for arbitrary N to obtain the fraction of ***C*s** in the stationary state x^*. From the results illustrated in figure 5.2, we observe that the higher the group size, the lower x^* for the same c/b, also, increasing c/b for fixed group size N leads to a decrease in the equilibrium fraction of cooperators x^*.

Case $Q > 1$

$Q > 1$ leads to a more complex scenario. In this case, the global benefit is only obtained when the minimum number of cooperators Q (with $Q > 1$) in the group is gathered. Only in that case cooperators share among them the required workload; otherwise, when $n_C < Q$, the effort of cooperators is in vain. The fitness difference is in this case given by (112)

$f_C(x) - f_D(x) =$

$$= \frac{c}{xN}\left\{N\frac{b}{c}\binom{N-1}{Q-1}x^Q(1-x)^{N-Q} - \left[1 + \sum_{n_C=0}^{Q-1}\binom{N}{n_C}x^{n_C}(1-x)^{N-n_C}\left(\frac{n_C}{Q}-1\right)\right]\right\} \tag{5.10}$$

The limit $Q = 1$ leads naturally to equation 5.9, already studied above in detail. In the case $N = Q = 2$ we obtain $x^* = \frac{c}{2b}$. This is an unstable fixed point; that is, we obtain a dynamics akin to that of a Stag-Hunt (**SH**) game for a group of size $N = 2$ in which we require all members of the group to cooperate in order for the benefit to be obtained.

For $N > 2$ and $Q > 1$ there is no analytical solution for equation 5.10, but we can solve it numerically, as depicted in figure 5.3. When $Q > 1$, a new evolutionary dynamics arises: the stable equilibria observed in figure 5.2 are replaced by a pair of roots, one stable and the other unstable. This divides the system into two basins of attraction, so depending on the initial fraction of cooperators in the population the system will evolve either towards a fully defective state or a coexistence of ***Cs*** and ***Ds***. Note that the fraction of cooperators in this coexistence decreases for increasing c/b and fixed Q (which is understandable since the cost c associated with the act of cooperating is higher), but importantly it *increases* for increasing Q and fixed c/b. While at first this could seem a paradox (since the requirements for the attainment of the public good are higher), it can be understood by taking into account the fact that the individual investment of each cooperator is c/Q – that is, the individual investment decreases with Q. This dynamics characterized by two basins of attraction typically vanishes for a critical c/b (112), above which a single stable fixed point remains for $x = 0$, similar to the **NPD**. Both $f_C(x)$ and $f_D(x)$ are polynomials of degree $N - 1$, and as such $g(x)$ would have at most $N - 1$ interior roots; however, it has been shown that for the **NSG** case the maximum possible number of roots is two (53, 112).

In fact the emergence of a pair of internal roots, a coordination and a coexistence, also occurs with the introduction of a threshold in other N-Person social dilemmas, such as the N-Person Prisoner's Dilemma (**NPD**) (a defectors' dominance dilemma) (116); and the N-Person Stag-Hunt Game (**NSH**) (a coordination dilemma) (105).

5.3.2 Finite Populations

For finite populations of size Z, the binomial sampling is replaced by the hyper-geometric sampling (sampling without replacement) presented in equations 4.8, which we repeat

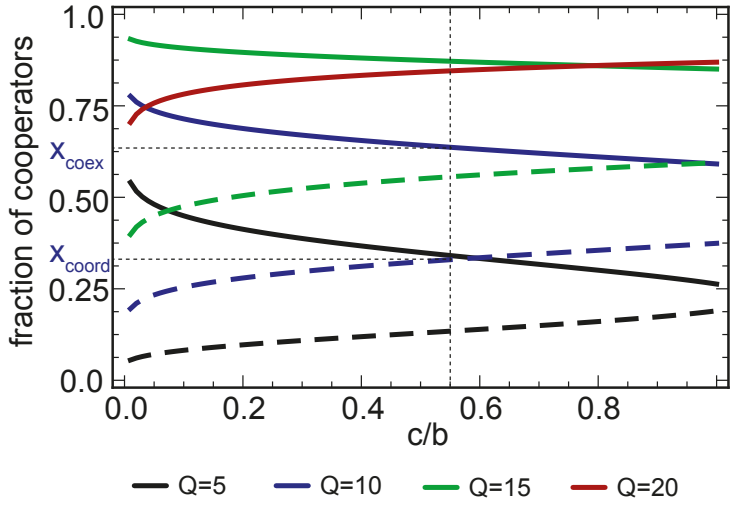

Figure 5.3: Evolutionary dynamics of the *N*-Person Snowdrift Game on infinite well-mixed populations - Internal equilibria of the replicator equation for the N-Person Snowdrift Game as a function of the ration c/b, for increasing threshold Q. Dashed lines correspond to coordination points, full lines correspond to coexistence points. Parameters: $N = 20$.

below:

$$f_C(j) = \binom{Z-1}{N-1}^{-1} \sum_{n_C=0}^{N-1} \binom{j-1}{n_C} \binom{Z-j}{N-n_C-1} \Pi_C(n_C+1) \tag{5.11a}$$

$$f_D(j) = \binom{Z-1}{N-1}^{-1} \sum_{n_C=0}^{N-1} \binom{j}{n_C} \binom{Z-j-1}{N-n_C-1} \Pi_D(n_C) \tag{5.11b}$$

For modeling the evolution of the population, we adopt a birth-death (**BD**) process combined with the pairwise comparison rule discussed in section 3.2.3.2 (77, 78, 79). In this case, we adopt a different update method than the one we have adopted in the previous chapter - the replicator dynamics analogue for finite populations - because for this project we want to adopt a different approach. Namely, in this chapter we will compute a numerical analogue of the *gradient of selection* for structured populations; the Fermi Imitation update method seems to us an appropriate choice for this purpose because it allows the study of the evolutionary dynamics for any intensity of selection.

In each time step, an individual A adopts the strategy of a randomly selected neigh-

bor B with a probability given by the Fermi distribution

$$p_{Fermi} = \frac{1}{1 + e^{-\beta(f_{s_B} - f_{s_A})}} \tag{5.12}$$

where β stands for the intensity of selection regulating the accuracy of the imitation process, and f_{s_A} (f_{s_B}) stands for the fitness of individual A (B) with strategy s_A (s_B). As a result, evolution proceeds as a balance between the probabilities to increase ($\mathcal{T}^+(j)$) and decrease ($\mathcal{T}^-(j)$) the number of ***C**s* in the population, j, which can be written as

$$\mathcal{T}^{\pm}(j) = \frac{j}{Z}\frac{Z-j}{Z-1}\left[1 + e^{\mp\beta(f_C(j) - f_D(j))}\right]^{-1} \tag{5.13}$$

The finite population equivalent of the gradient of selection $g(x)$ can be written as

$$G(j) \equiv \mathcal{T}^+(j) - \mathcal{T}^-(j) = \frac{j}{Z}\frac{Z-j}{Z-1}\tanh\left[\frac{\beta}{2}(f_C(j) - f_D(j))\right] \tag{5.14}$$

as discussed in more detail in section 3.2.3.2. The term $\frac{j}{Z}$ corresponds to the probability of selecting a cooperator in the population of size Z, while the term $\frac{Z-j}{Z-1}$ corresponds to the probability of selecting a defector among the $Z-1$ individuals that remain in the population (sampling is done without replacement). Please see Methods (section 5.8) for details.

The general dynamical picture remains the same as the one discussed for infinite populations as long as $Z \gg N$ (112), but as the group size approaches the population size the scenario changes: in figure 5.4 we show the gradient of selection $G(j/Z)$ with population size $Z = 10^2$ and group size between $N = 20$ and $N = 80$. As $N \sim Z$, cooperation becomes disadvantageous: the stable root is shifted to the left with increasing N, and the amplitude of $G(j/Z)$ also decreases.

5.4 The Gradient of Selection in Structured Populations

The gradient of selection $g(x)$ for infinite populations, and its analogue $G(j/Z)$ for finite populations, provide complete information concerning the evolutionary dynamics of the population. However, in structured populations, besides tracking how the number of cooperators and defectors varies in time, it is also necessary to track their location since their fitness depends on their social context. Because of this additional difficulty, the conventional approach adopted for the study of social dilemmas in structured populations is to evaluate the average final level of cooperation in the population after a convenient transient period, when starting from one particular initial condition

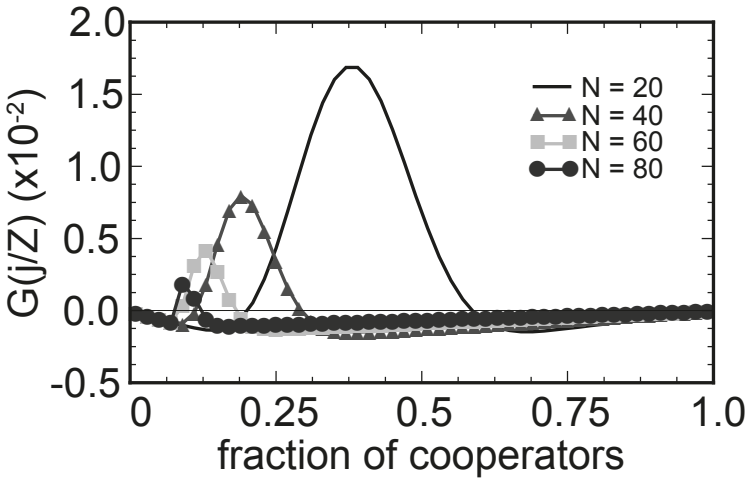

Figure 5.4: Evolutionary dynamics of the *N*-Person Snowdrift Game on finite, well-mixed populations for increasing group size *N* - Gradient of selection $G(j/Z)$ of the N-Person Snowdrift Game on finite, well-mixed populations for increasing group size N. Cooperation becomes disadvantageous as the group size N approaches the population size Z. Parameters: $Z = 10^2$, $Q = 1$, $b = 1.0$, $c = 0.2$.

(usually, 50% of ***Cs*** and ***Ds***). This was the approach we used in the previous chapter, for the **NPD** model. While the existence of coexistence points can be easily inferred from such results (since the population will evolve towards them and spend there a significant amount of time), nothing can be said about coordination points. Also, results obtained by following this approach correspond to one single initial condition j/Z, and may differ if we adopt a different initial condition.

In order to probe deeper into the evolutionary dynamics of the population under the **NSG**, we compute a numerical analogue of the gradient of selection in structured populations, the *average gradient of selection* (**AGoS**) (117), $G(j/Z)$, for the determination of which we compute the transition probabilities along the links of the network. For each individual i in the population that is a defector, one must calculate $\mathcal{T}_i^+ = k_i^{-1} \sum_{m=0}^{\bar{n_i}} \left[1 + e^{-\beta(f_m(t) - f_t(t))}\right]^{-1}$, where k_i is the degree of node i and $\bar{n_i}$ is the number of neighbors of i that are cooperators. Conversely, for each individual i that is a cooperator we calculate $\mathcal{T}_i^- = k_i^{-1} \sum_{m=0}^{\bar{n_i}} \left[1 + e^{-\beta(f_m(t) - f_t(t))}\right]^{-1}$, where $\bar{n_i}$ is the number of neighbors of i that are defectors. At a given time t of simulation p we define

$G_p = \mathcal{T}_p^+(j,t) - \mathcal{T}_p^-(j,t)$, with

$$\mathcal{T}_p^{\pm}(j,t) = Z^{-1} \sum_{i}^{\substack{\text{All } \textbf{\textit{Ds}} \\ \text{All } \textbf{\textit{Cs}}}} \mathcal{T}_i(t) \tag{5.15}$$

for a state with j cooperators in a population of size Z. The *time-dependent* **AGoS** at generation t_g (1 generation means Z iterations), $G^A(j,t_g)$, is then computed by averaging over the last Z time-steps, that is,

$$G^A(j,t_g) = c_j(t_g)^{-1} \sum_{t_g-1}^{t_g} \sum_{p=1}^{\Omega} G_p(j,t), \tag{5.16}$$

where $c_j(t_g)$ accounts for the number of times the population was observed in state j during generation t_g. Please see Methods (section 5.8) for details.

Figure 5.5 schematizes the method we adopt for determining the **AGoS**: the shaded area in figure 5.5A represents the period of interest for determining the gradient of selection for generation t_g; we perform several simulations for each initial condition j/Z and for each one, when the population crosses the shaded area, we register $\mathcal{T}_p^{\pm}(j,t)$ for the corresponding number of ***Cs*** in the population, j. $\mathcal{T}_p^{\pm}(j,t)$ corresponds to an average of the transition probabilities over all individuals in the population, as expressed in equation 5.15, measured along the links of the network that may give rise to a change of strategy; given that we adopt the Fermi Imitation update rule, these links correspond to those connecting nodes with different strategies.

In the following sections, we will use the conventional approach here mentioned as a departure point for introducing the gradient of selection.

5.5 Network Reciprocity in the *N*-Person Snowdrift Game

We will now start by investigating the behavior of the average final fraction of cooperators obtained when the population evolves according to the rules of the **NSG**, in line with the study conducted on the previous chapter for the N-Person Prisoner's Dilemma (**NPD**) (chapter 4).

The population is initialized with a random distribution of 50% of ***Cs*** and ***Ds*** in the nodes of the network. In each time-step of the evolution of the population, a randomly selected individual is given the opportunity to revise his strategy – that is, strategies are updated asynchronously. A strategy revision occurs according to the following method: a randomly chosen individual A chooses a random neighbor B; both evaluate their

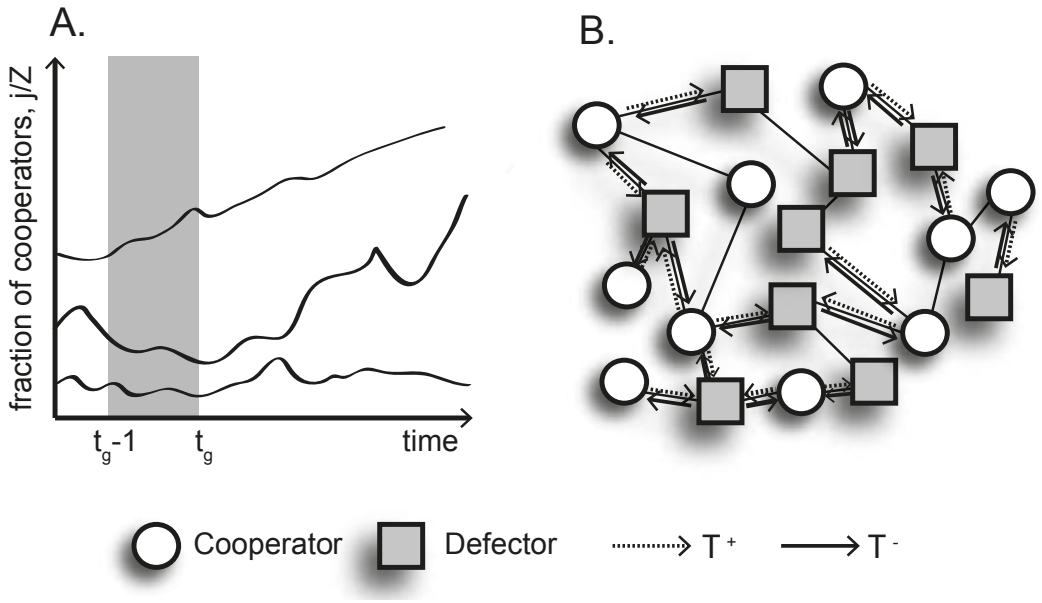

Figure 5.5: Determination of the analogue of the gradient of selection on structured populations - For the determination of the average gradient of selection (**AGoS**), we: **A.** perform several runs for each possible initial condition j/Z and, between the interval of interest $t_g - 1$ and t_g (for determining the **AGoS** in generation t_g) we register the transition probabilities $\mathcal{T}^{\pm}(j/Z)$ for each state j/Z in which the population is observed in that interval. In the scheme of panel A, we represent three runs in which the fraction of cooperators in the population evolves in time starting from three distinct initial conditions. **B.** Average transition probabilities $\mathcal{T}^{\pm}(j/Z)$ of the population in each instant t correspond to an average over all $\mathcal{T}^{\pm}$ computed along the links of the network connecting two individuals of different strategies.

individual fitnesses by accumulating the payoff obtained in all the games in which they participate. If individuals A and B have different strategies ($s_A \neq s_B$) A will imitate B with a probability proportional to the fitness difference $f_{s_B} - f_{s_A}$ and given by the Fermi distribution from statistical physics (references (77, 78, 79) and section 3.2.3.2). Note that, according to the conclusions from the previous chapter regarding how N-Person games should be formulated in structured populations, we will assume that each individual i always participates in $k_i + 1$ games (where k_i represents the number of neighbors of individual i): the one centered on himself plus the k_i games centered on his k_i neighbors.

We investigate the impact of population structure on the evolutionary dynamics

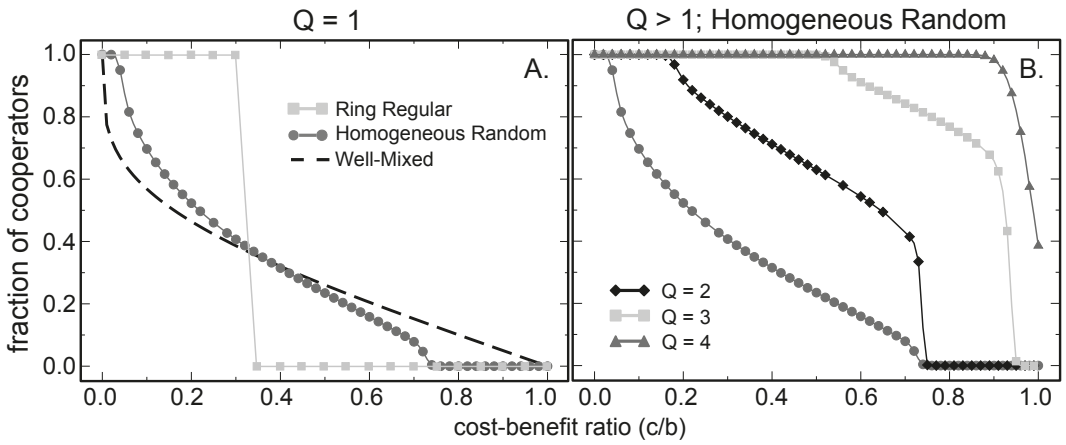

Figure 5.6: Average final fraction of cooperators for the networked *N*-Person Snowdrift Game - ring regular and homogeneous random networks - **A.** Average final fraction of cooperators in the **NSG** as a function of c/b for homogeneous populations. Line with full circles corresponds to the results of **HoRand** populations, line with filled squares corresponds to the results for ring regular populations, and dashed line corresponds to the infinite well-mixed limit, all for $Q = 1$. **B.** The increase in the coordination threshold Q leads to an increase on the level of cooperation obtained for a fixed c/b on homogeneous random populations. Parameters: $Z = 10^3$, $\langle k \rangle = 4$, and $\beta = 1.0$ for the simulations in structured populations.

of the **NSG**, and for that we consider three distinct network classes – ring regular, homogeneous random (**HoRand**) and scale-free Barabási-Albert (**BA**) networks. In homogeneous populations every individual takes part in the same number of games, all with the same size ($\langle k \rangle + 1$ in both cases). While in ring regular networks the neighborhoods of all individuals are arranged in the same regular manner, in **HoRand** networks neighborhoods are random – a distinctive fact that justifies why we opt for studying both network classes. However, this scenario does not take into account an important feature of social networks: its diversity. Often individuals face different number of collective dilemmas (depending on their social position) that may also have different sizes. Such levels of social diversity can be modeled by considering a heterogeneous network of interactions. Please see Methods (section 5.8) for details. In this section we investigate the impact of homogeneous networks on the evolutionary dynamics – heterogeneous networks will be the subject of the following section.

In figure 5.6A we compare the average final fraction of cooperators obtained on **HoRand** populations (line with filled circles) and ring regular populations (line with

filled squares) with their **WM** counterpart in the limit of infinite populations (dashed line) for $Q = 1$. The behavior is qualitatively similar in both the structured and the structureless cases: there is a monotonic decline from full cooperation to full defection as c/b increases. While in **Horand** populations the decline is smooth, in ring regular populations there is a sharp transition from full cooperation to full defection for $c/b = 0.3$. Figure 5.6B shows the impact of the threshold level Q on the overall levels of cooperation in **HoRand** populations. We observe that an increasing threshold Q leads to an increase on the level of cooperation for a fixed c/b, a feature that is also observed for **WM** populations (as illustrated in figure 5.3) and is qualitatively valid for other homogeneous graphs such as lattices and rings. This property was discussed in the context of **WM** populations (section 5.3), and the same justification can also be applied in this context if we notice that the investment made by each cooperator (c/Q) decreases with increasing Q. For $Q = 2$ and $Q = 3$ we observe a critical c/b after which the final fraction of cooperators starts to decrease until they reach a second critical c/b that marks an abrupt decline in the cooperation levels.

5.5.1 Ring Regular Networks

In figure 5.7A we represent the initial gradient of selection (that is, without performing any evolution in the population) for $Q = 1$ in ring regular networks, for several values of c/b. The results show that the global dilemma being played corresponds to a coexistence, and that the coexistence point is gradually shifted to the left (that is, gradually corresponds to a lower fraction of cooperators) for increasing c/b. Also, note that for $c/b = 0.35$ the gradient becomes fully negative, that is, regardless of the initial fraction of cooperators the population will be pushed towards a fully defective state. This is in accordance with the results shown in figure 5.6A: the cost-benefit ratio $c/b = 0.3$ marks the transition from full cooperation to full defection.

In face of these results, we now want to understand why the population evolves towards full cooperation, while the initial gradient of selection in figure 5.7A indicates the existence of a coexistence point for a relatively small fraction of cooperators in the population.

In a finite population, regardless of the internal stable points that may exist in the dynamics, the evolution only ceases when the population reaches one of the absorbing states, full cooperation or full defection, even though the fixation time in one of these states may be arbitrarily long. But is it just that what gives rise to the fully cooperative

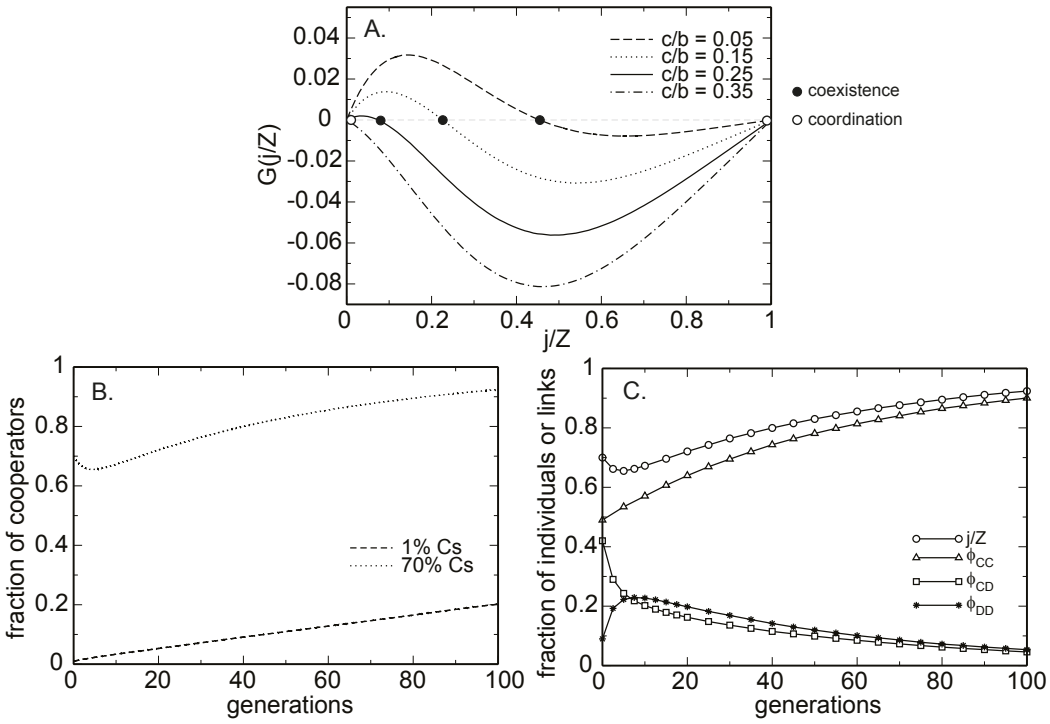

Figure 5.7: Evolutionary dynamics of the *N*-Person Snowdrift Game in ring regular networks - **A.** Gradients of selection $G(j/Z)$ for the **NSG** for some values of the ratio c/b, **B.** fraction of cooperators j/Z as a function of time (measured in generations), starting from above $x_{coexistence}$ (70% of cooperators) and below it (1% of cooperators) for $c/b = 0.15$, **C.** j/Z, ϕ_{CC}, ϕ_{DD} and ϕ_{CD} as a function of time, starting from 70% of cooperators, for $c/b = 0.15$. Parameters: $Z = 10^3$, $\langle k \rangle = 4$, $\beta = 1.0$.

population we observe in figure 5.6A? And if yes, why did the population fixate in full cooperation and not in full defection, as the fraction of cooperators in the coexistence level is relatively low? In order to understand better the origin of this result, we focus on a particular value of $c/b < 0.3$, and follow the time evolution of the fraction of cooperators starting from two different initial conditions – above and below the coexistence point $x_{coexistence}$ obtained for the same value of c/b in the infinite, well-mixed case, with $x_{coexistence} \approx 0.25$ (dashed line in figure 5.6A). In figure 5.7B we start from a population of 1% and 70% of cooperators respectively, randomly distributed in the network, and allow the population to evolve for 100 generations. Figure 5.7B shows that, although the final outcome after the 100 generations is the same (the population is heading to the absorbing state of full cooperation), the dynamic behavior observed

throughout evolution is quite different. While for the initial condition below $x_{coexistence}$ (1% of ***Cs***) the fraction of cooperators increases right from the start, for the initial condition above $x_{coexistence}$ (70% of ***Cs***) it starts by decreasing first, increasing only after a considerable amount of generations. To understand the origin of such behavior, we define the fraction of links between individuals i and j playing strategies s_i and s_j, $\phi_{s_i s_j}$, as

$$\phi_{s_i s_j} = \frac{\sum_{i=1}^{Z} \#s_i s_j \text{ links}}{\frac{Z\langle k \rangle}{2}} \tag{5.17}$$

where $\frac{Z\langle k \rangle}{2}$ is the total number of links of the network and s_i and s_j is either ***C*** or ***D***.

Figure 5.7C shows the average time evolution of these quantities when starting with a fraction of cooperators $x > x_{coexistence}$, along with the above defined quantities. Analysis of these results shows that isolated cooperators are the ones specifically being eliminated, i.e., cooperators and defectors on the population organize themselves increasingly more in an *assorted* manner – individuals that adopt a certain strategy are not isolated but organized in such a way that have at least one neighbor following the same strategy. This is corroborated by the several curves shown: ϕ_{CC} increases slightly, accompanied by a sudden decrease of ϕ_{CD}, representing the self-organization of cooperators and defectors; the maximum "saturation value" reached by ϕ_{DD} corresponds to the moment in which cooperators are less represented in the population. For these reasons, what we actually observing in figure 5.6 is not the end of evolution after an arbitrarily long period of time as a consequence of stochastic fluctuations, but a result of the gradual change in the global dilemma being played in the population caused by the self-organization of ***Cs*** and ***Ds*** in the network. For these values of c/b, regular structures can, therefore, be favorable for cooperation under the **NSG**, potentiating the self-organization of the population towards the full cooperation absorbing state.

5.5.2 Homogeneous Random populations

In order to understand the impact of the organization of strategies in the evolutionary dynamics of the **NSG** in **HoRand** populations, we initially distribute the strategies in the population according to two extreme methods. On the one hand, we distribute cooperators (and defectors) randomly in the population. On the other hand, we distribute cooperators in the population in such a way that each ***C*** has at least another ***C*** as neighbor. To distribute j cooperators in the population according to this second

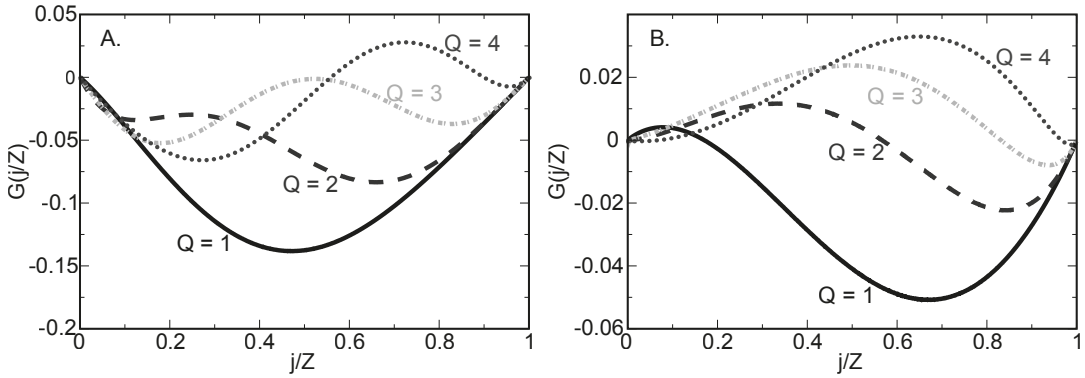

Figure 5.8: Initial gradient of selection for the *N*-Person Snowdrift Game on homogeneous random populations - Gradient of selection $G(j/Z)$ prior to population evolution when strategies are distributed **A.** randomly, and **B.** cooperators are distributed in a percolated way. Parameters: $Z = 10^3$, $\langle k \rangle = 4$, $\beta = 1.0$, $c/b = 0.7$.

method, we adopt the following procedure: we start by randomly choosing the first individual in the population to become a ***C***. If $j > 1$, after the first individual is assigned as cooperator, we randomly choose one of his neighbors in the network and assign him as cooperator. If $j > 2$, we create a list of cooperator individuals, and at each time step we choose one random cooperator i from this list, and then one random neighbor t of individual i. If individual t is not a cooperator yet, we assign him the cooperative strategy, and update the list of cooperators in the population. We proceed with this algorithm until all j cooperators are distributed in the population. Note that when individuals are distributed randomly in the population, for a sufficiently large population the probability that two cooperators are neighbors of each other is low.

The results for the initial gradients of selection for these two cases are shown in figure 5.8, for a cost-benefit ratio of $c/b = 0.7$. Note that these gradients of selection were obtained without evolving the population, they simply correspond to an evaluation of the probable direction of evolution depending on how strategies are initially distributed in the population.

Starting from the case $Q = 1$, the differences between the two distributions are striking: while for a random distribution of strategies the gradient is fully negative, for a distribution in which all cooperators have at least one cooperator as neighbor the global dilemma is transformed into a coexistence. This trend is maintained for higher values of Q: while for random distributions of strategies the gradient is or either totally negative, or exhibits a pair of coordination and coexistence internal fixed points, for a

distribution of strategies in which each cooperator has at least another cooperator as neighbor the gradient of selection always corresponds to a coexistence dilemma, and the level of cooperators in the coexistence increases with increasing Q. These results highlight the importance of the distribution of strategies in a structured population; note that these differences would have no meaning in a well-mixed population: in the **WM** scenario, there is no such thing as distributing strategies according to different methods (as all social positions are equivalent) and therefore for a given set of game parameters and j/Z the value of the gradient of selection will always be the same.

The update rule adopted here is non-innovative (section 3.2.3.2); this means that a cooperator surrounded by cooperators cannot change strategy (and likewise for a defector surrounded by defectors). More generally, with this update method "***C**s* breed ***C**s* and ***D**s* breed ***D**s*" (108) – along time, clusters of individuals exhibiting the same strategy are expected to emerge. Because the gradient of selection is highly sensitive to how individuals are distributed in the social network, we expect that it co-evolves with the self-organization of strategies in the population and maybe even similar to the one obtained in figure 5.8B. The **AGoS** will allow us to understand how the final fractions of cooperators depicted in figure 5.6 come to be, and more generically how the population structure affects the nature of the global dilemma played by the population.

Figure 5.9 allows the detailed study of the evolutionary dynamics in **HoRand** populations along time. Figure 5.9B shows the **AGoS** in **HoRand** populations, which can be compared both with its corresponding quasi-stationary distribution (figure 5.9) and the corresponding results for infinite **WM** populations (figure 5.9A). The **AGoS** was averaged over 125 generations after a transient of 25 generations – as the panel C of figure 5.9 shows, the population macro-dynamics takes at most 20 generations to reach a stationary regime. The vertical green dashed line shows the good agreement between the coexistence point x_{coex} (panel B) and the peak of the *quasi-stationary distribution* (panel D) for $Q = 3$.

First of all, it is worth comparing figures 5.8A (for the initial gradient of selection in **HoRand** populations, when the strategies are distributed randomly in the population and the initial gradient of selection is computed before any strategy revisions take place in the population) and figure 5.9C (which shows the evolution of the internal fixed points of the gradient of selection $G^A(j/Z)$ for the first 50 generations in **HoRand** populations). The starting point for the results shown in both these figures is exactly the same, in what concerns both the distribution of strategies and the population structure. However, a detailed analysis of the two figures shows that the internal roots shown in

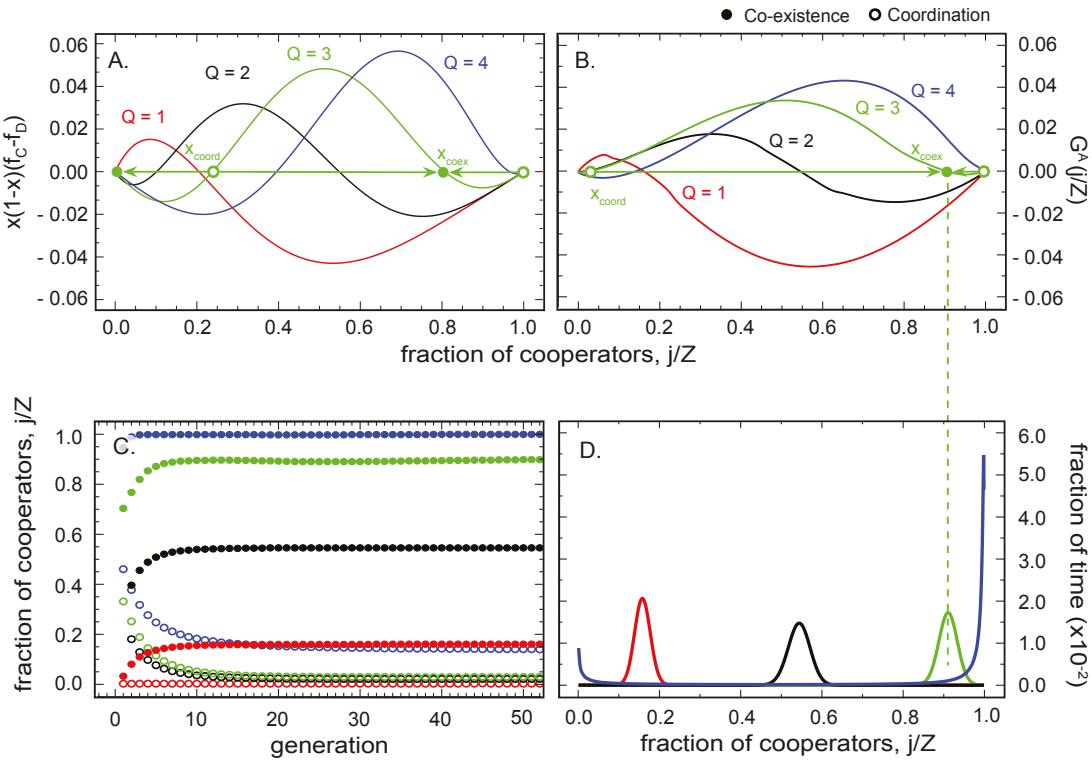

Figure 5.9: Gradient of selection for the *N*-Person Snowdrift Game on homogeneous random populations - **A.** Gradient of selection $g(x)$ in infinite, **WM** populations, **B.** average gradient of selection $G^A(j/Z)$ over 50 generations after a transient of 25 generations in finite populations structured along the links of **HoRand** networks, **C.** Internal fixed points of the $G^A(j,g)$ for the first 50 generations, and **D.** Stationary distributions computed for the situations described in **B.**. Parameters: $Z = 10^3$, $\langle k \rangle = 4$, $c/b = 0.6$, $\beta = 1.0$.[‡]

figure 5.9C for the first generation differ slightly from those shown in figure 5.8A for the initial gradient. This small discrepancy does not correspond to an error in our results but to the fact that the internal roots shown in figure 5.9C correspond to the roots of the gradients averaged over 1 generation (1 generation = Z iterations). For the particular case of the roots of the first generation, this means that they correspond to the roots of the average of the first Z iterations of the evolution of the population and in these iterations, due to the rearrangement of ***Cs*** and ***Ds*** in the population, emerge some internal roots, for some values of Q, that are still not present in the initial gradient of selection.

[‡]I thank my colleague in the ATP-group Flávio Pinheiro for this figure, as well as figures 5.10, 5.14

Comparing figures 5.9A and 5.9B for the gradients of selection in infinite **WM** populations and for the average gradient of selection $G^A(j/Z)$ after a transient period of 25 generations respectively, we observe that while the nature of the dilemma remains unchanged, **i) HoRand** networks facilitate coordination: regardless of the value of Q, the coordination point (x_{coord}) is shifted to the left (requiring less ***C*s**) when compared with its position in well-mixed populations (for $Q = 1, 2$ and 3 the coordination point is close to $1/Z$). That is, a lower minimum number of ***C*s** in the population is required for reaching the coexistence state. Furthermore, **ii)**, whenever individuals face stringent requirements to meet goals (large Q/N), the coexistence point (x_{coex}) is shifted to the right (coexistence involving more ***C*s**). In both cases we obtain a more favorable scenario for cooperation in **HoRand** structured populations compared to **WM** populations.

It is also noteworthy that, for large Q/N, the relative size of the two basins of attraction combined with stochastic effects renders full cooperation as the most prevalent state, whereas for low Q/N, the population will remain in the vicinity of the coexistence point (x_{coex}) most of the time.

The results in figure 5.9 allow the visualization of the gradients of selection for the particular value of cost-benefit ratio $c/b = 0.6$. In figure 5.10 we provide an overview of the evolutionary dynamics for the full range of c/b, by drawing the location of the interior roots of the **AGoS** for different values of Q (circles), in comparison with the well-mixed case (solid lines), showing how **HoRand** networks favor cooperation. This overall picture of the population dynamics supports the conclusions discussed above. Furthermore, both in **WM** and **HoRand** populations, x_{coex} shifts to lower values of the fraction (j/Z) of ***C*s** for larger values of c/b, a result reported in previous studies of the 2-person **SG** (64). Similarly, the critical c/b above which the nature of the dilemma is transformed to that of a **PD** is lower than that reported on **WM** populations (112), a fact that is particularly visible on panel B of figure 5.10.

5.6 Social diversity in the *N*-Person Snowdrift Game

Despite their theoretical interest, homogeneous networks are not good models for realistic social structures, as first noted in chapter 2. Instead, real social networks exhibit a marked degree of heterogeneity (a large number of individuals with few neighbors whereas a minority of the population have a large number of neighbors) combined with

and 5.15, which because of the tight schedule requirements of this thesis were obtained with his faster version of the program.

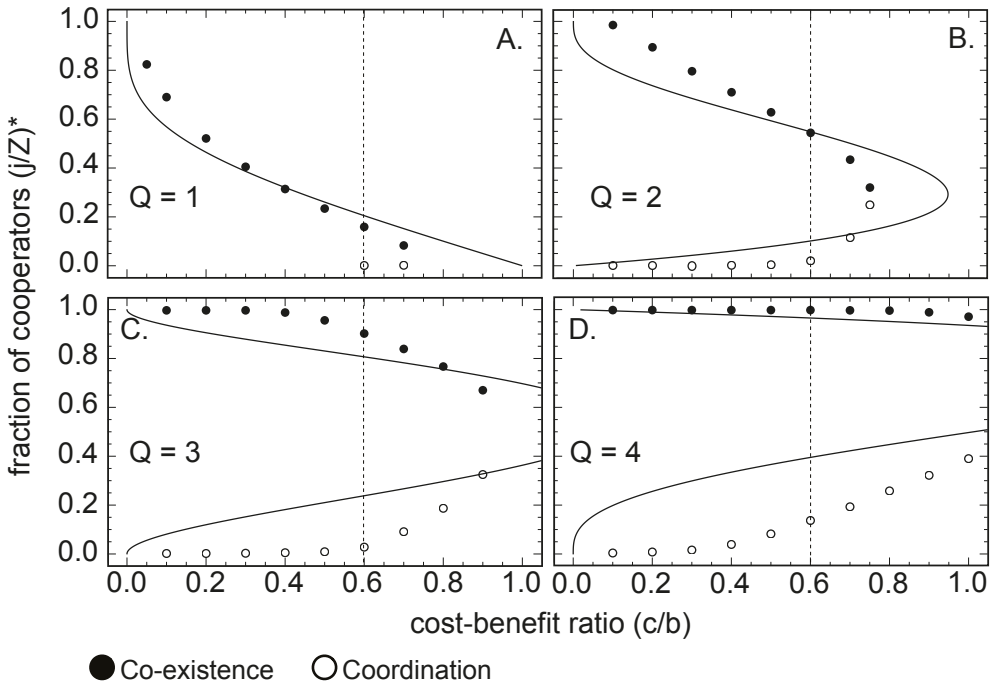

Figure 5.10: Average gradient of selection (AGoS) for the *N*-Person Snowdrift Game on homogeneous random populations - Location of the interior fixed points of the **AGoS** at the 75^{th} generation for **HoRand** populations (open and solid circles) as a function of c/b and for $1 \leq Q \leq 4$. The corresponding results for **WM** populations are drawn with solid lines for comparison. Vertical dashed lines indicate the values used in figure 5.9. Parameters: $Z = 10^3$, $\langle k \rangle = 4$ and $\beta = 1.0$ (for the dynamics on **HoRand** populations).

small-world effects, characteristics that are both present, albeit at extreme levels, on scale-free **BA** networks.

In figure 5.11 we represent the initial gradient of selection obtained in scale-free **BA** populations, when cooperators are distributed randomly (figure 5.11A) and when we assure that each and every cooperator has at least one cooperator as neighbor (figure 5.11B), for a cost-benefit ratio of $c/b = 0.7$. The difference observed between these two scenarios is even more pronounced than that observed for these two same scenarios in **HoRand** networks: while for the distribution of strategies adopted in figure 5.11A the initial gradient of selection is always negative regardless of the value of Q, with the distribution of strategies adopted in figure 5.11B the global game is totally transformed: the gradient becomes positive for all j/Z for all Q, akin to a Harmony Game. As we will show in the next section, this transition from a ***D***-dominance to a

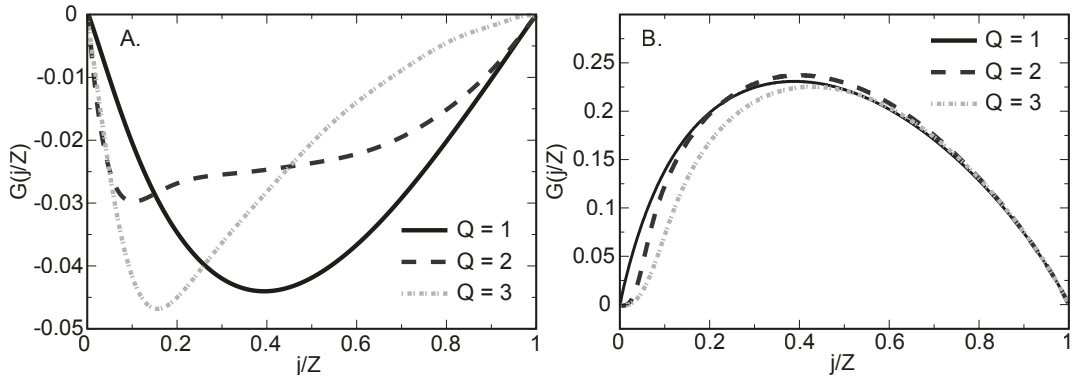

Figure 5.11: Initial Gradient of Selection for the *N*-Person Snowdrift Game on scale-free Barabási-Albert populations - Gradient of selection $G(j/Z)$ prior to population evolution when strategies are distributed **A.** randomly, and **B.** cooperators are distributed in such a way that each and every ***C*** has at least another ***C*** as neighbor. Parameters: $Z = 10^3$, $\langle k \rangle = 4$, $\beta = 1.0$, $c/b = 0.7$.

C-dominance game can be explained by the position of cooperators on the network according to node degree.

5.6.1 Biased distribution of strategies according to node degree

Taking into account the results of the previous section, here we adopt a biased distribution of strategies in the population according to node degree, and we show that by assigning ***C*s** preferentially to high connected nodes, the nature of the global social dilemma is gradually transformed. For the initial assignment of strategies to nodes, we define a probability p_{bias} of attributing strategy ***C*** to node x with connectivity k_x as

$$p_{bias} = \frac{k_i^\theta}{\sum_{j=0}^{Z-1} k_j^\theta} \tag{5.18}$$

where θ is the parameter that tunes the bias introduced for assigning ***C*s** preferentially to nodes of higher degree ($\theta > 0$) or lower degree ($\theta < 0$). The denominator $\sum_{j=0}^{Z-1} k_j^\theta$ stands for the proper normalization: the sum over the connectivities of all the nodes in the network, each connectivity to the power θ. For $\theta = 0$ we obtain $p_{bias} = \frac{1}{Z}$ and therefore we recover the conventional random assignment of strategies, independent of node degree.

Figure 5.12 shows the initial gradients of selection that are obtained for a biased distribution of strategies with $-1 \leq \theta \leq 1$, in scale-free **BA** populations. For $\theta = 0.0$, co-

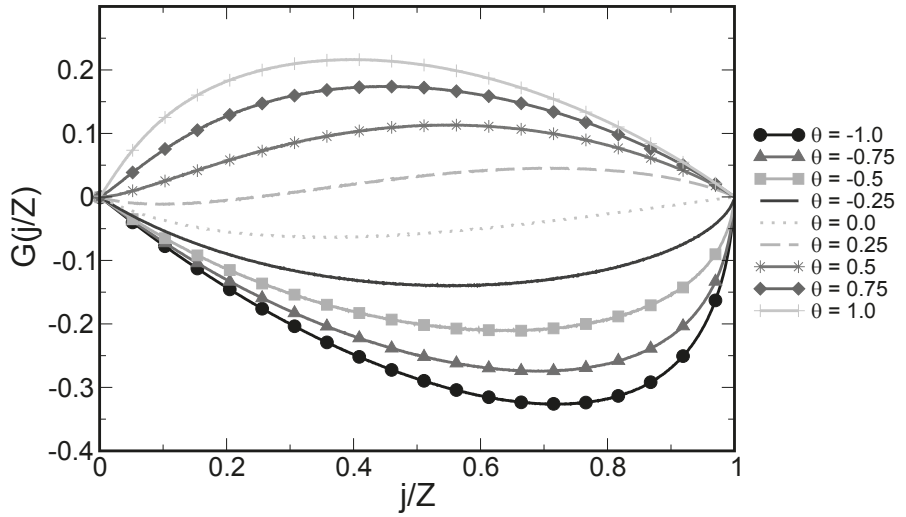

Figure 5.12: Gradients of selection for the *N*-Person Snowdrift Game in scale-free Barabási-Albert networks with biased distribution of strategies - Initial gradients of selection (prior to population evolution) for the N-Person Snowdrift Game in scale-free Barabási-Albert populations when strategies are distributed in a biased way according to the parameter θ in equation 5.18. When $\theta > 0$ ($\theta < 0$) cooperators are assigned preferentially to high (low) connected nodes. When $\theta = 0$, we recover the random assignment of strategies in the population. Parameters: $Z = 10^3$, $\langle k \rangle = 4$, $\beta = 1.0$, $c = 0.9$, $b = 1.0$.

operators and defectors are distributed randomly in the population and the gradient of selection depicted in figure 5.12 is in accordance with the results shown in figure 5.11A, only for a higher cost-benefit ratio c/b: the global dilemma, at a population level, corresponds to a ***D***-dominance game. For $\theta < 0$, cooperators are preferentially assigned to low connected nodes, and conversely defectors are assigned to higher connected nodes. Defectors in these positions will be more advantageous: they participate in more games, and in each game it is sufficient for them to encounter a single ***C*** to obtain the benefit. As a result, for $\theta < 0$ the global dilemma naturally continues to correspond to a ***D***-dominance game, and the amplitude of the gradient of selection increases as $|\theta|$ increases. That is, the population is pushed harder and harder in the direction of less ***C****s* in the population.

For $\theta > 0$, cooperators are preferentially assigned to high connected nodes, and as θ increases, the nature of the global dilemma is gradually transformed. For $\theta = 0.25$, we observe the emergence of a coordination point for $j/Z \approx 0.25$, and for $\theta \geq 0.5$ the global dilemma is transformed into a ***C***-dominance game, akin to a Harmony Game.

That is, despite the local rules of the game being always the same (the rules of the **NSG**), which in a well-mixed population correspond to a coexistence global dynamics, these can be highly altered when individuals are also defined by their specific position in their social network: for the same local rules, depending on where individuals are located and with whom they play the nature of the global dilemma can be surprisingly different.

This gradual transformation of the game from a ***D***-dominance dilemma to a ***C***-dominance for increasing θ in scale-free **BA** networks has to do with the particular growth mechanism of this class of networks. In scale-free **BA** networks the hubs are mostly interconnected, because of the preferential attachment of new nodes to higher connected nodes during network growth (see section 2.4). When we impose a preferential distribution of ***C****s* to high connected nodes, not only these individuals become more advantageous because they accumulate a higher fitness (higher than if they were assigned to a node with low connectivity), but also most cooperators will have at least one cooperator as neighbor. That is, the distribution of strategies we impose when $\theta \gg 0$ is very similar to that we imposed for obtaining the results shown in figure 5.11. We have verified this hypothesis by performing the same distributions of strategies in exponential networks (results not shown here), for which preferential attachment during network growth is replaced by random attachment.

5.6.2 Cooperators (and Defectors) on the Stars

In light of the results discussed in section 5.6.1, and of the analytical study we performed for the **NPD** (section 4.8), we now present an analogous study for the **NSG** (with $Q = 1$), resorting to the simple double star representative of characteristic substructures of scale-free **BA** networks. We will show that when both hubs agree on their strategies (be it both cooperators or both defectors) the invasion of their leaves is very easy. Furthermore, we will consider as an initial configuration the most disadvantageous situation for a cooperator (and simultaneously the most advantageous situation for a defector) and show how even in those circumstances the ***C*** strategy can spread and invade the whole double star.

Figure 5.13 depicts the most probable sequence of steps that occurs in the spreading of strategies in the double star, when we depart from the following distribution of strategies: a ***C***-hub surrounded by ***D***-leaves, and connected to another ***D***-hub whom in his turn is surrounded by ***C***-leaves. This corresponds simultaneously to the worse

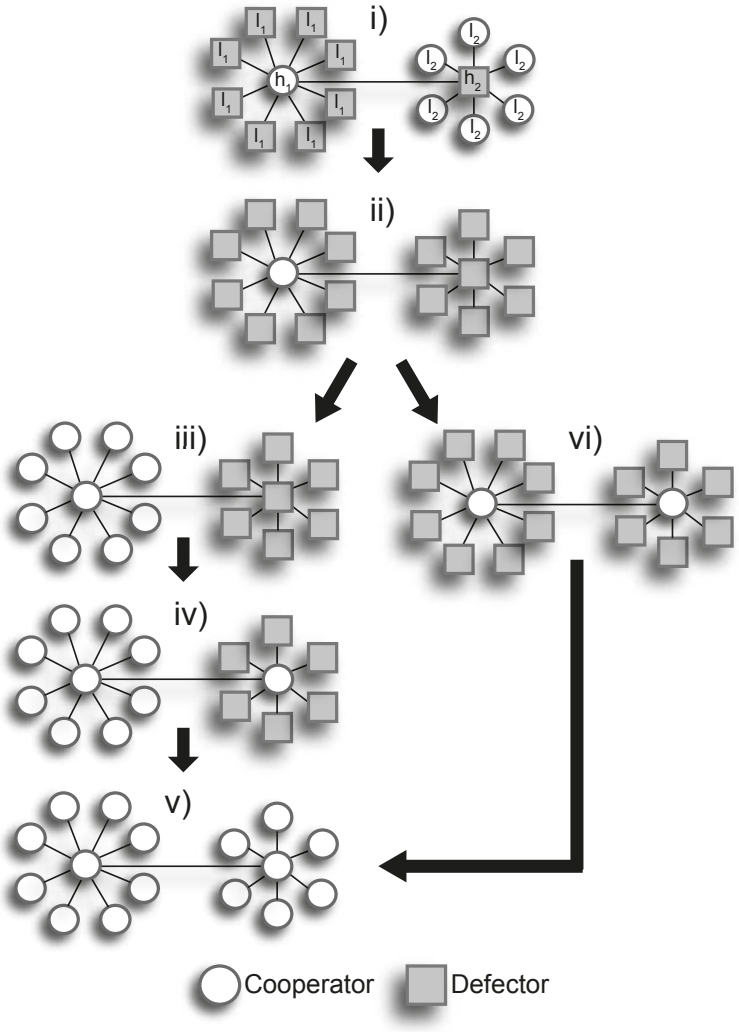

Figure 5.13: The invasion of the double star in the *N*-Person Snowdrift Game - The double star construction is composed of two centers (h_1 and h_2), the left one with $N-2$ leaves and the right one with $M-2$ leaves. The first configuration corresponds to the best situation for a ***D***, in the right center, and simultaneously to the worst situation for a ***C***, in the left hub.

configuration for a ***C*** (because he alone has to pay the effort to obtain the benefit in almost all the games in which he participates; note that we are studying the case $Q = 1$) and the best configuration for a ***D*** (there is always at least one cooperator in all the games in which he participates, and therefore he always obtains the benefit). In figure 5.13 we represent this initial configuration (configuration **i)**), as well as the

sequence of steps that may lead to the invasion of the whole double star by the ***C***-strategy. We assume that the left hub (h_1) has $N-2$ leaves, and the right hub (h_2) has $M-2$ leaves. As in the analysis performed for the **NPD** in section 4.8, for simplicity we neglect any other connections that the leaves of h_1 and h_2 may have. Our conclusions would remain qualitatively valid if those were included in our calculations, but our analysis would require further considerations regarding their connectivities.

Figure 5.13: from configuration i) to configuration ii)

In this initial configuration, we start by assessing the fitness of each individual to evaluate which strategy invasion is more probable to occur. The fitness of the ***C*** individual on the left hub (f_{C,h_1}), the fitness of the ***D*** individual on the right hub (f_{D,h_2}), the fitness of the ***D***-leaves of the left hub (f_{D,l_1}), and the fitness of the ***C***-leaves of the right hub (f_{C,l_2}) are, respectively, given by

$$f_{C,h_1} = Nb - (N-2)c - c - \frac{c}{M-1} = Nb - Nc + c - \frac{c}{M-1} \tag{5.19a}$$

$$f_{D,h_2} = Mb \tag{5.19b}$$

$$f_{D,l_1} = 2b \tag{5.19c}$$

$$f_{C,l_2} = 2b - \frac{c}{2} - \frac{c}{M-1} \tag{5.19d}$$

Taking into account that

$$f_{C,h_1} > f_{D,h_2} \Rightarrow \frac{c}{b} < \frac{N-M}{N-1+\frac{1}{M-1}}, \tag{5.20a}$$

$$f_{C,h_1} > f_{D,l_1} \Rightarrow \frac{c}{b} < \frac{N-2}{N-1+\frac{1}{M-1}}, \tag{5.20b}$$

$$f_{D,h_2} > f_{C,l_2} \Rightarrow Mb > 2b - \frac{c}{2} - \frac{c}{M-1}, \tag{5.20c}$$

four possibilities can occur with this configuration: the ***C***-hub, h_1, can either invade any of its leaves l_1, or invade the hub h_2; conversely, the ***D***-hub, h_2, can either invade any of its leaves l_2, or invade the hub h_1. Taking into account the fitness inequalities expressed in equations 5.20, we conclude that the less stringent inequality corresponds to the invasion of the leaves l_2 by the ***D***-hub h_2 ($f_{D,h_2} > f_{C,l_2}$ whenever $M \geq 2$). That is, this is the more probable scenario that can happen, and so we will assume that this

is the next possible configuration. Once one of the leaves l_2 is invaded by the ***D***-hub h_2, the fitnesses of h_2 and any of the cooperative l_2 now are

$$f_{D,h_2} = Mb \tag{5.21a}$$

$$f_{C,l_2} = 2b - \frac{c}{2} - \frac{c}{M-2} \tag{5.21b}$$

While the fitness of the ***D***-hub remains unaltered (because he always obtains the benefit b in all the games in which he participates), the fitness of the remaining ***C*** leaves decreases slightly, which means that invasion of the remaining ***C*** leaves l_2 by the ***D***-hub h_2 becomes progressively easier, and we reach configuration **ii)** in figure 5.13.

Figure 5.13: configuration ii)

Once configuration **ii)** is reached, the fitness of the ***C***-hub (f_{C,h_1}), the ***D*** leaves l_1 (f_{D,l_1}), and the ***D***-hub h_2 (f_{D,h_2}) correspond to

$$f_{C,h_1} = Nb - (N-2)c - 2c = Nb - Nc \tag{5.22a}$$

$$f_{D,l_1} = 2b \tag{5.22b}$$

$$f_{D,h_2} = 2b \tag{5.22c}$$

Given that

$$f_{C,h_1} > f_{D,l_1} \Rightarrow \frac{c}{b} < \frac{N-2}{N}, \tag{5.23}$$

and the same result holds for $f_{C,h_1} > f_{D,h_2}$, it is more probable for the ***C***-hub h_1 to invade either the ***D***-hub h_2 or the ***D***-leaves l_1 (than to be invaded by any of them). Regarding the possible invasions from the ***C***-hub to the leaves or the other hub, these are equally probable, and for that reason we will consider both possibilities. Of course, it is more probable that a leave l_1 is chosen to be invaded than the hub h_2, because they are in greater number. We will start by exploring all the consequences of the invasion of the ***D*** leaves l_1 by the ***C***-hub h_1, and in the end of that reasoning we will come back to this configuration and explore what happens when the ***C***-hub h_1 invades the ***D***-hub h_2.

Figure 5.13: from configuration ii) to configuration iii)

Once one of the leaves l_1 becomes ***C***, the fitnesses of the ***C***-hub (f_{C,h_1}) and of the remaining ***D***-leaves l_1 (f_{D,l_1}) are modified to

$$f_{C,h_1} = Nb - (N-3)c - \frac{c}{2} - \frac{c}{2} - c = Nb - Nc + c \tag{5.24a}$$

$$f_{D,l_1} = 2b \tag{5.24b}$$

which means that, while the fitness of the ***D***-leaves l_1 is unaltered regarding its value prior to this invasion, the fitness of the ***C***-hub slightly increases; therefore, the invasion of the remaining leaves becomes progressively easier and configuration **iii)** is attained.

Figure 5.13: from configuration iii) to configuration iv)

The fitnesses of the ***C***-hub (f_{C,h_1}) and of the ***D***-hub (f_{D,h_2}) now correspond to

$$f_{C,h_1} = Nb - (N-2)\frac{c}{2} - \frac{c}{N-1} - c \tag{5.25a}$$

$$f_{D,h_2} = 2b \tag{5.25b}$$

and

$$f_{C,h_1} > f_{D,h_2} \Rightarrow \frac{c}{b} < \frac{N-2}{\frac{N-2}{2} + \frac{1}{N-1} + 1} \tag{5.26}$$

This condition is deterministic whenever the numerator is greater than the denominator (since we assume $b > c$), that is, whenever

$$N - 2 > \frac{N-2}{2} + \frac{1}{N-1} + 1 \tag{5.27}$$

After a little algebra, we obtain that this condition is obeyed whenever $N > 5$, which is a small value. Furthermore, for $2 < N \leq 5$, this condition is also very likely to occur for rather high cost-benefit ratios c/b.

Figure 5.13: from configuration iv) to configuration v)

Once configuration **iv)** is reached, it is very easy for the cooperative strategy to invade the whole double star. The fitness of the ***C***-hub h_2 (f_{C,h_2}) and of the ***D*** leaves (f_{D,l_2}) can be written as

$$f_{C,h_2} = Mb - (M-2)c - \frac{c}{2} - \frac{c}{N} = Mb - Mc + \frac{3}{2}c - \frac{c}{N} \tag{5.28a}$$

$$f_{D,l_2} = 2b \tag{5.28b}$$

and we obtain

$$f_{C,h_2} > f_{D,l_2} \Rightarrow \frac{c}{b} < \frac{M-2}{M-\frac{3}{2}-\frac{1}{N}} \tag{5.29}$$

which is a valid inequality for most values of $c/b < 1.0$, and therefore it is possible and probable that the ***C***-hub h_2 invades the leaves l_2. Furthermore, when the first leaf is invaded, the fitnesses of the ***C***-hub h_2 and of the remaining defective leaves l_2 become

$$f_{C,h_2} = Mb - (M-3)c - \frac{c}{2} - \frac{c}{2} - \frac{c}{N} = Mb - Mc + 2c - \frac{c}{N} \tag{5.30a}$$

$$f_{D,l_2} = 2b \tag{5.30b}$$

That is, while the fitness of the ***D***-leaves l_2 remains unchanged, the fitness of the ***C***-hub h_2 slightly increases; and therefore the invasion of the remaining defective leaves becomes easier, and we eventually reach configuration **v)**, in which all individuals in the double star are ***C*s**.

Figure 5.13: configuration vi) to configuration v)

When, in the double star, both centers are ***C*s**, and all the remaining nodes (the leaves) are ***D*s**, we may write the fitness of either one of the centers (f_{C,h_1} and f_{C,h_2}) and either of the leaves (f_{D,l_1} and f_{D,l_2}) as

$$f_{C,h_1} = Nb - (N-2)c - \frac{c}{2} - \frac{c}{2} = Nb - Nc + c \tag{5.31a}$$

$$f_{C,h_2} = Mb - Mc + c \tag{5.31b}$$

$$f_{D,l_1} = f_{D,l_2} = 2b \tag{5.31c}$$

Depending on the relationship between N and M, it will be either the l_1 leaves or the l_2 leaves the first ones to get invaded by the corresponding hubs. For simplicity, now we will consider $N > M$. In this case, it will be more probable that the l_1 leaves get invaded first (because the left hub has a higher fitness), according to

$$f_{C,h_1} > f_{D,l_1} \Rightarrow \frac{c}{b} < \frac{N-2}{N-1} \tag{5.32}$$

which is a valid condition for most values of c/b. When one of the leaves becomes a cooperator, the fitness of the ***C***-center (f_{C,h_1}) and of the remaining ***D***-leaves (f_{D,l_1}) is

modified to

$$f_{C,h_1} = Nb - (N-3)c - \frac{c}{2} - \frac{c}{3} - \frac{c}{2} = Nb - Nc + \frac{5}{3}c \tag{5.33a}$$

$$f_{D,l_1} = 2b \tag{5.33b}$$

and

$$f_{C,h_1} > f_{D,l_1} \Rightarrow \frac{c}{b} < \frac{N-2}{N-5/3} \tag{5.34}$$

which is a less strict condition than the one we have met before in equation 5.32, meaning that it becomes increasingly easier to invade the remaining ***D*** leaves. The situation is symmetrical in the right hub, and therefore the double star evolves until reaching configuration **v)**.

We are aware that, while in the previous chapter we considered the replicator dynamics analogue in structured populations as an update method, here we are considering the Fermi Imitation update method. In the replicator dynamics individuals only imitate the strategy of neighbors that have a fitness larger than theirs (that is, selection is strong), while in the Fermi process individuals can imitate, with a certain probability (regulated by the intensity of selection β) the strategy of individuals with a lower fitness. Nevertheless, we have verified that even for high values of the cost-benefit ratio c/b, close to 1, the double star is totally invaded by the cooperative strategy even for the intensity of selection $\beta = 1.0$ considered here. Higher values of the intensity of selection β reduce, on average, the evolutionary time taken to reach the full cooperative state of the double star starting from the configuration **i)** described in figure 5.13.

5.6.3 Average Gradient of Selection in Heterogeneous Populations

We now proceed to explore the more general scenario $Q \geq 1$ in scale-free **BA** networks, by analyzing the corresponding average gradients of selection. Figure 5.14 depicts the trajectories of the internal points of the gradient of selection for the first 150 generations of evolutionary time. The intrinsically dual nature (co-existence and coordination) of the **NSG** creates a multitude of internal roots which result from the occurrence of evolutionary deadlocks associated with particular motifs of the network (117, 118), reflected in the appearance of quasi-stationary states close to full cooperation and full defection. For this reason, and contrary to the case of **HoRand** networks, the **AGoS** in scale-free **BA** networks does not converge rapidly into a stationary state, due to the continuous invasion and counter-invasion induced by highly connected nodes.

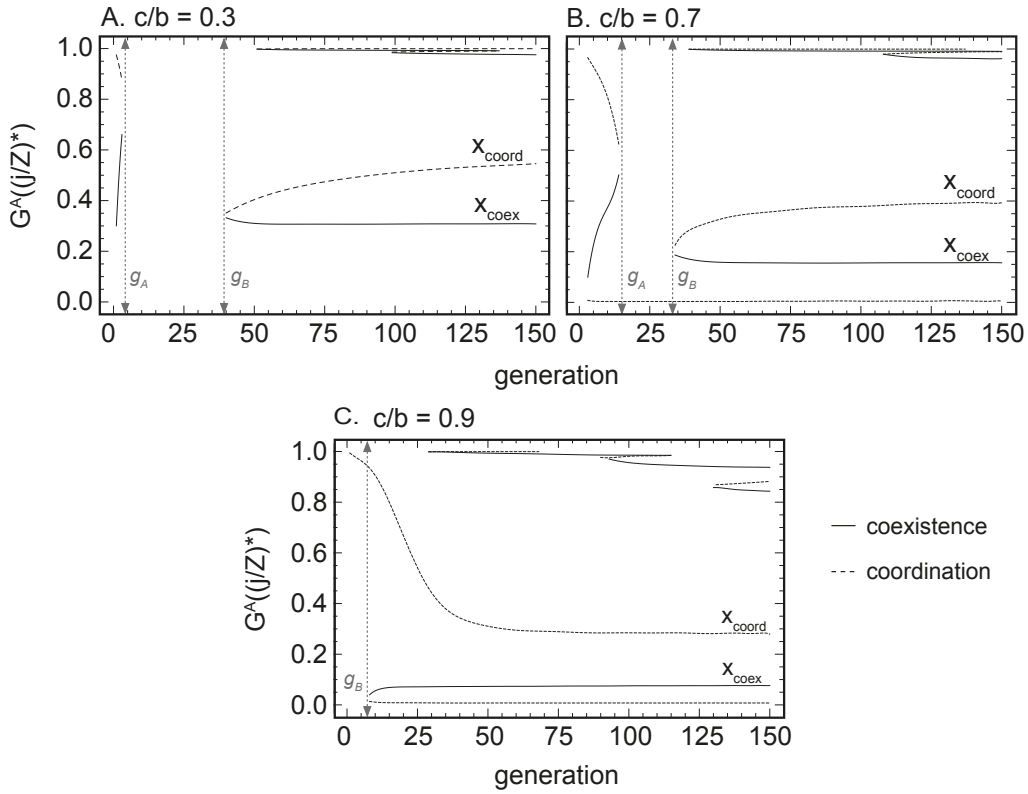

Figure 5.14: Trajectories of the internal points of the average gradient of selection (AGoS) during the first 150 generations for the *N*-Person Snowdrift Game on scale-free Barabási-Albert populations - We consider **A.** c/b=0.3, **B.** $c/b = 0.7$, **C.** $c/b = 0.9$ respectively. Each curve corresponds to the fit of the obtained points: dashed (full) lines correspond to the trajectory of coordination (co-existence) points. Parameters: $Z = 10^3$, $\langle k \rangle = 4$, $\beta = 1.0$.

For $Q = 1$ we observe a transition phase during the first 50 generations at which the population-wide dynamics changes abruptly. This phase is characterized by two bifurcations: the first in which two internal points bifurcate at generation g_A and a second when at generation g_B a bifurcation gives rise to two internal points (x_{coex} and x_{coord}) that will mainly dominate the evolutionary dynamics. Overall, we see that g_A (g_B) increases (decreases) with increasing c/b, a fact that is particularly evident in figures 5.14A and 5.14B. The effective dilemma between generations g_A and g_B is akin to a *Harmony Game*, that is, the fraction of cooperators tends to increase regardless of the state j/Z.

We also note the existence of a critical c/b value $(0.7 < c/b \leq 0.9)$ at which g_A and

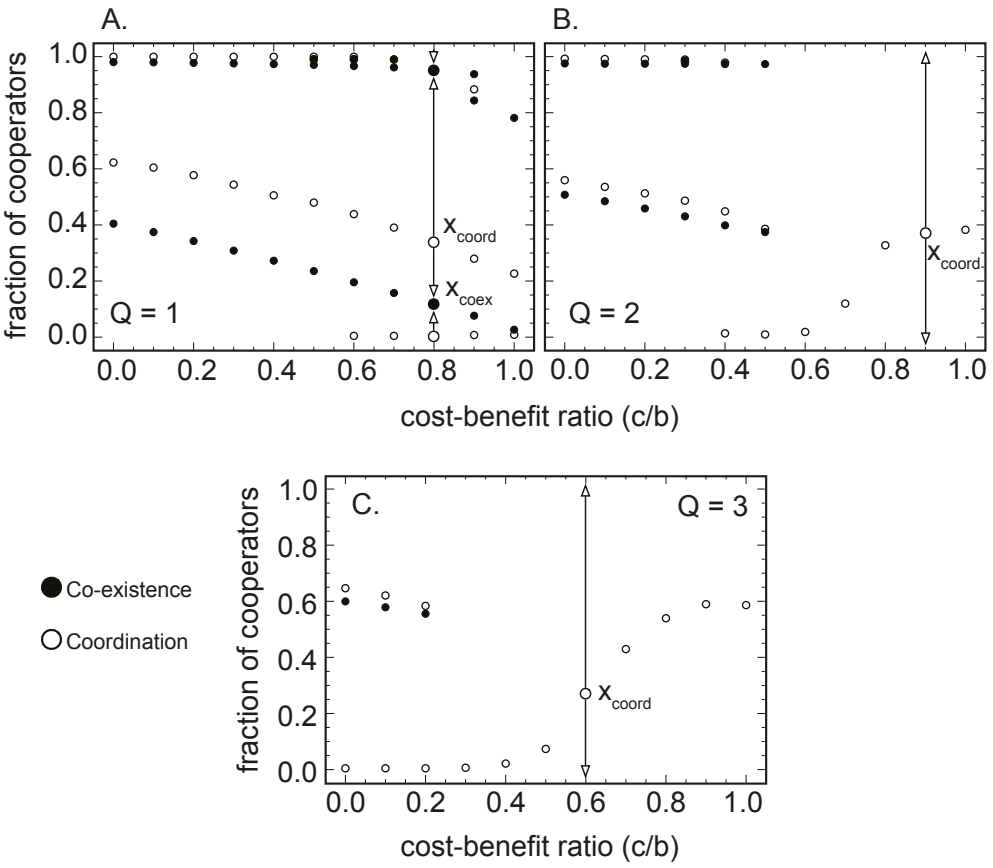

Figure 5.15: Evolutionary dynamics of the *N*-Person Snowdrift Game on scale-free Barabási-Albert populations - Position of the internal roots of $G^A(j/Z, g)$ at the 150^{th} generation as a function of c/b for: **A.** $Q = 1$, **B.** $Q = 2$, and **C.** $Q = 3$. Solid (open) circles indicate a co-existence (coordination) point. Parameters: $Z = 10^3$, $\langle k \rangle = 4$, $\beta = 1.0$.

g_B merge resulting in a different dynamical pattern, as the transient period akin to a Harmony Game is omitted – results depicted in figure 5.14C. However, we continue to observe a bifurcation which gives rise to a coexistence point, x_{coex}, now closer to $j/Z = 0.0$.

Figure 5.15, similar to figure 5.10 but now for scale-free **BA** populations, provides the location of the internal roots of $G^A(j, t_g)$ at the 150^{th} generation as a function of c/b. We consider the cases $Q = 1$ to $Q = 3$, the latter corresponding to impose unanimity of cooperation for the smallest groups of the population (for our particular choice of the average connectivity $\langle k \rangle$, for which we used $\langle k \rangle = 4$).

For $Q = 1$, we observe that the population-wide dynamics is characterized by two

basins of attraction, each dominated by a co-existence point. Overall, whenever highly connected nodes (hubs) are ***Ds***, the population may remain in a co-existence state for low values of the fraction of ***Cs***, since some intermediate degree nodes (and their neighborhood) may remain cooperating. Differently, whenever hubs adopt a cooperative behavior, the population is driven towards a co-existence point in which a small fraction of ***Ds*** may free ride when located on the leaves (low degree nodes) of the network. Between these two regimes, the stochastic nature of the evolutionary process, together with the method adopted for the computation of the **AGoS**, allows one to observe the fingerprints of short-lived *equilibria*, as shown in figure 5.15, whereas the size of each basin of attraction is ultimately defined by the strength of the dilemma, i.e., by the cost-to-benefit ratio c/b.

As we increase the coordination requirements needed to achieve a collective benefit ($Q > 1$, see figure 5.15), local co-existences become harder to achieve which, combined with harsher dilemmas (large c/b), in the long run lead the population-wide dynamics towards pure coordination, with a single unstable root and two stable monomorphic states. For large values of Q and c/b, it is noteworthy that global coordination can be reached for values of c/b in which widespread defection would pervade in well-mixed populations (i.e. $Q = 1$ and $c/b = 1.0$), showing how heterogeneous networks may transform a defection dominance dilemma into a coordination problem.

5.7 Discussion

The present study shows the impact of the population structure in the dynamics of cooperative collective action associated with the **NSG**. Due to its twofold nature of coordination and coexistence (112) – in well-mixed populations the game exhibits a pair of coordination and coexistence points when a threshold Q is introduced – the **NSG** is more complex than most dilemmas previously studied in structured populations (119, 120).

In order to handle such a degree of complexity, we have studied the global dynamics (117) created by each network structure, and compared it with the results previously obtained in unstructured populations (111, 112). We show that evolution on homogeneous networks exhibits a population-wide behavior qualitatively similar to that observed in well-mixed populations. Notwithstanding, homogeneous social structures are able to reduce the efforts needed to achieve a stable fraction of cooperators which, in turn, increases with increasing Q. Heterogeneous networks, on the other hand, lead to

more complex evolutionary dynamics scenarios, with a multitude of internal *equilibria*, whereas for high value of c/b and $Q > 1$, the increasing difficulty to locally coordinate actions transforms the overall population-wide dynamics into a coordination problem.

Finally, our results support the idea that stringent requirements to achieve a collective benefit significantly raise the chances of cooperation, thereby escaping the tragedy of the commons.

5.8 Methods

5.8.1 Population structure

We compare the evolutionary dynamics on both homogeneous and heterogeneous networks. As representative of the former, we consider ring regular networks in which the neighborhood of all nodes is regularly organized in the same fashion; and homogeneous random networks (**HoRand**) (23), obtained by randomly swapping the ends of pairs of links of a ring regular network. As representative of the latter, we take scale-free networks generated with the Barabási-Albert algorithm (**BA**) of growth and preferential attachment (section 2.4 and reference (24)). In all simulations, networks remain fixed throughout evolution. We consider populations of size $Z = 10^3$ and average connectivity $\langle k \rangle = 4$.

5.8.2 Evolution

In each game round, a randomly chosen individual A is given the opportunity to revise his strategy, by comparing it with the one adopted by a randomly chosen neighbor B. Individuals A and B assess their individual fitness by accumulating the payoff obtained from the $k_i + 1$ games (with $i \in \{A, B\}$) in which they participate: the one centered on themselves, and the ones centered on their k_i neighbors. If individuals A and B have different strategies ($s_A \neq s_B$) A imitates B according to the Fermi Imitation process (references (77, 78, 79) and section 3.2.3.2), with probability given by the Fermi distribution from statistical physics

$$p_{Fermi} = \frac{1}{1 + e^{-\beta\left(f_{s_B} - f_{s_A}\right)}} \tag{5.35}$$

Note that individual A can still imitate individual B if $f_{s_A} > f_{s_B}$, the Fermi imitation process allows for occasional mistakes in the decision-making process.

5.8.3 Simulations

We evaluate the steady state by averaging the *final fraction of cooperators* after 1500 generations (see panels A and B of figure 5.6) starting with 50% of ***C**s* and ***D**s* placed randomly in the population. We also compute the *quasi-stationary distribution*, that is the fraction of time the system spends in each non-monomorphic state j ($j \in \{1, ..., Z-1\}$) along the first 2500 generations (1 generation = Z time-steps) over 5 x 10^4 simulations (see panel D of figure 5.9), starting from an initial random composition of strategies in the population. Concerning the determination of the *average gradient of selection* (**AGoS**) (117), for each individual i we compute the probability that this individual changes behavior at time t,

$$\mathcal{T}_i(t) = \frac{1}{k_i} \sum_{m=1}^{\bar{n_i}} \frac{1}{1 + e^{-\beta(f_m(t) - f_i(t))}}, \tag{5.36}$$

where k_i stands for the degree of node i and $\bar{n_i}$ for the number of neighbors of i having a different strategy. At a given time t of simulation p we define

$$G_p(j,t) = \mathcal{T}_p^+(j,t) - \mathcal{T}_p^-(j,t) \tag{5.37}$$

with

$$\mathcal{T}_p^{\pm}(j,t) = \frac{1}{Z} \sum_{\substack{\text{All } \boldsymbol{C}s \\ \text{All } \boldsymbol{D}s}}^{i=1} \mathcal{T}_i(t) \tag{5.38}$$

for a state with j ***C**s* in a population of size Z. The *time-dependent* **AGoS** at generation t_g is then computed by averaging over the last Z time-steps, that is,

$$G^A(j,t_g) = c_j(t_g)^{-1} \sum_{t_g-1}^{t_g} \sum_{p=1}^{\Omega} G_p(j,t) \tag{5.39}$$

where $c_j(t_g)$ accounts for the number of times the system was observed in state j during generation t_g. For a given network type, we perform $\Omega = 2.5 \times 10^7$ simulations (using 10^2 networks of each type) starting from random initial conditions.

6

Peer Influence (of cooperation and more)

6.1 Introduction

A brief search on the Internet reveals that there are approximately two hundred notable, well-known social networking websites currently online, a number that corresponds only to those that have the highest number of members and excludes thousands of other, smaller, online social networks (121). Of these, Facebook is currently the largest online social network, with more than $908\ 000\ 000$ members, approximately $1/7$ of the total world population.

The advent of the World Wide Web has enabled the popularity and massive access to online social networks, and as a consequence has made it possible to obtain large amounts of data on them. Data from social networks is valuable in the sense that it can help to shed a light on how humans interact with each other, how they react to the information transmitted by their peers (do they imitate them? can they be influenced by them?), and how these interactions are affected by the structure of that social network. In fact, the study of social networks goes back far farther than the networks' modern day computer incarnations: the true foundation of the field is attributed to the psychiatrist Jacob Moreno, a Romanian immigrant in America, who in the 1930s became interested in the dynamics of social interactions within groups of people (122). However, until recently, because of the effort involved in compiling them, it was impossible to obtain networks with more than a few dozens or hundreds of elements. Nowadays,

there is no reason why social networks cannot be as large as the Internet or the World Wide Web; the difficulties that previously existed in gathering the data are now the handling of the enormous amounts of data available for academic studies. Such constraints, together with privacy issues, are now determinant for the size of the social networks available nowadays. This growing tendency to socialize online carries with it a huge research potential: not only the evolution of the social structure is registered, but also all the interactions. Some centuries from now, if this data is accessible it will provide a very valuable resource to study human culture in this century.

Behaviors or strategies (as to cooperate or defect) are examples of information that propagates in social networks – other examples can be emotions, gossip, ideas, fads. How this information flows and what determines the flow patterns has become extremely valuable with applications extending to all areas of human activity. Several studies have focused on the role played by social networks on the spread of information between individuals, by making use of email and blog databases, and online social networks such as Twitter and Facebook (123, 124, 125, 126). Both empirical studies and theoretical models have shown how social networks affect the propagation of health issues (127, 128, 129), ideas (130), criminal behavior (131, 132), economic decisions (133, 134, 135), school achievement (136) and cooperation (52, 65, 120), among other human traits.

Recently, Fowler and Christakis (137, 138, 139, 140, 141, 142, 143, 144) undertook a series of statistical analyses applied to several social networks, in order to study the propagation of traits on those social networks. They focused on the Framingham Heart Study (**FHS**) database (145), from which they obtained a social network and analyzed correlations between individuals for traits as diverse as smoking habits, alcohol consumption, loneliness, obesity, happiness or cooperation. Correlations reflect the relative probability (when compared with a random arrangement) that two individuals share the same trait, as a function of their social distance, defined as the smallest number of hops connecting those individuals in the social network. Besides the social network obtained from the **FHS** database, other social networks were studied. A sample from the Facebook social network was used to check whether the individuals were smiling or if they exhibited signs of overweight on their profile pictures. Also, data from the National Longitudinal Study of Adolescent Health (Add Health) (146) was used to investigate how habits of sleep and marijuana consumption propagated on that social network. All these studies revealed the emergence of similar and non-trivial patterns of correlation: individuals were positively correlated up to a social distance between 2

and 4. These results reveal that not only our "friends", but also our friends' friends, and even our friends' friends' friends, exhibit a positive correlation of traits. That is, when studying the example of propagation of the smoking habits in social networks, Fowler and Christakis discovered that it is likely that the 1^{st}, 2^{nd} and 3^{rd} neighbors of a smoker are also smokers.

These results are surprising in several aspects. The first one, concerning the fact that the traits analyzed were of very different nature, and because of that we expect that their propagation follows different "rules" – how we opt for a given profile picture is different from how we decide to cooperate or defect with someone, or from how we decide for a more or less healthy meal. Nonetheless, the adoption of these behaviors/traits, although following different dynamical rules, reveals a similar global pattern. On the other hand, these similar patterns were obtained for social networks with different topological properties. From the network data that we were able to collect from the published papers, we observed that while the **FHS** and the Facebook networks exhibited a degree distribution akin to that of exponential networks, the degree distribution of the AddHealth network could be modeled more closely by the Erdös-Renyi model. Furthermore, these networks have sizes that span from a few hundreds to a few thousands, and average connectivities that range from values as low as 2 or 3, to values of more than one dozen.

We use the term *peer influence* when referring to this empirical observation that individuals influence the behavior of their nearest neighbors. Here we investigate the degree of peer influence that emerges from different dynamical processes propagating in networked populations – the spread of cooperative strategies, opinions and diseases. Individuals are assigned to the nodes of a complex network, whereas links between them represent interactions. We show that, for each network class considered, *different* processes lead to *identical* degrees of influence, suggesting that peer influence does not depend on the process at stake. On the other hand, we find that simple topological properties of the underlying social networks, such as the average connectivity and the clustering coefficient, ultimately determine the intensity of influence observed, which systematically falls between 2 and 3 for typical social networks, in agreement with the results stemming from empirical analyses of correlations in present (137, 138, 139, 140, 142, 143, 144) and past (147) social networks.

6.2 Dynamical Processes

We adopt three dynamical processes to investigate peer influence: the 2-person Prisoner's Dilemma as representative of the propagation of cooperative strategies (section 6.2.1); the Voter Model as representative of opinion dynamics (section 6.2.2); and the Susceptible-Infected-Recovered epidemic model as representative of disease spreading dynamics (section 6.2.3). We adopt these three particular dynamical processes because we believe they are representative of the majority of processes that occur on social networks, and because there exist several results already in the literature in which we can base our research.

6.2.1 Evolution of Cooperation

In contrast with the previous two chapters, we now focus on 2-person one-shot social dilemmas, in particular the Prisoner's Dilemma game (**PD**) – although we also confirmed our conclusions with other 2-person social dilemmas, namely the Snowdrift Game (**SG**) and the Stag-Hunt game (**SH**), all discussed in chapter 2. In the case of the 2-person Prisoner's Dilemma, individuals can either cooperate or defect with all of their (first) neighbors, with returns of $R = 1$ for mutual cooperation, $P = 0$ for mutual defection, $S = -\lambda$ when playing ***C*** against ***D***, and $T = 1 + \lambda$ when playing ***D*** against ***C***, where $\lambda > 0$ measures both the temptation to defect and the fear of being cheated. This can be summarized in the payoff matrix

$$\begin{array}{c} \\ \boldsymbol{C} \\ \boldsymbol{D} \end{array} \begin{array}{c} \begin{array}{cc} \boldsymbol{C} & \boldsymbol{D} \end{array} \\ \begin{pmatrix} 1 & -\lambda \\ 1+\lambda & 0 \end{pmatrix} \end{array}, \lambda > 0 \tag{6.1}$$

We adopt the Fermi Imitation update rule already discussed in chapter 3 (section 3.2.3.2 and references (77, 78, 79)). When the 2-person one-shot **PD** is played in a population without any social structure, the population evolves towards full defection, a fate which may change when individuals are embedded in a social network represented by means of a graph (65, 120, 148) in which structural diversity is ubiquitous (65, 149, 150).

6.2.2 Opinion Dynamics

In practice, the population dynamics of peer-influence need not be fitness driven by any type of social dilemma. To this end, we adopt a simple model of opinion formation

– the Voter Model (**VM**) (151). This model owes its name to the fact that it was first proposed to model, in a very simple manner, a voter's attitude towards one particular subject or election. In general, in the literature exist several different variants of the Voter Model concerning how an individual adopts a given opinion, and in general there can be n_{VM} different opinions in the population. However, we will consider the simplest case of only two possible different opinions ($n_{VM} = 2$). We consider that in each time-step a randomly chosen individual A adopts the opinion of a random neighbor B with probability p_{VM}. Due to its simplicity, there are several studies on this model not only on **WM** populations but also on structured populations (152, 153, 154, 155).

6.2.3 Epidemics

Information transmission has been sometimes regarded as "contagious" (130, 156), similar to the propagation of infectious diseases. As an example, we employ the Susceptible-Infected-Recovered model (**SIR**), a model created in 1927 by W. Kermack and A. McKendrick (157), in which individuals can be in a Susceptible (***S***), Infected (***I***) or Recovered (***R***) epidemiological state. Flow of individuals in this model is characterized as $\boldsymbol{S} \xrightarrow{\alpha} \boldsymbol{I} \xrightarrow{\gamma} \boldsymbol{R}$, where α and γ are the rates of infection and recovery, respectively[†]. This means that a susceptible individual meets an infected individual and gets infected with a probability determined by the infection rate α. Later, that infected individual may recover according to the recovery rate γ.

Assuming a well-mixed population of constant size $Z = S(t) + I(t) + R(t)$ (where $S(t)$, $I(t)$ and $R(t)$ represent the number of susceptible, infected and recovered individuals in the population as a function of time t, respectively), evolution is characterized by the coupled differential equations

$$\frac{dS(t)}{dt} = -\alpha S(t)I(t) \tag{6.2a}$$

$$\frac{dI(t)}{dt} = \alpha S(t)I(t) - \gamma I(t) \tag{6.2b}$$

$$\frac{dR(t)}{dt} = \gamma I(t) \tag{6.2c}$$

[†]It should be stressed that we are committing an abuse of notation: the symbols α and γ, which in section 4.8.2 of chapter 4 denote fitness differences, are now used to denote the infection and recovery rates in the **SIR** epidemic model respectively.

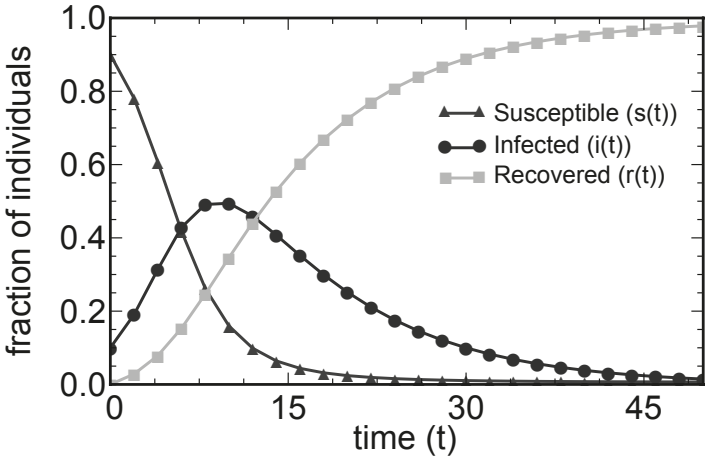

Figure 6.1: Evolutionary dynamics of the Susceptible-Infected-Recovered (SIR) epidemic model on well-mixed populations - Fraction of susceptible $(s(t) = S(t)/Z)$, infected $(i(t) = I(t)/Z)$ and recovered $(r(t) = R(t)/Z)$ in a **WM** population as a function of time t. Parameters: $\alpha = 0.5$, $\gamma 0.1$, $s(0) = 0.9$, $i(0) = 0.1$.

Alternatively, we may define the normalized variables $s(t) = \frac{S(t)}{Z}$, $i(t) = \frac{I(t)}{Z}$ and $r(t) = \frac{R(t)}{Z}$ that stand for the fraction of susceptible, infected and recovered individuals in the population over time.

An important quantity on epidemiology is the *basic reproduction ratio* R_0, defined as the expected number of infections generated by a single infected individual in a completely susceptible population. An infectious disease is said to be *endemic* if the fraction of infected individuals increases over time, that is,

$$\frac{di(t)}{dt} > 0 \Leftrightarrow \alpha s(t) i(t) - \gamma i(t) > 0 \Leftrightarrow \frac{\alpha s(t) i(t)}{\gamma} > i(t) \tag{6.3}$$

As R_0 is defined considering the secondary infections caused by a single infected in a population of susceptible individuals, we have $s(0) \approx 1$, and therefore an infectious disease is said to be endemic when $R_0 > 1$. Correspondingly, an infectious disease will die out whenever $R_0 < 1$. In figure 6.1 we illustrate how disease spreads in a well-mixed population for a particular choice of parameters. We have numerically integrated[†] the set of equations 6.2 and assumed, as initial conditions, that $r(0) = 0$. $s(0) = 0.9$ and $i(0) = 0.1$.

[†]For a fixed population size an exact solution for **SIR** can be obtained by applying direct integration methods, please check (158) for details.

In the following sections, we adopt a stochastic version of the **SIR** epidemic model on networks, which proceeds as follows: in each time-step, a randomly chosen infected individual can recover with rate γ; if not, we evaluate the possibility of infecting a randomly chosen susceptible neighbor according to rate α. The study of epidemic processes on complex networks has been subject to intense attention over the last years (159, 160, 161, 162, 163, 164). This is important to understand how contagious traits (not only diseases but also emotions or rumors, for instance) propagate on social networks and what can be done to prevent it (in the case of diseases) or foster it (in the case of publicity, for instance).

6.3 Measuring Peer Influence

In order to measure the degree of peer influence, we let the dynamical process evolve in the network (of size Z). If j is the number of individuals exhibiting a certain trait, we calculate the probability $P_n(j/Z)$ that two individuals at a distance n from each other share that same trait. The social distance between individuals corresponds to the smallest number of *hops* separating two members of a complex network, as illustrated in figure 6.2. At the end of the simulations, for each j/Z we calculate the average of $P_n(j/Z)$, $\epsilon_n^{ev}(j/Z) = \langle P_n(j/Z) \rangle$. We then subtract from this value its random component $\epsilon_n^{rand}(j/Z)$, that is, we perform the difference $\Delta\epsilon_n(j/Z) = \epsilon_n^{ev}(j/Z) - \epsilon_n^{rand}(j/Z)$. $\epsilon_n^{rand}(j/Z)$ is the average probability that a node shares the same trait with nodes located at a social distance n resulting from a random distribution of traits.

In figure 6.3A we illustrate $\epsilon_n^{ev}(j/Z)$ for a Prisoner's Dilemma game played on a ring regular network after a transient period – in this case, we measure the correlations between cooperators as a function of the fraction j/Z of cooperators in the population, and for that reason $\epsilon_n^{ev}(j/Z)$ is an increasing function of j/Z. If we measured the average probability of a defector finding another defector at a social distance n (that is, if we measured correlations between defectors), it would be a decreasing function of j/Z. Also, note that in the example depicted in figure 6.3A for a fixed j/Z the value of $\epsilon_n^{ev}(j/Z)$ decreases for increasing social distance.

The quantity that we use in order to measure the degree of peer influence is $\delta_n(j/Z)$, with

$$\delta_n(j/Z) = \frac{\Delta\epsilon_n(j/Z)}{|\Delta\epsilon_1(j/Z)|}, \tag{6.4}$$

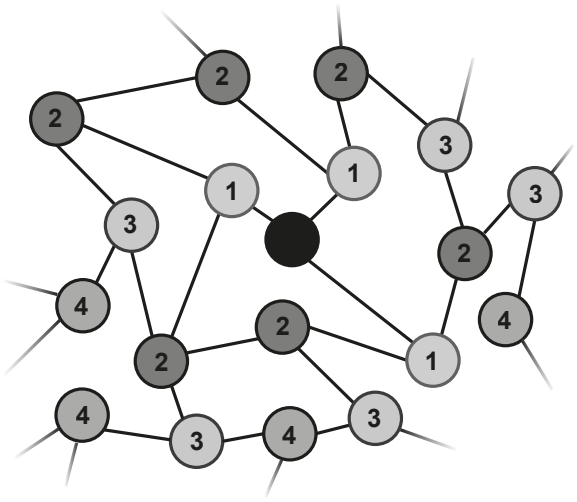

Figure 6.2: Social distances in a social network - Social distance of a given node to the focal individual (black circle) defined as the shortest number of hops between the two.

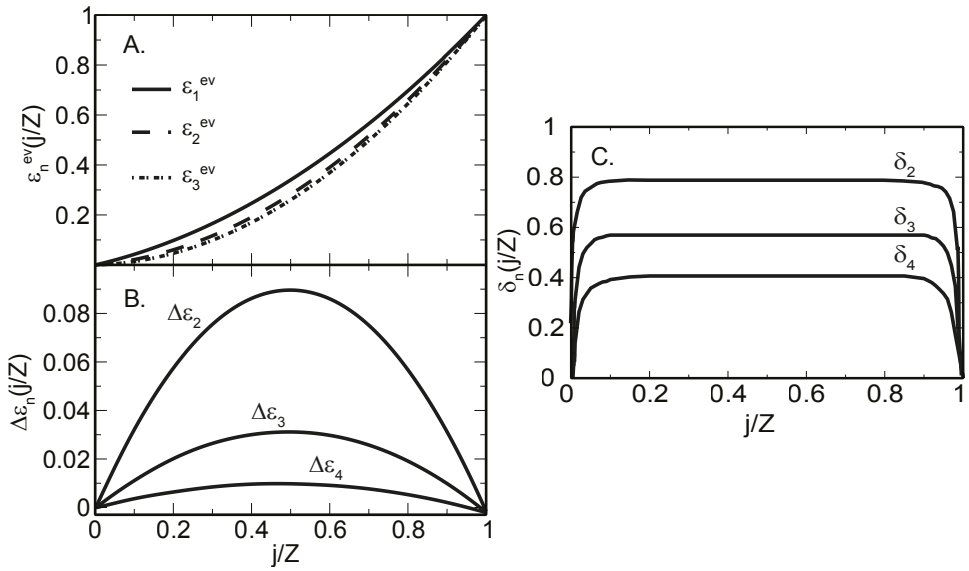

Figure 6.3: Determination of $\delta_n(j/Z)$ - **A.** $\epsilon_n^{ev}(j/Z)$ as a function of the fraction of co-operators in the population j/Z for the social distances $n = 1$ to $n = 3$, **B.** $\Delta\epsilon_n(j/Z) = \epsilon_n^{ev}(j/Z) - \epsilon_n^{rand}(j/Z)$ as a function of j/Z for the social distances $n = 2$ to $n = 4$, **C.** $\delta_n(j/Z)$ as a function of j/Z for the social distances $n = 2$ to $n = 4$. $\delta_n(j/Z)$ remains approximately constant for most values of j/Z. These examples correspond to the values obtained for the **PD** game in ring regular networks. Parameters: $Z = 10^3$, $\langle k \rangle = 4$, $\lambda = 0.03$, $\beta = 1.0$.

In equation 6.4, $|\Delta\epsilon_1(j/Z)|$ ensures a convenient normalization; we take the absolute value so that $\delta_n(j/Z)$ is only affected by the change of sign of the numerator, $\Delta\epsilon_n(j/Z)$. figure 6.3B illustrates some $|\Delta\epsilon_n(j/Z)|$ for the social distances $n = 2$ to $n = 4$, and figure 6.3C illustrates the value of $\delta_n(j/Z)$ for $n = 2$ to $n = 4$ – for correlations between cooperators in a Prisoner's Dilemma played on a ring regular population. Given the normalization we chose, $\delta_n(j/Z)$ is approximately constant and independent of j/Z. The expression we have adopted for $\delta_n(j/Z)$ mimics the one adopted in the empirical work of Fowler and Christakis, allowing a direct comparison between theoretical and experimental results. In our case, we simply added a normalization factor such that we obtain an approximately constant $\delta_n(j/Z)$ regardless of the value of j/Z, something that does not occur in their case.

As a final remark, we would like to stress that an analytical study of this problem would be extremely difficult, if not impossible. While estimating the values of ϵ_1^{ev} is feasible in homogeneous networks by making use of the pair approximation method (section 3.3.4 and reference (99)), estimating the correlations for higher social distances n would require tracking the frequency of larger motifs in the network (that is, larger than merely pairs of nodes), and would require obtaining the solution of systems of equations of several ordinary differential equations. For these reasons, here we rely solely on computational simulations of these dynamical processes on complex networks.

6.4 Universality of Peer Influence

We will now analyze the patterns of correlations obtained for the three dynamical processes discussed in section 6.2 – the Prisoner's Dilemma (**PD**), the Voter Model (**VM**) and the **SIR** epidemic model. Given the structural diversity of social networks (1, 52, 150, 165, 166, 167, 168, 169) in which some individuals interact more often than others, we investigate the role that diversity in the number of social ties, average connectivity and clustering play in the emerging patterns of correlations. To this end, we will use various types of static networks: random, exponential and scale-free networks (1, 149, 165, 166). Individuals are assigned to nodes, with the links between them representing a social interaction. Homogeneous random networks (**HoRand**) were obtained by repeatedly swapping the ends of pairs of randomly chosen links of a regular ring. Heterogeneous scale-free networks were obtained combining growth and preferential attachment, following the model proposed by Barabási and Albert (**BA**)

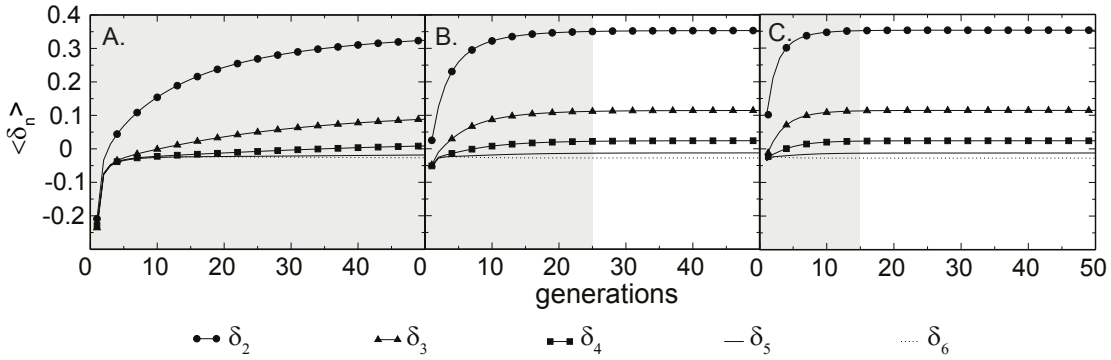

Figure 6.4: Temporal evolution of δ_n for the Voter Model for homogeneous random populations - Correlations δ_n for the first 50 generations for the Voter Model with **A.** probability $p_{VM} = 0.1$, **B.** $p_{VM} = 0.5$ and **C.** $p_{VM} = 1.0$. Note that different values of p_{VM} only lead to an overall rescaling of the evolutionary timescale without altering the qualitative results. Shaded areas correspond to the transient period until all δ_n reach stationary values (on panel **A** no stationary value is reached in the period represented). Parameters: $Z = 10^3$, $\langle k \rangle = 4$.

(24, 166). Exponential networks were obtained by adopting the same algorithm, with preferential attachment being replaced by random attachment (166). Random networks were built adopting the limit $p_{rewire} = 1$ of the Watts-Strogatz model (7), in which all links are rewired.

In the case of the Prisoner's Dilemma game, we assume that individuals revise their strategies based on the perceived success of others. Following the Fermi Imitation update method (section 3.2.3.2 and references (77, 78, 79)), an individual A with strategy s_A imitates a randomly chosen neighbor B with strategy s_B ($s_A \neq s_B$) with probability $p = \left[1 + e^{-\beta\left(f_{s_B} - f_{s_A}\right)}\right]^{-1}$, where f_A (f_B) stands for the fitness of A (B) and β denotes the intensity of selection.

In the case of the Voter Model, individuals adopt with probability p_{VM} the opinion of a randomly chosen neighbor. In figure 6.4 we represent the results obtained for the evolution of the behavioral correlations $\langle \delta_n \rangle$ for the Voter Model and various values of p_{VM}. We represent by $\langle \delta_n \rangle$ the average of $\delta_n(j/Z)$ over all j/Z; in other cases, further ahead, it will be more useful to consider only the value of δ_n at a single state j/Z. We observe that the value of p_{VM} determines the transient period after which the behavioral correlations stabilize: the smaller the value of p_{VM}, the larger this transient period. Nevertheless, the value of the correlations $\langle \delta_n \rangle$ after the transient period is

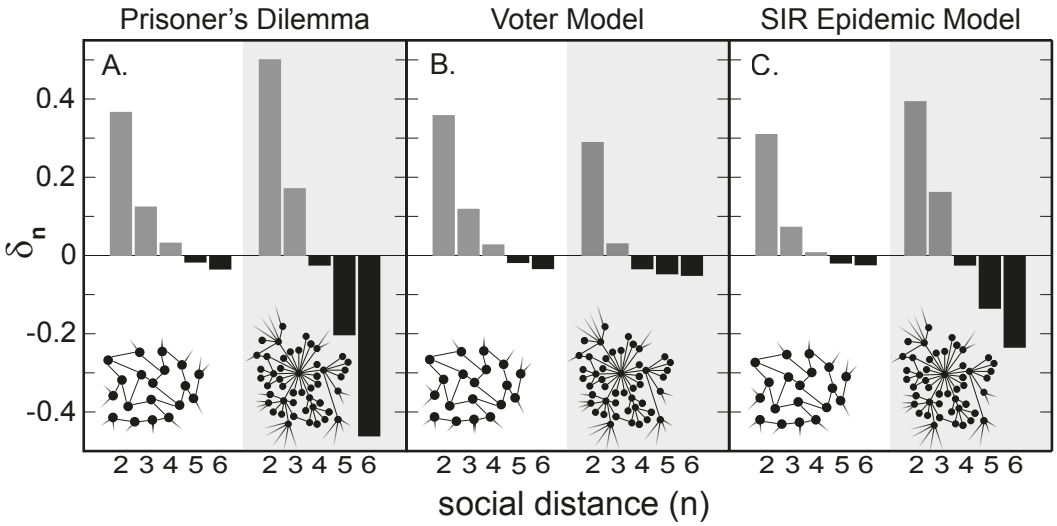

Figure 6.5: Peer influence in social networks - Behavioral correlations $\langle \delta_n \rangle$ in homogeneous networks (random, white background) and heterogeneous networks (scale-free generated with Barabási-Albert algorithm, grey background) for the following traits and processes: Correlations among **A.** cooperators in the **PD** game, **B.** individuals with the same opinion in the **VM**, and **C.** recovered individuals in the **SIR** epidemic model. Normalization ensures that $\delta_1 = 1.0$ in all cases. Parameters: $Z = 10^3$, $\langle k \rangle = 4$, $p_{VM} = 1$ (Voter Model), $\lambda = 0.03$, $\beta = 1.0$ (Prisoner's Dilemma), $\alpha = \gamma = 0.5$ (**SIR**).

the same regardless of the value of p_{VM}, and for this reason we wil adopt its maximum value ($p_{VM} = 1$) to ensure faster computational simulations. The results for the temporal evolution of behavioral correlations $\langle \delta_n \rangle$ for the Voter Model in scale-free **BA** networks (not shown here) are qualitatively equivalent (regarding the impact of the value of p_{VM} on the transient period towards the stationary state).

Now, we proceed to compare the correlations $\langle \delta_n \rangle$ for the three different dynamical processes adopted – Prisoner's Dilemma (**PD**), Voter Model (**VM**) and **SIR** epidemic model. These results for δ_n are shown in figure 6.5 for both homogeneous networks (random, in panels with white background) and heterogeneous networks (scale-free **BA**, in panels with gray background). Figure 6.5A shows the $\langle \delta_n \rangle$ associated with the evolutionary dynamics of cooperators and defectors interacting with each of their neighbors via the 2-person Prisoner's Dilemma (**PD**) game. We define $n_{critical}$ ($n_{critical} = 3$ in references (137, 138, 139, 140, 142, 143, 144) and $n_{critical} = 2$ in reference (147)) as the largest distance n for which δ_n remains positive. $n_{critical}$ systematically exhibits a value between 2 and 3, which depends only on how connected in-

dividuals are and if one's own neighbors are also neighbors of each other (measured by the clustering coefficient; these dependencies will be discussed in detail in section 6.6). We have chosen the particular value $\lambda = 0.03$ for the Prisoner's Dilemma because that corresponds to a coexistence global dilemma in homogeneous random networks and to a ***C***-dominance game in scale-free **BA** networks. That is, with this value we could ensure that we found both strategies (cooperate and defect) in the population. However, we have verified that our conclusions remain qualitatively valid for other λ values, if we allow different transient periods.

Figure 6.5 demonstrates that the $n_{critical}$ value does not depend on the underlying dynamical process that determines how information flows. We have also verified that these values of $n_{critical}$ are not sensitive to the parameters inherent to each dynamical process. We find that the same degrees of peer influence also apply to other famous social dilemmas, such as the Stag-Hunt Game (43) or the Snowdrift Game (39), as well as alternative update rule parameters (77), which affect mainly the overall time-scale of the population dynamics as it evolves towards the stationary state.

6.5 Finite size effects

To investigate finite size effects, we study below how the correlations behave as a function of the network size. Let us denote by $\langle \sigma_n \rangle$ the average fraction of the population that has neighbors at a social distance n, and by $\langle \eta_n \rangle$ the average size of a neighborhood of order n. These two quantities turn out to play an important role in the characterization of the finite-size effects one necessarily observes when dealing with populations as small as $Z = 10^3$.

Figure 6.6 shows how $\langle \eta_n \rangle$ varies with the social distance n for different values of the population size Z, both for **HoRand** and scale-free **BA** networks. In both network classes, these functions reach their single peak at intermediate values of n, which are systematically smaller in heterogeneous networks than in homogeneous ones. This, in turn, leads to averages sizes "at peak" somewhat larger for heterogeneous networks. With increasing population size Z, we observe that peaks shift to larger n, therefore warranting better statistics for larger values of n.

Figure 6.7, in turn, shows how $\langle \sigma_n \rangle$ changes with the social distance n for different values of the population size Z, both for **HoRand** and scale-free **BA** networks. Clearly, for low n all individuals in the population have neighbors at that social distance, even for small population sizes $(Z = 10^3)$ and irrespective of network class. The differences

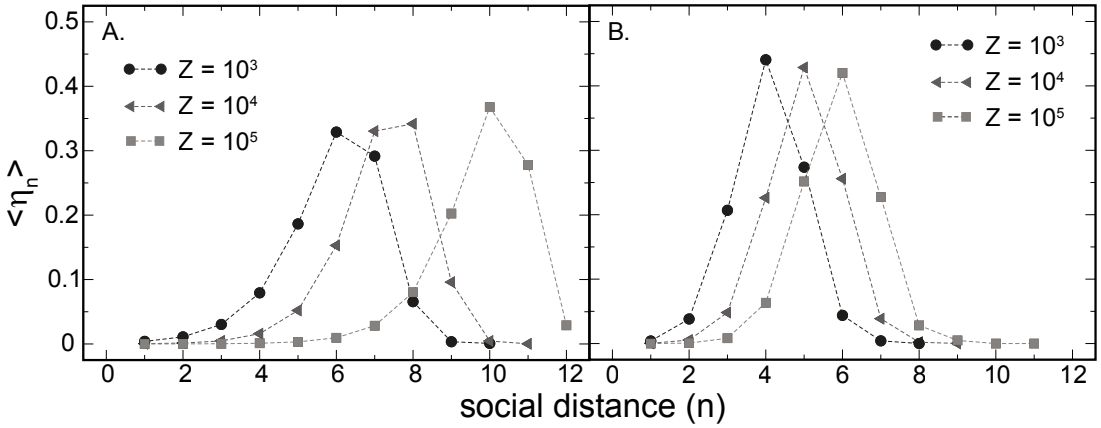

Figure 6.6: Normalized average size of n^{th} neighborhoods, $\langle \eta_n \rangle$, in homogeneous random and scale-free Barabási-Albert networks of variable size - $\langle \eta_n \rangle$ is plotted as a function of social distance n and for different values of population size Z for both homogeneous random (panel **A.**) and heterogeneous scale-free Barabási-Albert (panel **B.**) networks. Each point corresponds to an average over 10 different realizations of the corresponding networks with average connectivity $\langle k \rangle = 4$.

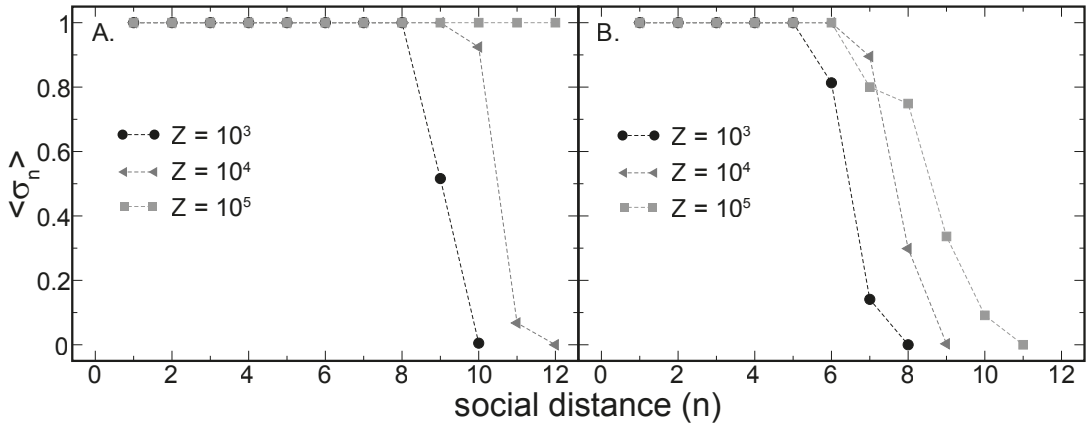

Figure 6.7: Average fraction of individuals with n^{th} neighborhood, $\langle \sigma_n \rangle$, in homogeneous random and scale-free Barabási-Albert networks of variable size - $\langle \sigma_n \rangle$ is plotted as a function of social distance n and for different values of population size Z for both homogeneous random (panel **A.**) and heterogeneous scale-free Barabási-Albert (panel **B.**) networks. Each point corresponds to an average over 10 different realizations of the corresponding networks, with average connectivity $\langle k \rangle = 4$.

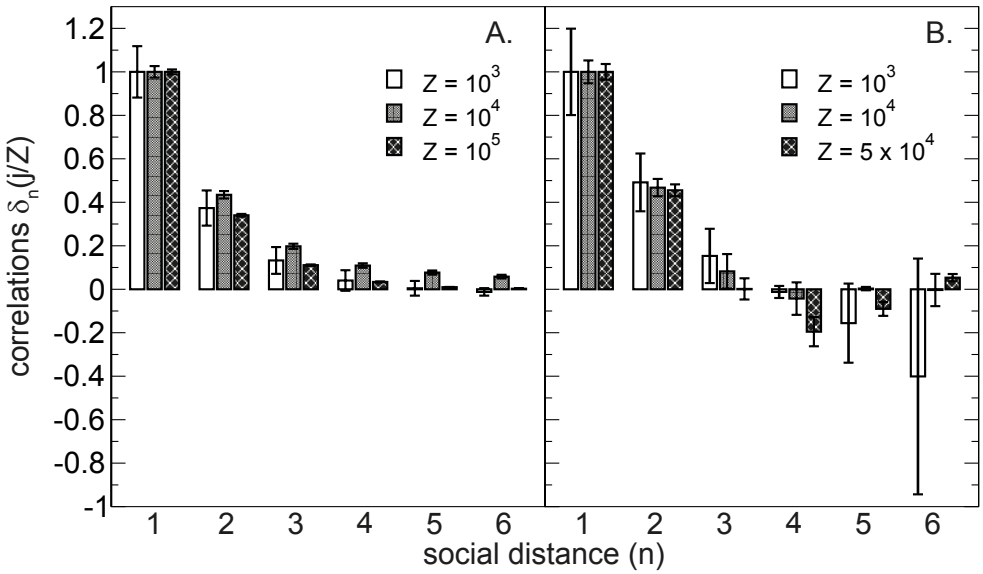

Figure 6.8: Peer influence in social networks – finite size effects - δ_n in homogeneous random networks (panel **A.**) and heterogeneous networks (scale-free generated with the Barabási-Albert algorithm – panel **B.**) for correlations among cooperators in the Prisoner's Dilemma. Normalization ensures that δ_1 in all cases. All values were obtained for networks of average degree $\langle k \rangle = 4$.

show up for larger n. After a critical social distance (which depends on the population size and network class), $\langle \sigma_n \rangle$ undergoes a sudden drop, which occurs systematically for lower values of n in heterogeneous networks. This behavior strongly influences the statistics associated with the computation of the correlations δ_n, since larger values of $\langle \sigma_n \rangle$ ensure better statistics for δ_n.

With these results at hand, we have performed extensive numerical simulations to investigate the impact of these two factors in the accuracy obtained in the determination of δ_n for the dynamical processes under study. In figure 6.8 we demonstrate how correlations and errors depend on the population size for the Prisoner's Dilemma, for both homogeneous random networks (figure 6.8A) and scale-free **BA** networks (figure 6.8B). The uncertainty decreases with increasing population size Z, for fixed social distance n. While for small network sizes there is a lower bound on the uncertainty which cannot be further decreased, in view of the small network diameter and the limited values of $\langle \sigma_n \rangle$ and $\langle \eta_n \rangle$, for larger networks correlations for large values of n approach a random pattern, as one would naturally expect. More important, the positive

values of the correlations obtained for small n, however, remain robust and statistically significant with increasing network size and the existence (*and* actual value) of the critical social distance remains unchanged whenever we define such critical value as the one above which positive correlations become statistically irrelevant. The behavior of correlations and errors with population size is qualitatively equivalent for the other dynamical processes, namely the Voter Model and the **SIR** epidemic model (results not shown here).

6.6 Dependence of $n_{critical}$ on network topological properties

Besides being heterogeneous, social networks often exhibit high clustering coefficients (166), contrary to the negligible values that characterize the ones used in figure 6.5. To evaluate the impact of this property, we generated networks with arbitrary clustering coefficient by swapping the ends of pairs of links chosen according to the algorithm defined in (170), starting from a network with a given degree distribution, designed beforehand using the algorithms described in the Methods section (section 6.8).

In figure 6.9 we show how the values of $n_{critical}$ for scale-free networks remain limited between 2 and 3, irrespectively of their clustering coefficient and average degree. Similar results, not presented here, are obtained for other heterogeneous networks, such as random and exponential networks. Indeed, to break down these surprisingly steady values of $n_{critical}$, one must artificially produce highly sparse, highly clustered and strictly homogeneous networks where all nodes share the same number of partners, such as regular rings or lattices (figure 6.9, panels A, C and E). However, it is worth emphasizing that social networks are intrinsically heterogeneous (150, 165), and as such it is remarkable how resilient $n_{critical}$ is to changes in realistic topological features. This said, $n_{critical}$ shows an overall tendency to increase with increasing levels of clustering, mostly whenever networks are sparse.

6.7 Discussion

Overall, our results suggest that the extent of peer influence emerges as a natural outcome of dynamical processes on structured populations, being pervasive in a wide-range of phenomena occurring in social networks. Despite the importance of social networks in defining the paths and ends of the dynamical processes they support, showing how important it is to address and understand social dynamics from a complex

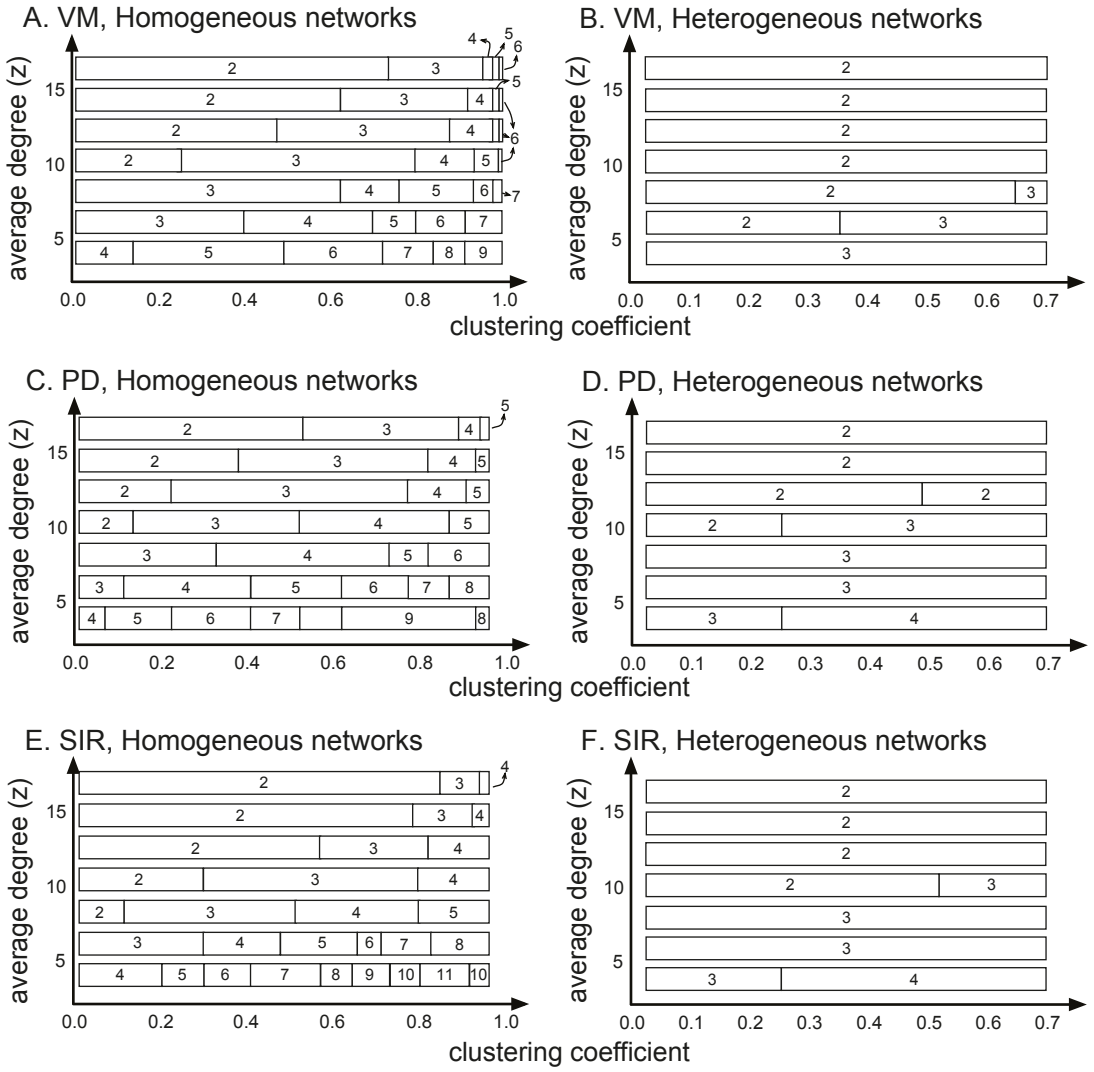

Figure 6.9: Dependence of $n_{critical}$ on the clustering coefficient and average connectivity $\langle k \rangle$ - $n_{critical}$ in **A.** homogeneous and **B.** heterogeneous (scale-free) networks for different values of the clustering coefficient and average connectivity $\langle k \rangle$. Results were obtained for populations of size $Z = 10^3$ among individuals: with the same opinion in the Voter Model (panels **A.** and **B.**), cooperators in the Prisoner's Dilemma (panels **C.** and **D.**), and recovered individuals in the **SIR** epidemic model (panels **E.** and **F.**). We normalized the clustering coefficient of each homogeneous network by the corresponding values for a ring regular network with the same (average) connectivity. Values of $n_{critical}$ were obtained for $\delta_n(j/Z = 0.5)$ when all δ_n have reached a stationary value.

networks perspective (117, 171, 172), the patterns of peer-influence they exhibit are extremely resilient and surprisingly independent of their structure.

On the other hand, our results also show how networks naturally entangle individuals into interactions of many-body nature: Indeed, social networks effectively extend, in non-trivial ways, the dyadic interactions we started from. The fact that the distance between any two individuals in social networks is small (18) and comparable to $n_{critical}$ further enhances the significance of the present results, as they stress how our individual actions may have wide repercussions on every other individual of the network.

6.8 Methods

6.8.1 Population structure

We investigate the role that degree distribution, average connectivity and clustering coefficient play in the emerging patterns of correlations. To this end, we consider (homogeneous) random, exponential and scale-free networks. Homogeneous random networks were obtained by repeatedly swapping the ends of pairs of randomly chosen links of a regular ring. Heterogeneous scale-free networks were obtained combining growth and preferential attachment, following the model proposed by Barabási and Albert (24). Exponential networks were obtained by adopting the same algorithm, with preferential attachment replaced by random attachment (24). Random networks were built adopting the limit $p_{rewire} = 1$ of the Watts-Strogatz model (7), in which all links are rewired. We consider 10 different realizations of each class of network, and networks remain fixed throughout all the evolution of the dynamical processes.

6.8.2 Network Topological Properties

The social distance n between two individuals in the population corresponds to the shortest path length between those two individuals. Shortest path lengths between any pair of individuals in the network are determined by applying the Dijkstra's algorithm (173). In the particular problem at study, it consists of the following: for a given node i, we start by determining the first neighbors of i, attributing them a social distance of $n = 1$. Each of these nodes is tagged so as to identify that their social distance to i has already been determined. This avoids some effects that could be introduced by clustering, namely a given node being identified as being at two different social distances. Then we proceed to determine the first neighbors of each of i's neighbors; in

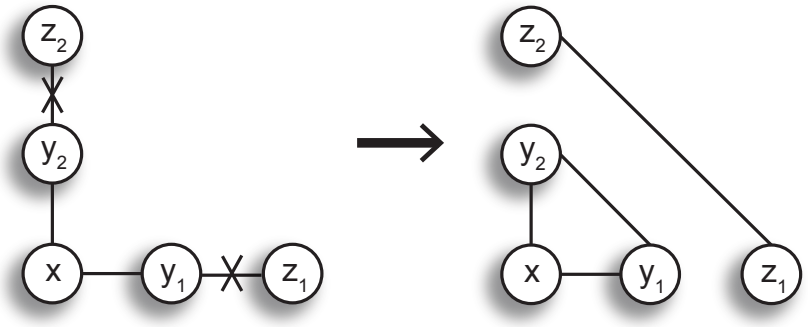

Figure 6.10: Increasing clustering coefficient of networks of arbitrary degree distribution - In each iteration, we select two distinct neighbors y_1 and y_2 of a randomly chosen node x; then we select a neighbor z_1 of y_1 and a neighbor z_2 of y_2, ensuring that $x \neq y_1 \neq y_2 \neq z_1 \neq z_2$. Between these 5 chosen nodes exist 4 edges, namely $\{\{x, y_1\}, \{x, y_2\}, \{y_1, z_1\}, \{y_2, z_2\}\}$; if edges $\{\{y_1, y_2\}, \{z_1, z_2\}\}$ do not exist, we create those links, deleting in their place the links $\{\{y_1, z_1\}, \{y_2, z_2\}\}$ – this way we create a triangle between nodes x, y_1 and y_2. This rewiring is accepted if it does not produce a disconex network, and if it increases the clustering coefficient of the entire network.

case they are not tagged yet, they will be identified as being at a social distance $n = 2$ of node i. We proceed with this algorithm until we reach the desired social distance n for the given simulation.

We employ the method described in (170) for increasing the clustering coefficient of a given simulated network without altering its degree distribution, which consists of iteratively applying rewirings that increase network clustering without altering its degree distribution, as schematized in figure 6.10.

6.8.3 Evolution

We adopt three distinct dynamical processes to model social dynamics: the 2-person Prisoner's Dilemma (**PD**) (sections 6.2.1 and reference (174)), the Voter Model (**VM**) (section 6.2.2 and reference (151)) and the Susceptible-Infected-Recovered (**SIR**) epidemic model (section 6.2.3 and reference (157)). In opposition to the work exposed in the previous chapters, here we assume that all interactions are pairwise.

In each round, a randomly chosen individual is given the opportunity to revise its state, be it a strategy (in the case of the **PD**), an opinion (in the case of the **VM**) or an epidemiological state (in the case of the **SIR** epidemic model). That is, trait updates

are asynchronous. In the case of the **VM**, a randomly chosen individual A adopts the opinion of a randomly chosen first neighbor B with a probability p_{VM} constant in time. Since this update method is non-innovative (individuals can only adopt a certain strategy when at least one of his neighbors is using it) the evolution of the population ceases when it reaches either one of the monomorphic states. In the case of the **SIR** epidemic model, a randomly chosen infected individual either recovers with a probability γ; or, if not, we evaluate if he has any susceptible neighbor and if that is the case he infects a randomly chosen susceptible neighbor with probability α. Maintaining a list of the infected individuals in the population at every time t, and in each instant randomly choosing one individual from that list instead of from the whole population helps to speed the simulations. Finally, in the case of the **PD**, we assume that individual fitness corresponds to the accumulated payoff from all pairwise interactions in which individuals participate with their first neighbors. Individuals revise their strategies according to the Fermi imitation update method (references (77, 78, 79) and section 3.2.3.2), which consists of the following: a randomly chosen individual A chooses a random first neighbor B to compare strategies. If individuals A and B have different strategies ($s_A \neq s_B$), A imitates B with a probability proportional to the fitness difference $f_{s_B} - f_{s_A}$, and given by the Fermi distribution from statistical physics,

$$p_{Fermi} = \frac{1}{1 + e^{-\beta(f_{s_B} - f_{s_A})}}. \tag{6.5}$$

where β regulates the intensity of selection.

6.8.4 Evaluation of Correlations

We evaluate the likelihood $\delta_n(j/Z)$ that two individuals at a social distance n self-organize in the same trait, with

$$\delta_n(j/Z) = \frac{\Delta\epsilon_n(j/Z)}{|\Delta\epsilon_1(j/Z)|}, \tag{6.6}$$

where $\Delta\epsilon_n(j/Z) = \epsilon_n^{ev}(j/Z) - \epsilon_n^{rand}(j/Z)$. The expression we have adopted for $\delta_n(j/Z)$ mimics the one adopted in the empirical work of Fowler and Christakis, allowing a direct comparison between theoretical and experimental results. In our case, we simply added a normalization factor such that we obtain an approximately constant $\delta_n(j/Z)$ regardless of the value of j/Z, something that does not occur in their case. However, we have checked that our conclusions remain qualitatively valid when adopting their method.

To obtain $\epsilon_n^{ev}(j/Z)$, we simulate each process for all possible initial conditions. For the **PD** and **VM** dynamics and for each initial j/Z, we randomly distribute traits and evolve the population for a transient period until all δ_n have reached a stationary state, in which $|\delta_n(G=x)-\delta_n(G=x-5)|<\xi$, for all δ_n, where G denotes generations of evolutionary time (1 generation = Z iterations). We took $\xi=0.02$ and computed the average correlations during the final 5 generations. After each trait update we determine, for each individual, the fraction of those who exhibit the same trait at a distance n. The value of ϵ_n^{ev} for that particular configuration of strategies and for that instant t corresponds to $\epsilon_n^{ev}(j/Z;t)=\frac{\sum_{i=0}^{Z}\epsilon_{n,i}^{ev}}{Z}$ where $\epsilon_{n,i}^{ev}$ corresponds to the fraction of individuals at a social distance n of individual i that exhibit the same trait as i. Note that we normalize by the size of the population, Z, and not by the number of individuals that exhibit the trait we are investigating (and for which it makes sense of talking about this average probability). We have made this choice so as to be able to relate the values obtained for ϵ_n^{ev} with the gradients of selection in structured populations, an issue that will be subject to further investigation in the near future. Furthermore, we have confirmed that normalizing by the number of individuals that exhibit a given trait, instead of normalizing by the population size, does not qualitatively alter our conclusions regarding the patterns observed for $n_{critical}$.

We perform 10^5 different runs for each initial condition. For the dynamics of the *Susceptible-Infected-Recovered* model, and for each initial fraction of ***S**s* and ***I**s* (we initialize the population without any recovered individuals), we evolve the population until an absorbing state is reached (i.e. no ***I*** individuals left) and measure the correlations among all ***R**s*. In this case, δ_n was computed averaging over 10^8 runs for each initial condition. In what concerns the determination of $\epsilon_n^{rand}(k/N)$, we average over 10^3 simulations in which the traits are randomly distributed onto the nodes of the corresponding network.

The standard deviation σ_{δ_n} associated with each value of δ_n is computed as follows:

$$\sigma_{\delta_n}=\delta_n\sqrt{\left(\frac{\sigma_{\Delta\epsilon_n}}{\Delta\epsilon_n}\right)^2+\left(\frac{\sigma_{\Delta\epsilon_1}}{\Delta\epsilon_1}\right)^2-2\frac{\mathrm{Cov}\left[\Delta\epsilon_n,\Delta\epsilon_1\right]}{\Delta\epsilon_n\Delta\epsilon_1}} \tag{6.7}$$

where $\sigma_{\Delta\epsilon_n}$ is the standard deviation associated with the difference $\Delta\epsilon_n(j/Z)=\epsilon_n^{ev}(j/Z)-\epsilon_n^{rand}(j/Z)$ and is given by

$$\sigma_{\Delta\epsilon_n}=\sqrt{\sigma^2_{\epsilon_n^{ev}}+\sigma^2_{\epsilon_n^{rand}}} \tag{6.8}$$

and the covariance $\mathrm{Cov}\left[\Delta\epsilon_n, \Delta\epsilon_1\right]$ of the differences $\Delta\epsilon_n(j/Z) = \epsilon_n^{ev}(j/Z) - \epsilon_n^{rand}(j/Z)$ and $\Delta\epsilon_1(j/Z) = \epsilon_1^{rand}(j/Z) - \epsilon_1^{rand}(j/Z)$ is given by

$$\mathrm{Cov}\left[\Delta\epsilon_n, \Delta\epsilon_1\right] = \mathrm{E}\left[\Delta\epsilon_n\Delta\epsilon_1\right] - \mathrm{E}\left[\Delta\epsilon_n\right]\mathrm{E}\left[\Delta\epsilon_1\right] \tag{6.9}$$

Taking into account that

$$\Delta\epsilon_n\Delta\epsilon_1 = \epsilon_n^{ev}\epsilon_1^{ev} + \epsilon_n^{ev}\epsilon_1^{rand} - \epsilon_n^{rand}\epsilon_1^{ev} - \epsilon_n^{rand}\epsilon_1^{rand} \tag{6.10}$$

the only quantity that can prevent us from ensuring that $\mathrm{Cov}\left[\Delta\epsilon_n, \Delta\epsilon_1\right] = 0$ is the product $\epsilon_n^{ev}\epsilon_1^{ev}$. However, as an approximation and for computational efficiency (the denominator $\Delta\epsilon_n\Delta\epsilon_1$ in equation 6.7 can reach very small values that lead to some problems when computing σ_{δ_n}) we will consider $\mathrm{Cov}\left[\Delta\epsilon_n, \Delta\epsilon_1\right] = 0$. Note that, if $\mathrm{Cov}\left[\Delta\epsilon_n, \Delta\epsilon_1\right] > 0$, this would cause a smaller standard deviation σ_{δ_n}, so the results we present on this chapter correspond to the worst case possible.

Given the large size of some of populations that were studied in this chapter, for computational efficiency we opted for parallelizing the simulations and obtaining the values of δ_n for each network separately. We computed the final average value and associated standard deviation by resorting to the following formula (175):

$$\sigma^2 = \frac{n_x^2\sigma_x^2 + n_y^2\sigma_y^2 - n_y\sigma_x^2 - n_y\sigma_y^2 - n_x\sigma_x^2 - n_x\sigma_y^2 + n_xn_y\sigma_x^2 + n_xn_y\sigma_y^2 + n_xn_y\left(\bar{X} - \bar{Y}\right)^2}{\left(n_x + n_y - 1\right)\left(n_x + n_y\right)} \tag{6.11}$$

where n_x and n_y represent the number of trials performed to obtain the average value of variables x and y, as well as the associated standard deviations, σ_x and σ_y (which are $\overline{X}$ and $\overline{Y}$ respectively). In this case, we have $n_x = n_y$.

7

Final Conclusions and Outlook

We analyzed the evolutionary dynamics of cooperation in structured populations and studied in detail, using different approaches, two collective social dilemmas of cooperation: The N-Person Prisoner's Dilemma, and the N-Person Snowdrift Game. Furthermore, we studied how peer influence emerges from dyadic interactions in three distinct dynamical processes modeled in structured populations, demonstrating the many-body implications arising from pairwise interactions.

Regarding the N-Person Prisoner's Dilemma, we have shown that diversity in the number and size of the games in which individuals participate, as well as diversity in the contributions made by cooperators, leads to a very significant improvement in the levels of cooperation observed in the population. That is, whenever the act of giving is considered more important than the amount that is given, cooperation blooms. This effect is robust with respect to the details of the evolutionary dynamics, the updating strategy (synchronous versus asynchronous) and even to errors. Furthermore, we provide a detailed analytical study of the mechanism responsible for the boost in cooperation observed in highly heterogeneous networks, when cooperators' contributions are rescaled by the number of games in which individuals participate. By making use of sub-structures representative of the architecture of scale-free Barabási-Albert networks, we have shown that even in the worst configurations possible for cooperators it is still possible, and probable, for the cooperative strategy to propagate.

We have also evaluated the impact of structured populations on the evolutionary dynamics of the N-Person Snowdrift Game – but in this case, we followed a different approach, more appropriate to deal with a social dilemma which, from the outset, promotes the coexistence between cooperators and defectors. We computed a numerical

analogue of the gradient of selection in complex networks that provides a complete (mean-field) description of the evolution of the population for all possible initial conditions. We show that evolution on homogeneous networks exhibits a population-wide behavior qualitatively similar to that observed in well-mixed populations. Evolution in heterogeneous networks reveals the emergence of a multitude of internal equilibria and of more complex evolutionary dynamics scenarios. The heterogeneity in the number of connections of each individual generally turns the global dilemma into a coordination dilemma.

Finally, we measured the degree of peer influence between individuals exhibiting the same trait (strategy, opinion or epidemiological state) in simulations of dyadic dynamical processes for different network classes. We have shown that the pattern of peer influence observed is independent of the particular dynamical process adopted, being determined by the network class and particular topological properties (clustering coefficient and average connectivity). With respect to this last point, we perform a detailed study of the dependence of the degree of peer influence on the average connectivity and clustering coefficient on both homogeneous and heterogeneous (scale-free Barabási-Albert) networks. Real social networks are highly heterogeneous and exhibit high values of clustering coefficient, and in these cases the degree of peer influence we observe is very robust and similar to the results we had previously observed.

We believe our work is an important contribution to the understanding of the evolutionary dynamics of cooperation. During the research several interesting problems emerged and they will be the focus of future research. The same applies to our study of peer influence in social networks, which can also be explored in more detail. Definitely, the road ahead is exiting and encouraging, given the capacity of the methods used have to provide clear cut answers.

Finally, it would be very interesting to test the models discussed in this thesis with social experiments involving humans. This poses many difficulties, both in setting up the experiments and also in analyzing the results. Because of the inherent difficulties, while theoretically this research is very rich, experiments that can corroborate the models are still lacking. Fortunately, this trend has been changing in the last years with new experiments being set up making use of the numerous possibilities that the Internet nowadays offers us.

References

[1] S. N. DOROGOVTSEV AND J. F. F. MENDES. *Evolution of Networks: From Biological Nets to the Internet and WWW*. Oxford University Press, 2003.

[2] M.E.J. NEWMAN. *Networks: an introduction*. Oxford University Press, 2010.

[3] **Wolfram Mathematica**. *Available from http://www.wolfram.com/*.

[4] **Mark Newman's personal website**. *Available from http://www-personal.umich.edu/ mejn/*.

[5] S. MARTIN, W.M. BROWN, R. KLAVANS, AND K.W. BOYACK. **OpenOrd: an open-source toolbox for large graph layout**. In *Conference on Visualization and Data Analysis*, pages 786806–786806–11, 2011.

[6] **Gephi, an open source graph visualization and manipulation software**. *Available from http://gephi.org/*.

[7] D.J. WATTS AND S.H. STROGATZ. **Collective dynamics of small-world networks**. *Nature*, **393**(6684):440–442, 1998.

[8] M.E.J. NEWMAN, D.J. WATTS, AND S.H. STROGATZ. **Random graph models of social networks**. *Proceedings of the National Academy of Sciences*, **99**(Suppl 1):2566–2572, 2002.

[9] S.N. SOFFER AND A. VÁZQUEZ. **Network clustering coefficient without degree-correlation biases**. *Physical Review E*, **71**(5):057101, 2005.

[10] S. BORNHOLDT, H.G. SCHUSTER, AND J. WILEY. *Handbook of graphs and networks*. Wiley Online Library, 2003.

[11] P. GLEISER AND L. DANON. **Community Structure in Jazz**. *Advances in Complex Systems*, **6**:565–573, 2003.

[12] M.E.J. NEWMAN. **Finding community structure in networks using the eigenvectors of matrices**. *Physical Review E*, **74**(3):036104, 2006.

[13] J.G. WHITE, E. SOUTHGATE, J.N. THOMSON, AND S. BRENNER. **The structure of the nervous system of the nematode Caenorhabditis elegans**. *Philosophical Transactions of the Royal Society of London. B, Biological Sciences*, **314**(1165):1–340, 1986.

[14] **Marvel Universe Social Graph**. *Available from http://exposedata.com/marvel/*.

[15] **Infochimps**. *Available from http://www.infochimps.com/datasets/marvel-universe-social-graph/*.

[16] A. RAPOPORT. **Contribution to the theory of random and biased nets**. *Bulletin of Mathematical Biology*, **19**(4):257–277, 1957.

[17] R. SOLOMONOFF AND A. RAPOPORT. **Connectivity of random nets**. *Bulletin of Mathematical Biology*, **13**(2):107–117, 1951.

[18] J. TRAVERS AND S. MILGRAM. **An experimental study of the small world problem**. *Sociometry*, pages 425–443, 1969.

[19] S. MILGRAM. *Obedience to authority: An experimental view*. Harper & Row, 1974.

[20] P.S. DODDS, R. MUHAMAD, AND D.J. WATTS. **An experimental study of search in global social networks**. *Science*, **301**(5634):827–829, 2003.

[21] J. LESKOVEC AND E. HORVITZ. **Planetary-scale views on a large instant-messaging network**. In *Proceeding of the 17th International Conference on World Wide Web*, pages 915–924. ACM, 2008.

[22] J. UGANDER, B. KARRER, L. BACKSTROM, AND C. MARLOW. **The anatomy of the facebook social graph**. *Arxiv preprint arXiv:1111.4503*, 2011.

[23] FC SANTOS, JF RODRIGUES, AND JM PACHECO. **Epidemic spreading and cooperation dynamics on homogeneous small-world networks**. *Physical Review E*, **72**(5):056128, 2005.

[24] A. L. BARABÁSI AND R. ALBERT. **Emergence of scaling in random networks**. *Science*, **286**:509–512, 1999.

[25] P.L. KRAPIVSKY, S. REDNER, AND F. LEYVRAZ. **Connectivity of growing random networks**. *Physical Review Letters*, **85**(21):4629–4632, 2000.

[26] A.L. BARABÁSI, R. ALBERT, AND H. JEONG. **Mean-field theory for scale-free random networks**. *Physica A: Statistical Mechanics and its Applications*, **272**(1):173–187, 1999.

[27] S.N. DOROGOVTSEV, J.F.F. MENDES, AND A.N. SAMUKHIN. **Structure of growing networks with preferential linking**. *Physical Review Letters*, **85**(21):4633, 2000.

[28] R. COHEN AND S. HAVLIN. **Scale-free networks are ultrasmall**. *Physical Review Letters*, **90**(5):58701, 2003.

[29] G. BIANCONI AND A.L. BARABÁSI. **Competition and multiscaling in evolving networks**. *EPL (Europhysics Letters)*, **54**:436–442, 2001.

[30] S.N. DOROGOVTSEV AND J.F.F. MENDES. **Scaling properties of scale-free evolving networks: Continuous approach**. *Physical Review E*, **63**(5):056125, 2001.

[31] A. WAGNER. **How the global structure of protein interaction networks evolves**. *Proceedings of the Royal Society of London. Series B: Biological Sciences*, **270**(1514):457–466, 2003.

[32] A. VÁZQUEZ, M. BOGUNÁ, Y. MORENO, R. PASTOR-SATORRAS, AND A. VESPIGNANI. **Topology and correlations in structured scale-free networks**. *Physical Review E*, **67**(4):046111, 2003.

[33] J. VON NEUMANN AND O. MORGENSTERN. *Theory of Games and Economic Behavior*. Princeton University Press, 1944.

[34] R.J. AUMANN AND M. MASCHLER. **Game theoretic analysis of a bankruptcy problem from the Talmud**. *Journal of Economic Theory*, **36**(2):195–213, 1985.

[35] R.A. EPSTEIN. *The theory of gambling and statistical logic*. Academic Press, 2009.

[36] A.A. COURNOT. *Recherches sur les principes mathématiques de la théorie des richesses/par Augustin Cournot*. L. Hachette, 1838.

[37] E. BOREL AND J. VILLE. *Applications aux jeux de hasard*. Gauthier-Vilars, 1938.

[38] J. NASH. **Non-cooperative games**. *The Annals of Mathematics*, **54**(2):286–295, 1951.

[39] R. SUGDEN. *The economics of rights, co-operation and welfare*. Blackwell Oxford, 1986.

[40] B. RUSSELL. *Common sense and nuclear warfare*. AMS Press, 1968.

[41] J.M. SMITH AND G.R. PRICE. **The Logic of Animal Conflict**. *Nature*, **246**:15–18, 1973.

[42] J. J. ROUSSEAU. **Discourse on the Origin and Foundations of Inequality among Men**. *The First and Second Discourses*, 1755.

[43] B. SKYRMS. *The stag hunt and the evolution of social structure*. Cambridge University Press, 2004.

[44] GARRETT HARDIN. **The Tragedy of the Commons**. *Science*, **162**(3859):1243–1248, 1968.

[45] K. SIGMUND. *The calculus of selfishness*. Princeton University Press, 2009.

[46] E. OSTROM. *Governing the commons: The evolution of institutions for collective action*. Cambridge University Press, 1990.

[47] R. BOYD AND P.J. RICHERSON. **The evolution of reciprocity in sizable groups**. *Journal of Theoretical Biology*, **132**(3):337–356, 1988.

[48] P. KOLLOCK. **Social dilemmas: The anatomy of cooperation**. *Annual Review of Sociology*, **24**:183–214, 1998.

[49] R.M. DAWES. **Social dilemmas**. *Annual Review of Psychology*, **31**(1):169–193, 1980.

[50] C. HAUERT, N. HAIDEN, AND K. SIGMUND. **The dynamics of public goods**. *Discrete and Continuous Dynamical Systems Series B*, **4**:575–588, 2004.

[51] C. HAUERT, A. TRAULSEN, H. BRANDT, M.A. NOWAK, AND K. SIGMUND. **Via freedom to coercion: the emergence of costly punishment**. *Science*, **316**(5833):1905–1907, 2007.

[52] F.C. SANTOS, M.D. SANTOS, AND J.M. PACHECO. **Social diversity promotes the emergence of cooperation in public goods games**. *Nature*, **454**(7201):213–216, 2008.

[53] C.S. GOKHALE AND A. TRAULSEN. **Evolutionary games in the multiverse**. *Proceedings of the National Academy of Sciences*, **107**(12):5500–5504, 2010.

[54] K. BINMORE. **Playing fair: Game theory and the social contract, Vol. I**. *Cambridge, Massachussets: MIT Press*, **1**:104, 1994.

[55] M. ARCHETTI AND I. SCHEURING. **Review: Game theory of public goods in one-shot social dilemmas without assortment**. *Journal of Theoretical Biology*, **299**:9–20, 2011.

[56] C. PACKER, D. SCHEEL, AND A.E. PUSEY. **Why lions form groups: food is not enough**. *American Naturalist*, **136**(1):1–19, 1990.

[57] E.C. YIP, K.S. POWERS, AND L. AVILÉS. **Cooperative capture of large prey solves scaling challenge faced by spider societies**. *Proceedings of the National Academy of Sciences*, **105**(33):11818–11822, 2008.

[58] K.N. RABENOLD. **Cooperative enhancement of reproductive success in tropical wren societies**. *Ecology*, **65**(3):871–885, 1984.

[59] U. MOTRO. **Co-operation and defection: playing the field and the ESS**. *Journal of Theoretical Biology*, **151**(2):145–154, 1991.

[60] C. HAUERT, M. HOLMES, AND M. DOEBELI. **Evolutionary games and population dynamics: maintenance of cooperation in public goods games**. *Proceedings of the Royal Society B: Biological Sciences*, **273**(1600):2565–2571, 2006.

[61] J.M. SMITH. *Evolution and the Theory of Games*. Cambridge University Press, 1982.

[62] J.M. SMITH. **Game theory and the evolution of fighting**. *On evolution*, pages 8–28, 1972.

[63] J.M. SMITH. **The theory of games and the evolution of animal conflicts**. *Journal of Theoretical Biology*, **47**(1):209–221, 1974.

[64] C. HAUERT AND M. DOEBELI. **Spatial structure often inhibits the evolution of cooperation in the snowdrift game**. *Nature*, **428**(6983):643–646, 2004.

[65] F.C. SANTOS AND J.M. PACHECO. **Scale-free networks provide a unifying framework for the emergence of cooperation**. *Physical Review Letters*, **95**(9):98104, 2005.

[66] H.P. YOUNG. **The evolution of conventions**. *Econometrica: Journal of the Econometric Society*, **61**(1):57–84, 1993.

[67] M. KANDORI, G.J. MAILATH, AND R. ROB. **Learning, mutation, and long run equilibria in games**. *Econometrica: Journal of the Econometric Society*, **61**(1):29–56, 1993.

[68] N.G. VAN KAMPEN. *Stochastic processes in physics and chemistry*. North Holland, 2007.

[69] S. KARLIN AND H. M. TAYLOR. *A First Course in Stochastic Processes, Second Edition*. Academic Press, 2 edition, April 1975.

[70] R.A. FISHER. *The genetical theory of natural selection*. Clarendon Press, 1930.

[71] S. WRIGHT. **Evolution in Mendelian populations**. *Genetics*, **16**(2):97–159, 1931.

[72] S.J. RUSSELL AND P. NORVIG. *Artificial intelligence: a modern approach*. Prentice Hall, 2010.

[73] M.J. OSBORNE. *An introduction to game theory*, **198**. Oxford University Press, 2004.

[74] R.S. SUTTON AND A.G. BARTO. *Reinforcement learning: An introduction*, **1**. Cambridge University Press, 1998.

[75] C.W. GARDINER. *Stochastic methods*. Springer, 1985.

[76] H. GINTIS. *Game theory evolving: A problem-centered introduction to modeling strategic behavior*. Princeton University Press, 2000.

[77] A. TRAULSEN, M.A. NOWAK, AND J.M. PACHECO. **Stochastic dynamics of invasion and fixation**. *Physical Review E*, **74**(1):011909, 2006.

[78] A. TRAULSEN, M.A. NOWAK, AND J.M. PACHECO. **Stochastic payoff evaluation increases the temperature of selection**. *Journal of Theoretical Biology*, **244**(2):349–356, 2007.

[79] A. TRAULSEN, J.M. PACHECO, AND M.A. NOWAK. **Pairwise comparison and selection temperature in evolutionary game dynamics**. *Journal of Theoretical Biology*, **246**(3):522–529, 2007.

[80] M.A. NOWAK AND K. SIGMUND. **The evolution of stochastic strategies in the prisoner's dilemma**. *Acta Applicandae Mathematicae*, **20**(3):247–265, 1990.

[81] J.M. SMITH AND E. SZATHMÁRY. *The major transitions in evolution*. Oxford University Press, USA, 1997.

[82] M.A. NOWAK. **Five rules for the evolution of cooperation**. *Science*, **314**(5805):1560–1563, 2006.

[83] W.D. HAMILTON. **The genetical evolution of social behaviour. II**. *Journal of Theoretical Biology*, **7**(1):17–52, 1964.

[84] G.S. WILKINSON. **Reciprocal food sharing in the vampire bat**. *Nature*, **308**(5955):181–184, 1984.

[85] G.S. WILKINSON. **Food sharing in vampire bats**. *Scientific American*, **262**(2):64–71, 1990.

[86] R.L. TRIVERS. **The evolution of reciprocal altruism**. *Quarterly Review of Biology*, **46**(1):35–57, 1971.

[87] R. AXELROD AND W.D. HAMILTON. **The evolution of cooperation**. *Science*, **211**(4489):1390–1396, 1981.

[88] P. MOLANDER. **The optimal level of generosity in a selfish, uncertain environment**. *Journal of Conflict Resolution*, **29**(4):611–618, 1985.

[89] M.A. NOWAK AND K. SIGMUND. **A strategy of win-stay, lose-shift that outperforms tit-for-tat in the Prisoner's Dilemma game**. *Nature*, **364**(6432):56–58, 1993.

[90] P. SEABRIGHT. *The company of strangers: A natural history of economic life*. Princeton University Press, 2010.

[91] C. KESER. **Trust and reputation building in e-commerce**. CIRANO Working Papers 2002s-75, CIRANO, 2002.

[92] P. RESNICK, R. ZECKHAUSER, J. SWANSON, AND K. LOCKWOOD. **The value of reputation on eBay: A controlled experiment**. *Experimental Economics*, **9**(2):79–101, 2006.

[93] M.A. NOWAK AND K. SIGMUND. **Evolution of indirect reciprocity by image scoring**. *Nature*, **393**:573–7, June 1998.

[94] M.A. NOWAK AND K. SIGMUND. **Evolution of indirect reciprocity**. *Nature*, **437**(7063):1291–1298, 2005.

[95] R. BSHARY AND A.S. GRUTTER. **Image scoring and cooperation in a cleaner fish mutualism**. *Nature*, **441**(7096):975–978, 2006.

[96] Ç. AKÇAY, V.A. REED, S.E. CAMPBELL, C.N. TEMPLETON, AND M.D. BEECHER. **Indirect reciprocity: song sparrows distrust aggressive neighbours based on eavesdropping**. *Animal Behaviour*, **80**(6):1041–1047, 2010.

[97] J.R. STEVENS AND M.D. HAUSER. **Why be nice? Psychological constraints on the evolution of cooperation**. *Trends in Cognitive Sciences*, **8**(2):60–65, 2004.

[98] M.A. NOWAK AND R.M. MAY. **Evolutionary games and spatial chaos**. *Nature*, **359**(6398):826–829, 1992.

[99] H. MATSUDA, N. OGITA, A. SASAKI, AND K. SATO. **Statistical mechanics of population**. *Progress of Theoretical Physics*, **88**(6):1035–1049, 1992.

[100] W.S. BROECKER. **Climatic change: are we on the brink of a pronounced global warming?** *Science*, **189**(4201):460–463, 1975.

[101] T. PFEIFFER AND M.A. NOWAK. **Climate change: all in the game**. *Nature*, **441**(7093):583–584, 2006.

[102] C. HAUERT, S. DE MONTE, J. HOFBAUER, AND K. SIGMUND. **Volunteering as red queen mechanism for cooperation in public goods games**. *Science*, **296**(5570):1129–1132, 2002.

[103] G. SZABÓ AND C. HAUERT. **Phase transitions and volunteering in spatial public goods games**. *Physical Review Letters*, **89**(11):118101, 2002.

[104] C. HAUERT AND G. SZABÓ. **Prisoner's dilemma and public goods games in different geometries: compulsory versus voluntary interactions**. *Complexity*, **8**(4):31–38, 2003.

[105] J.M. PACHECO, F.C. SANTOS, M.O. SOUZA, AND B. SKYRMS. **Evolutionary dynamics of collective action in N-person stag hunt dilemmas**. *Proceedings of the Royal Society B: Biological Sciences*, **276**(1655):315–321, 2009.

[106] H. OHTSUKI, C. HAUERT, E. LIEBERMAN, AND M.A. NOWAK. **A simple rule for the evolution of cooperation on graphs and social networks**. *Nature*, **441**(7092):502–505, 2006.

[107] C. BOEHM. *Hierarchy in the forest: The evolution of egalitarian behavior*. Harvard University Press, 2001.

[108] F.C. SANTOS AND J.M. PACHECO. **A new route to the evolution of cooperation**. *Journal of Evolutionary Biology*, **19**(3):726–733, 2006.

[109] R. BOYD AND S. MATHEW. **A narrow road to cooperation**. *Science*, **316**(5833):1858–1859, 2007.

[110] F.C. SANTOS, V.V. VASCONCELOS, M.D. SANTOS, P.N.B. NEVES, AND J.P. PACHECO. **Evolutionary Dynamics of Climate Change under Collective-Risk Dilemmas**. *Mathematical Models and Methods in Applied Sciences (M3AS)*, **22**(supp01):1140004, 2012.

[111] D.F. ZHENG, H.P. YIN, C.H. CHAN, AND P.M. HUI. **Cooperative behavior in a model of evolutionary snowdrift games with N-person interactions**. *Europhysics Letters*, **80**(1):18002, 2007.

[112] M.O. SOUZA, J.M. PACHECO, AND F.C. SANTOS. **Evolution of cooperation under N-person snowdrift games**. *Journal of Theoretical Biology*, **260**(4):581–588, 2009.

[113] F.C. SANTOS AND J.M. PACHECO. **Risk of collective failure provides an escape from the tragedy of the commons**. *Proceedings of the National Academy of Sciences*, **108**(26):10421–10425, 2011.

[114] P.E. STANDER. **Cooperative hunting in lions: the role of the individual**. *Behavioral Ecology and Sociobiology*, **29**(6):445–454, 1992.

[115] C. HAUERT, F. MICHOR, M.A. NOWAK, AND M. DOEBELI. **Synergy and discounting of cooperation in social dilemmas**. *Journal of Theoretical Biology*, **239**(2):195–202, 2006.

[116] J.M. PACHECO, F.C. SANTOS, M.O. SOUZA, AND B. SKYRMS. **Evolutionary dynamics of collective action**. *The Mathematics of Darwin's Legacy*, pages 119–138, 2011.

[117] F.L. PINHEIRO, J.M. PACHECO, AND F.C. SANTOS. **From Local to Global Dilemmas in Social Networks**. *PLoS ONE*, **7**(2):e32114, 2012.

[118] J. GÓMEZ-GARDEÑES, J. PONCELA, L. MARIO FLORÍA, AND Y. MORENO. **Natural selection of cooperation and degree hierarchy in heterogeneous populations**. *Journal of theoretical biology*, **253**(2):296–301, 2008.

[119] M. PERC AND A. SZOLNOKI. **Coevolutionary games - A mini review**. *BioSystems*, **99**(2):109–125, 2010.

[120] G. SZABÓ AND G. FÁTH. **Evolutionary games on graphs**. *Physics Reports*, **446**(4-6):97–216, 2007.

[121] **Wikipedia's List of Social Networking Websites**. *Available from http://en.wikipedia.org/wiki/List-of-social-networking-websites*.

[122] J.L. MORENO. **Who shall survive?: A new approach to the problem of human interrelations.** 1934.

[123] K. LEWIS, J. KAUFMAN, M. GONZALEZ, A. WIMMER, AND N.A. CHRISTAKIS. **Tastes, ties, and time: A new social network dataset using Facebook. com**. *Social Networks*, **30**(4):330–342, 2008.

[124] J.P. ONNELA AND F. REED-TSOCHAS. **Spontaneous emergence of social influence in online systems**. *Proceedings of the National Academy of Sciences*, **107**(43):18375–18380, 2010.

[125] M. CHA, H. HADDADI, F. BENEVENUTO, AND K.P. GUMMADI. **Measuring user influence in Twitter: The million follower fallacy**. In *4th International AAAI Conference on Weblogs and Social Media (ICWSM)*, 2010.

[126] E. BAKSHY, J.M. HOFMAN, W.A. MASON, AND D.J. WATTS. **Everyone's an influencer: quantifying influence on twitter**. In *Proceedings of the Fourth ACM International Conference on Web Search and Data Mining*, pages 65–74. ACM, 2011.

[127] M. KEELING. **The implications of network structure for epidemic dynamics**. *Theoretical Population Biology*, **67**(1):1–8, 2005.

[128] J.G. TROGDON, J. NONNEMAKER, AND J. PAIS. **Peer effects in adolescent overweight**. *Journal of Health Economics*, **27**(5):1388–1399, 2008.

[129] H.S. NAIR, P. MANCHANDA, AND T. BHATIA. **Asymmetric social interactions in physician prescription behavior: The role of opinion leaders**. *Journal of Marketing Research*, **47**(5):883–895, 2010.

[130] L. BETTENCOURT, A. CINTRÓN-ARIAS, D.I. KAISER, AND C. CASTILLO-CHÁVEZ. **The power of a good idea: Quantitative modeling of the spread of ideas from epidemiological models**. *Physica A: Statistical Mechanics and its Applications*, **364**:513–536, 2006.

[131] E.L. GLAESER, B. SACERDOTE, AND J.A. SCHEINKMAN. **Crime and Social Interactions**. *The Quarterly Journal of Economics*, **111**(2):507–548, 1996.

[132] A. CALVÓ-ARMENGOL AND Y. ZENOU. **Social Networks and Crime Decisions: The Role of Social Structure in Facilitating Delinquent Behavior**. *International Economic Review*, **45**(3):939–958, 2004.

[133] M. BERTRAND, E.F.P. LUTTMER, AND S. MULLAINATHAN. **Network effects and welfare cultures**. Technical report, National Bureau of Economic Research, 1998.

[134] A. CALVÓ-ARMENGOL. **Job contact networks**. *Journal of Economic Theory*, **115**(1):191–206, 2004.

[135] L. COHEN, A. FRAZZINI, AND C. MALLOY. **The Small World of Investing: Board Connections and Mutual Fund Returns**. Working Paper 13121, National Bureau of Economic Research, May 2007.

[136] B. SACERDOTE. **Peer effects with random assignment: Results for Dartmouth roommates**. Technical report, National Bureau of Economic Research, 2000.

[137] N.A. CHRISTAKIS AND J.H. FOWLER. **The spread of obesity in a large social network over 32 years**. *New England Journal of Medicine*, **357**(4):370–379, 2007.

[138] N.A. CHRISTAKIS AND J.H. FOWLER. **The collective dynamics of smoking in a large social network**. *New England Journal of Medicine*, **358**(21):2249–2258, 2008.

[139] N.A. CHRISTAKIS AND J.H. FOWLER. **Dynamic Spread of Happiness in a Large Social Network: Longitudinal Analysis Over 20 Years in the Framingham Heart Study**. *British Medical Journal*, **337**:1–9, 12 2008.

[140] J.T. CACIOPPO, J.H. FOWLER, AND N.A. CHRISTAKIS. **Alone in the crowd: The structure and spread of loneliness in a large social network.** *Journal of Personality and Social Psychology*, **97**(6):977–991, 2009.

[141] N.A. CHRISTAKIS AND J.H. FOWLER. *Connected: The surprising power of our social networks and how they shape our lives*. Little, Brown and Company, 2009.

[142] J.H. FOWLER AND N.A. CHRISTAKIS. **Cooperative behavior cascades in human social networks**. *Proceedings of the National Academy of Sciences of the United States of America*, **107**(12):5334–5338, 2010.

[143] S.C. MEDNICK, N.A. CHRISTAKIS, AND J.H. FOWLER. **The spread of sleep loss influences drug use in adolescent social networks**. *PloS one*, **5**(3):e9775, 2010.

[144] J.N. ROSENQUIST, J. MURABITO, J.H. FOWLER, AND N.A. CHRISTAKIS. **The spread of alcohol consumption behavior in a large social network**. *Annals of Internal Medicine*, **152**(7):426–433, 2010.

[145] **Framingham Heart Study**. *Available from http://www.framinghamheartstudy.org/*.

[146] **National Longitudinal Study of Adolescent Health**. *Available from http://www.cpc.unc.edu/projects/addhealth/*.

[147] C.L. APICELLA, F.W. MARLOWE, J.H. FOWLER, AND N.A. CHRISTAKIS. **Social networks and cooperation in hunter-gatherers**. *Nature*, **481**(7382):497–501, 2012.

[148] F.C. SANTOS, J.F. RODRIGUES, AND J.M. PACHECO. **Graph topology plays a determinant role in the evolution of cooperation**. *Proceedings of the Royal Society B: Biological Sciences*, **273**(1582):51–55, 2006.

[149] F.C. SANTOS, J.M. PACHECO, AND T. LENAERTS. **Evolutionary dynamics of social dilemmas in structured heterogeneous populations**. *Proceedings of the National Academy of Sciences of the United States of America*, **103**(9):3490–3494, 2006.

[150] F.C. SANTOS, J.M. PACHECO, AND T. LENAERTS. **Cooperation prevails when individuals adjust their social ties**. *PLoS Computational Biology*, **2**(10):1284–1291, 2006.

[151] T.M. LIGGETT. *Stochastic interacting systems: contact, voter, and exclusion processes*, **324**. Springer Verlag, 1999.

[152] V. SOOD, T. ANTAL, AND S. REDNER. **Voter models on heterogeneous networks**. *Physical Review E*, **77**(4):041121, 2008.

[153] F. VAZQUEZ AND V.M. EGUÍLUZ. **Analytical solution of the voter model on uncorrelated networks**. *New Journal of Physics*, **10**:063011, 2008.

[154] C. CASTELLANO, D. VILONE, AND A. VESPIGNANI. **Incomplete ordering of the voter model on small-world networks**. *EPL (Europhysics Letters)*, **63**:153, 2003.

[155] P.L. KRAPIVSKY. **Kinetics of monomer-monomer surface catalytic reactions**. *Physical Review A*, **45**(2):1067, 1992.

[156] E. HATFIELD, J.T. CACIOPPO, AND R.L. RAPSON. *Emotional contagion*. Cambridge University Press, 1994.

[157] W. O. KERMACK AND A. G. MCKENDRICK. **A Contribution to the Mathematical Theory of Epidemics**. *Proceedings of the Royal Society of London. Series A*, **115**(772):700–721, 1927.

[158] G. SHABBIR, H. KHAN, AND M.A. SADIQ. **A note on exact solution of SIR and SIS epidemic models**. *Arxiv preprint arXiv:1012.5035*, 2010.

[159] R. PASTOR-SATORRAS AND A. VESPIGNANI. **Epidemic spreading in scale-free networks**. *Physical Review Letters*, **86**(14):3200–3203, 2001.

[160] S. VAN SEGBROECK, F.C. SANTOS, AND J.M. PACHECO. **Adaptive contact networks change effective disease infectiousness and dynamics**. *PLoS Computational Biology*, **6**(8):e1000895, 2010.

[161] J. VERDASCA, M.M. TELO DA GAMA, A. NUNES, N.R. BERNARDINO, J.M. PACHECO, AND M.C. GOMES. **Recurrent epidemics in small world networks**. *Journal of Theoretical Biology*, **233**(4):553–561, 2005.

[162] M.M. TELO DA GAMA AND A. NUNES. **Epidemics in small world networks**. *The European Physical Journal B-Condensed Matter and Complex Systems*, **50**(1):205–208, 2006.

[163] Y. MORENO, R. PASTOR-SATORRAS, AND A. VESPIGNANI. **Epidemic outbreaks in complex heterogeneous networks**. *The European Physical Journal B-Condensed Matter and Complex Systems*, **26**(4):521–529, 2002.

[164] R. PASTOR-SATORRAS AND A. VESPIGNANI. **Epidemic dynamics and endemic states in complex networks**. *Physical Review E*, **63**(6):066117, 2001.

[165] L.A.N. AMARAL, A. SCALA, M. BARTHÉLÉMY, AND H.E. STANLEY. **Classes of small-world networks**. *Proceedings of the National Academy of Sciences*, **97**(21):11149–11152, 2000.

[166] R. ALBERT AND A.L. BARABÁSI. **Statistical mechanics of complex networks**. *Reviews of Modern Physics*, **74**:47–97, Jan 2002.

[167] J.M. PACHECO, A. TRAULSEN, AND M.A. NOWAK. **Active linking in evolutionary games**. *Journal of Theoretical Biology*, **243**(3):437–443, 2006.

[168] H. OHTSUKI, M.A. NOWAK, AND J.M. PACHECO. **Breaking the symmetry between interaction and replacement in evolutionary dynamics on graphs**. *Physical Review Letters*, **98**(10):108106–108109, 2007.

[169] J.P. ONNELA, J. SARAMÄKI, J. HYVÖNEN, G. SZABÓ, D. LAZER, K. KASKI, J. KERTÉSZ, AND A.L. BARABÁSI. **Structure and tie strengths in mobile communication networks**. *Proceedings of the National Academy of Sciences*, **104**(18):7332, 2007.

[170] S. BANSAL, S. KHANDELWAL, AND L. MEYERS. **Exploring biological network structure with clustered random networks**. *BMC Bioinformatics*, **10**(1):405, 2009.

[171] A. BARRAT, M. BARTHÉLEMY, AND A. VESPIGNANI. *Dynamical processes on complex networks*. Cambridge University Press, 2008.

[172] D. LAZER, A. PENTLAND, L. ADAMIC, S. ARAL, A. BARABÁSI, D. BREWER, N.A. CHRISTAKIS, N. CONTRACTOR, J. FOWLER, M. GUTMANN, T. JEBARA, G. KING, M. MACY, D. ROY, AND M. VAN ALSTYNE. **Computational Social Science**. *Science*, **323**(5915):721–723, 2009.

[173] E.W. DIJKSTRA. **A note on two problems in connexion with graphs**. *Numerische Mathematik*, **1**(1):269–271, 1959.

[174] A. RAPOPORT AND A.M. CHAMMAH. *Prisoner's dilemma: A study in conflict and cooperation*, **165**. University of Michigan Press, 1965.

[175] T.C. HEADRICK. *Statistical Simulation: Power Method Polynomials and other Transformations*. Taylor & Francis, 2009.